Ozone-Based Advanced Oxidation Processes for Removing Contaminants of Emerging Concern from Digestate Supernatant
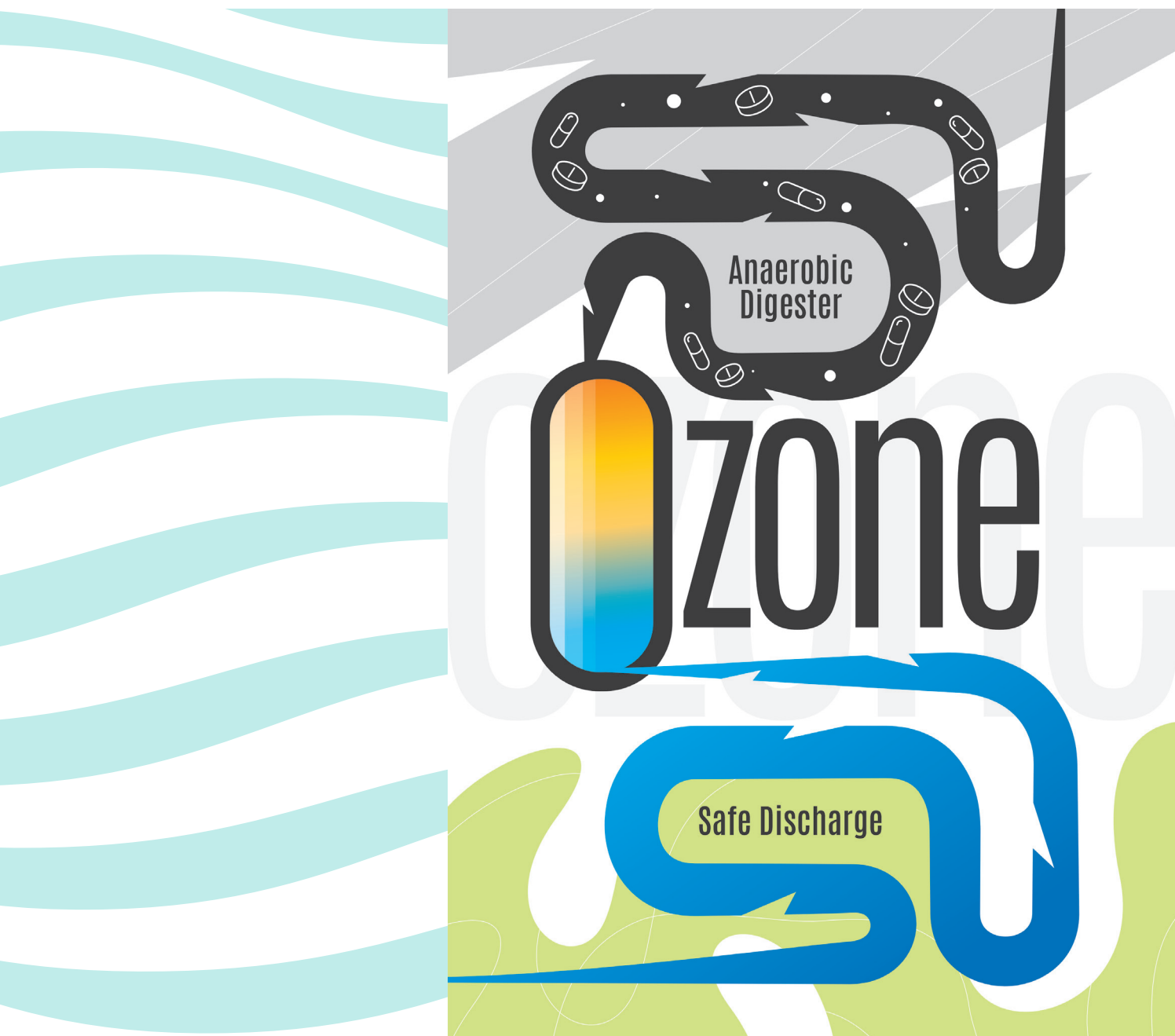## Application and Modeling

Moradi, N.

Important note
To cite this publication, please use the final published version (if applicable).
Please check the document version above.

Ozone-Based Advanced Oxidation Processes for Removing Contaminants of Emerging Concern from Digestate Supernatant: Application and Modeling

Nazanin Moradi

Ozone-Based Advanced Oxidation Processes for Removing Contaminants of Emerging Concern from Digestate Supernatant: Application and Modeling

DISSERTATION

for the purpose of obtaining the degree of doctor

at Delft University of Technology

by the authority of the Rector Magnificus Prof.dr.ir. T.H.J.J. van der Hagen,

chair of the Board for Doctorates

and

in fulfilment of the requirement of the Rector of IHE Delft

Institute for Water Education, Prof.dr. E.J. Moors,

to be defended in public on

Monday, 28 October 2024 at 17:30 hours

in Delft, the Netherlands

by

Nazanin MORADI

Master of Science in Environmental Health Engineering,

Isfahan University of Medical Sciences

born in Mahshar, Iran

This dissertation has been approved by the promotors.

Composition of the doctoral committee:

Rector Magnificus TU Delft	chairperson
Rector IHE Delft	vice-chairperson
Prof.dr. D. Brdjanovic	IHE Delft / TU Delft, promotor
Prof.dr.ir. M.C.M. van Loosdrecht	TU Delft, promotor

Independent members:

Prof.dr. B. Bina	Isfahan university of medical science, Iran
Prof.dr.ir. J.B. van Lier	TU Delft
Prof.dr. C.A. Madera Parra	University del Valle Cali, Colombia
Prof.dr. M. Matošić	University of Zagreb, Croatia
Prof.dr.ir. M.K. de Kreuk	TU Delft, reserve member

This research was conducted under the auspices of the Graduate School for Socio-Economic and Natural Sciences of the Environment (SENSE)

To my younger self, who did not give up…

ACKNOWLEDGEMENTS

SUMMARY

Organic waste constitutes a substantial portion of global waste, posing environmental challenges. Anaerobic Digestion (AD) plants offer a circular bioeconomy solution by converting organic waste into renewable energy and nutrients. While AD primarily yields methane, the resulting nutrient-rich digestate holds significant agronomic value for land applications. However, the direct application of digestate is banned in several countries due to environmental and health hazards, including the presence of contaminants of emerging concern (CECs). This circumstance leads to landfilling as the primary alternative—a non-sustainable solution.

This thesis explores the application of ozone-based Advanced Oxidation Processes (AOPs) as a potential post-AD treatment for liquid digestate, aligning with the fundamental objectives of fostering sustainable circular economy practices in waste management.

Chapter 1 serves as the foundation, highlighting the prevalence of organic waste on a global scale and elucidating the environmental challenges associated with CECs in digestate. This chapter addresses the gap in knowledge and formulates research questions to explore the feasibility of utilizing ozone-based AOPs for the removal of CECs from liquid digestate.

In Chapter 2, the primary objective is the evaluation of ozonation as a post-AD treatment for efficiently removing CECs. The chapter aims to determine the required ozone dose for CECs removal from digestate, understand the overall impact of the digestate matrix on the removal kinetic rate, and conduct a toxicity assay. The lab-scale experiments within a bubble column reactor successfully demonstrates the effectiveness of ozonation. Despite the challenging nature of the digestate matrix, which reduces the removal efficiency to 1% of the maximum observed in demineralized water, the determined ozone dose of 0.48 mg O_3/mg DOC is sufficient for removing all studied CECs. This falls within the reported range of ozone doses for other water matrices. The finding of acute toxicity assay shows a decrease of at least 18.1% during the 5-hour ozonation period. The result of this chapter shows that despite the significant ozone consumption, the required ozone dose for complete CECs removal from digestate supernatant is within or lower than the reported range for other water matrices. This suggests that ozonation could be a viable post-AD treatment strategy to generate a cleaner stream before discharge or land application.

In Chapter 3, a mathematical model is formulated to describe the ozonation process in digestate. The primary focus is on understanding the impact of digestate, characterized by a high load of organic matter, on ozone consumption during treatment. Given the

energy-intensive nature of ozone technology, the chapter underlines the importance of predicting ozone consumption to assess the cost-effectiveness of the process as a potential post- AD treatment. Analysis of data gathered during the long-term ozonation of digestate reveals an increase in ozone consumption influenced by the complex digestate matrix, exposing a knowledge gap in understanding key parameters governing the ozonation process. This chapter addresses a research gap in ozone modeling by incorporating ammonia into the ozone decomposition matrix (the Petersen matrix) and considering the influence of alkalinity on the oxidation of other components. The insights contribute to the understanding of the ozonation process within complex water matrices like digestate. Key conclusions from this chapter include the effective prediction of ozone consumption, elucidation of component oxidation, and the necessity of considering interactions between water matrix components for accurate process description and prediction of ozone consumption before experimental work.

Chapter 4 extends the mathematical framework in the previous chapter, utilizing the calibrated model to predict the removal of contaminants of emerging concern (CECs) in diverse water matrices. With a primary focus on the digestate matrix, the objective is to identify inhibitory factors influencing the removal of persistent CECs during ozonation. Experimental exploration examines the individual and combined effects of matrix components on CECs removal, revealing DON-N as the most inhibitory factor. The developed model, integrating CECs removal rates and inhibition factors, showcases high predictive accuracy across diverse water matrices. The key advantage of this model, setting it apart from other prediction models, is its independence from parameters such as RCT. By relying solely on fundamental water matrix characterizations including DOC, DON-N, ammonia and alkalinity, the model streamlines the prediction process for the abatement of CECs during ozonation. This unique feature enhances the efficiency and applicability of the model, making it a simple tool for assessing CECs removal in diverse water matrices without the prerequisite of extensive preliminary experimentation.

Chapter 5 explores a pilot-scale hybrid system, UVOX Redox®, which combines UV light with ozone treatment for the removal of contaminants of emerging concern (CECs) from digestate in two distinct AD plants. Housed within a hybrid mobile technology called NOMAD, explicitly designed for digestate treatment, the UVOX pilot introduces an innovative methodology applicable to small-scale and decentralized AD plants. The chapter underscores the efficiency of UVOX in removing CECs, demonstrating high removal efficiency, cost-effectiveness, and energy reduction, thus making it a pragmatic and viable solution for full-scale applications. Additionally, the chapter introduces the UVT surrogate method, establishing robust correlations with DOC and CECs removal. This improvement enables the easy monitoring of treatment efficacy, offering a reliable means to assess the system's performance. The findings of this chapter contribute to the practical implementation of UVOX, aligning with broader goals related to sustainable digestate recycling and the advancement of circular economy strategies.

Chapter 6 summarizes the key findings of this thesis and outlines future perspectives to enhance and extend this research.

This thesis presents a comprehensive investigation into the application of ozone-based AOPs for digestate treatment, providing practical solutions that advance the implementation of sustainable practices within the circular bioeconomy.

SAMENVATTING

Biologisch afval vormt een aanzienlijk deel van al het afval en geeft milieuproblemen. Anaerobe vergistingsinstallaties bieden een circulaire oplossing door organisch afval om te zetten in hernieuwbare energie en voedingsstoffen. Hoewel anaerobe vergisting voornamelijk methaan oplevert, heeft het resulterende voedingsrijke digestaat aanzienlijke agronomische waarde voor landtoepassingen. Echter, directe toepassing van digestaat is in verschillende landen verboden vanwege milieu- en gezondheidsrisico's, waaronder de aanwezigheid van opkomende verontreinigende stoffen (CEC's). Deze omstandigheid leidt tot storten als voornaamste alternatief, een niet-duurzame oplossing.

Dit proefschrift onderzoekt de toepassing van op ozon gebaseerde geavanceerde oxidatieprocessen (AOP's) als mogelijke nabehandeling voor vloeibare digestaat, in lijn met de doelstellingen van het bevorderen van duurzame circulaire economie praktijken in afvalbeheer.

Hoofdstuk 1 dient als inleiding, waarbij de alomtegenwoordigheid van organisch afval op wereldwijde schaal wordt benadrukt en de milieuproblemen geassocieerd met opkomende verontreinigende stoffen (CEC's) in digestaat worden toegelicht. Dit hoofdstuk behandelt de kenniskloof en formuleert onderzoeksvragen om de haalbaarheid van het gebruik van op ozon gebaseerde geavanceerde oxidatieprocessen (AOP's) voor het verwijderen van CEC's uit vloeibaar digestaat te onderzoeken.

In Hoofdstuk 2 is het primaire doel de evaluatie van ozonisatie als een post anaerobe vergisting -behandeling voor het efficiënt verwijderen van opkomende verontreinigende stoffen (CEC's). Het hoofdstuk beoogt de benodigde ozondosis te bepalen voor de verwijdering van CEC's uit digestaat, inzicht te krijgen in de algehele impact van de digestaatmatrix op de verwijderingskinetiek, en een toxiciteitstest uit te voeren. De laboratoriumexperimenten in een bellenkolomreactor laten met succes de effectiviteit van ozonisatie zien. Ondanks de uitdagende aard van de digestaatmatrix, waardoor de verwijderingsefficiëntie wordt teruggebracht tot 1% van het maximum waargenomen in gedemineraliseerd water, is de bepaalde ozondosis van 0,48 mg O_3/mg DOC voldoende voor het verwijderen van alle bestudeerde CEC's. Dit valt binnen het gerapporteerde bereik van ozondoses voor andere watermatrices. De bevindingen van de acute toxiciteitstest tonen een afname van minstens 18,1% gedurende de 5 uur durende ozonisatieperiode. De resultaten van dit hoofdstuk tonen aan dat ondanks het aanzienlijke ozonverbruik, de benodigde ozondosis voor volledige verwijdering van CEC's uit digestaat supernatant gelijk of lager is dan het gerapporteerde bereik voor andere watermatrices. Dit suggereert dat ozonisatie een haalbare nabehandelingsstrategie voor digestaat zou kunnen zijn om een schonere stroom te genereren vóór lozing of toepassing op het land.

In Hoofdstuk 3 wordt een wiskundig model geformuleerd om het ozonatieproces in digestaat te beschrijven. De primaire focus ligt op het begrijpen van de impact van digestaat, gekenmerkt door een hoge belasting van organisch materiaal, op ozonverbruik tijdens de behandeling. Gezien de energie-intensieve aard van ozontechnologie, benadrukt het hoofdstuk het belang van het voorspellen van ozonverbruik om de kosteneffectiviteit van het proces als mogelijke digestaat behandeling te beoordelen. Analyse van gegevens verzameld tijdens de langdurige ozonatie van digestaat toont een toename in ozonverbruik beïnvloed door de complexe digestaatmatrix, waarmee een kenniskloof wordt blootgelegd met betrekking tot het begrijpen van sleutelparameters die het ozonatieproces beheersen. Dit hoofdstuk behandelt een gemis in ozonmodellering door ammoniak op te nemen als factor in het ozonverbruik (de Petersen-matrix) en rekening te houden met de invloed van alkaliniteit op de oxidatie van andere componenten. De inzichten dragen bij aan het begrip van het ozonatieproces binnen complexe watermatrices zoals digestaat. Belangrijke conclusies uit dit hoofdstuk omvatten de effectieve voorspelling van ozonverbruik, verheldering van invloed van ammonium en alkaliniteit, en de noodzaak om interacties tussen watermatrixcomponenten te overwegen voor een nauwkeurige beschrijving van het proces en voorspelling van ozonverbruik vóór experimenteel werk.

Hoofdstuk 4 breidt het wiskundige kader uit dat in het vorige hoofdstuk is ontwikkeld, waarbij het gekalibreerde model wordt gebruikt om de verwijdering van opkomende verontreinigende stoffen (CEC's) in diverse watermatrices te voorspellen. Met een primaire focus op de digestaatmatrix is het doel om remmende factoren te identificeren die van invloed zijn op de verwijdering van persistente CEC's tijdens ozonisatie. Middels experimenteel onderzoek werd de individuele en gecombineerde effecten van matrixcomponenten op de verwijdering van CEC's onderzocht, waarbij blijkt dat opgelost organisch stikstof de meest remmende factor is. Het ontwikkelde model, waarin verwijderingssnelheden van CEC's en remmingsfactoren zijn geïntegreerd, vertoont een hoge voorspellende nauwkeurigheid over diverse watermatrices. Het belangrijkste voordeel van dit model, ten opzichte van eerdere modellen, is de onafhankelijkheid van parameters zoals RCT-waarde. Door uitsluitend te vertrouwen op fundamentele eigenschappen van watermatrices, waaronder opgelost organisch koolstof en stikstof, ammoniak en alkaliniteit, vereenvoudigt het model het voorspellingsproces voor de oxidatie van CEC's tijdens ozonisatie. Deze unieke eigenschap verbetert de efficiëntie en toepasbaarheid van het model, waardoor het een eenvoudig instrument wordt voor het beoordelen van CEC-verwijdering in diverse watermatrices zonder de noodzaak van uitgebreide voorafgaande experimenten.

Hoofdstuk 5 onderzoekt een pilootschaal hybride systeem, UVOX Redox®, dat UV-licht combineert met ozonbehandeling voor de verwijdering van opkomende verontreinigende stoffen (CEC's) uit digestaat in twee verschillende vergistingsinstallaties. Geïntegreerd in een hybride mobiele technologie genaamd NOMAD, specifiek ontworpen voor digestaatbehandeling, introduceert de UVOX-pilot een innovatieve methodologie die

toepasbaar is op kleinschalige en gedecentraliseerde vergistingsinstallaties. Het hoofdstuk benadrukt de efficiëntie van UVOX bij het verwijderen van CEC's, waarbij hoge verwijderingsefficiëntie, kosteneffectiviteit en energiereductie worden gedemonstreerd, waardoor het een pragmatische en haalbare oplossing is voor grootschalige toepassingen. Daarnaast introduceert het hoofdstuk de UVT-surrogaatmethode, die robuuste correlaties tussen opgelost organisch koolstof en CEC's-verwijdering vaststelt. Deze verbetering maakt het eenvoudig om de behandeling efficiëntie te monitoren en biedt een betrouwbaar middel om de prestaties van het systeem te beoordelen. De bevindingen van dit hoofdstuk dragen bij aan de praktische implementatie van UVOX, in lijn met bredere doelen met betrekking tot duurzame recycling van digestaat en de bevordering van strategieën voor de circulaire economie.

Hoofdstuk 6 vat de belangrijkste bevindingen van deze scriptie samen en schetst toekomstige perspectieven om dit onderzoek te verbeteren en uit te breiden.

Deze scriptie presenteert een gedetailleerd onderzoek naar de toepassing van op ozon gebaseerde geavanceerde oxidatieprocessen voor de behandeling van digestaat, en biedt praktische oplossingen die de implementatie van duurzame technologieën binnen de circulaire bio-economie bevorderen.

CONTENTS

1

INTRODUCTION

1.1 BACKGROUND

Organic waste constitutes a high percentage of global waste composition, ranging from 28% in high-income countries to a massive 64% in low-income countries, with an average of 46% worldwide. Resulting greenhouse gas (GHG) emissions poses a serious climate change threat. In the EU, 1.4 billion tons of manure are produced each year; however, less than 10% is currently actively managed (Worldbank.org).

Within the paradigm of circular bioeconomy, Anaerobic Digestion (AD) plants emerge as important hubs capable of recovering valuable renewable energy and nutrients from diverse organic waste streams. Anaerobic digestion is a promising process to convert organic waste to bioenergy. Beyond methane production, growing attention has focused on the recycling and reuse of the effluent stream generated by anaerobic digesters, known as digestate. This nutrient-rich liquid fraction is suitable for nutrient recovery or for irrigation and land application (Wang et al., 2023). However, direct application of digestate to soil or its discharge can lead to undesirable consequences, including GHG emissions (Crolla et al., 2013; Wang and Lee, 2021), acidification, eutrophication, and a reduction in worm populations through high ammonium-N loading rates (Moinard et al., 2021). Moreover, the presence of contaminants of emerging concern (CECs), particularly pharmaceuticals, adds a layer of complexity to the environmental implications of digestate.

Over the past few decades, the agricultural sector has witnessed a surge in the use of active pharmaceutical compounds, including antibiotics, non-steroidal anti-inflammatory drugs (NSAIDs), and hormones, for purposes such as animal growth and disease control (Kasumba et al., 2020; Nurk et al., 2019; Widyasari-Mehta et al., 2016). These compounds, characterized by their non-biodegradable nature, present challenges during the anaerobic digestion of livestock manure. While the anaerobic digestion process can eliminate some pharmaceuticals through biodegradation or sorption, it struggles with non-biodegradable compounds, leading to a considerable percentage of these compounds persisting in the resulting digestate. Consequently, the discharge of digestate into the environment contributes to environmental hazards, including the rise of antibiotic-resistant genes and bacteria (Liu et al., 2018; Yang et al., 2022b).

Different approaches including additives (Zhang et al., 2018; Zhou et al., 2021), pretreatment such as thermal method (Yin et al., 2020), advanced anaerobic system and co-digestion methods (Huang et al., 2018) have been investigated to improve removal of antibiotics during anaerobic digestion process. Although these methods were successful in increasing antibiotic removal during anaerobic digestion process, a significant portion of these compounds still is reported to end up in digestate derived from manure and slurries, with concentrations ranging from 120 μg/L for tetracycline to 66,400 μg/L for chlortetracycline, for instance (Kasumba et al., 2020; Nurk et al., 2019). Therefore, discharge of digestate can pose potential environmental hazards and contribute to the

increased proliferation of antibiotic-resistant genes (ARGs) and antibiotic-resistant bacteria (ARBs) (Gurmessa et al., 2020; Reygaert, 2018; Yang et al., 2022a).

1.2 TECHNOLOGIES TO REMOVE CECs

Various methods have been employed to remove CECs from drinking water and wastewater. These methods include biological, physical and chemical treatments (Kumar et al., 2023).

Biological treatment such as membrane bioreactors, bio-filtration, microbial and enzymatic processes are considered as low energy-intensive treatments, but with low to moderate removal efficiency (Kumar et al., 2023; Stadlmair et al., 2018).

The advantage of physical treatment, such as membrane separation and adsorption, is the absence of toxic by-product (Ahmed et al., 2017). However, there are disadvantages associated with physical treatment. For instance, membranes, while effective in separation, do not mineralize CECs (Konieczny et al., 2011; Yue et al., 2020). The residual of these compounds accumulates in the concentrate and necessitates additional treatment (Yang et al., 2022a; Yu et al., 2019). Adsorption, although proficient in transferring CECs from the liquid phase to the adsorbent (Vinayagam et al., 2022), raises sustainability concerns due to its non-degradative nature (Yang et al., 2022a).

Nevertheless, chemical treatment including advance oxidation processes (AOPs) are among the most promising methods in removing CECs by degrading and oxidizing the parent compounds rather than transferring them into another phase (Dong et al., 2022; Sgroi et al., 2021; Wang et al., 2023a). A wide range of AOPs have been applied to remove CECs in lab, pilot, and full scale. This range includes ozone-based AOPs, UV-based AOPs, electrochemical AOPs (eAOP), catalytic AOPs (cAOP), and physical AOPs (pAOP) (Miklos et al., 2018).

Figure 1.1 represent processes of different degrees of implementation from well-established AOPs to the processes that are only tested at laboratory scale yet.
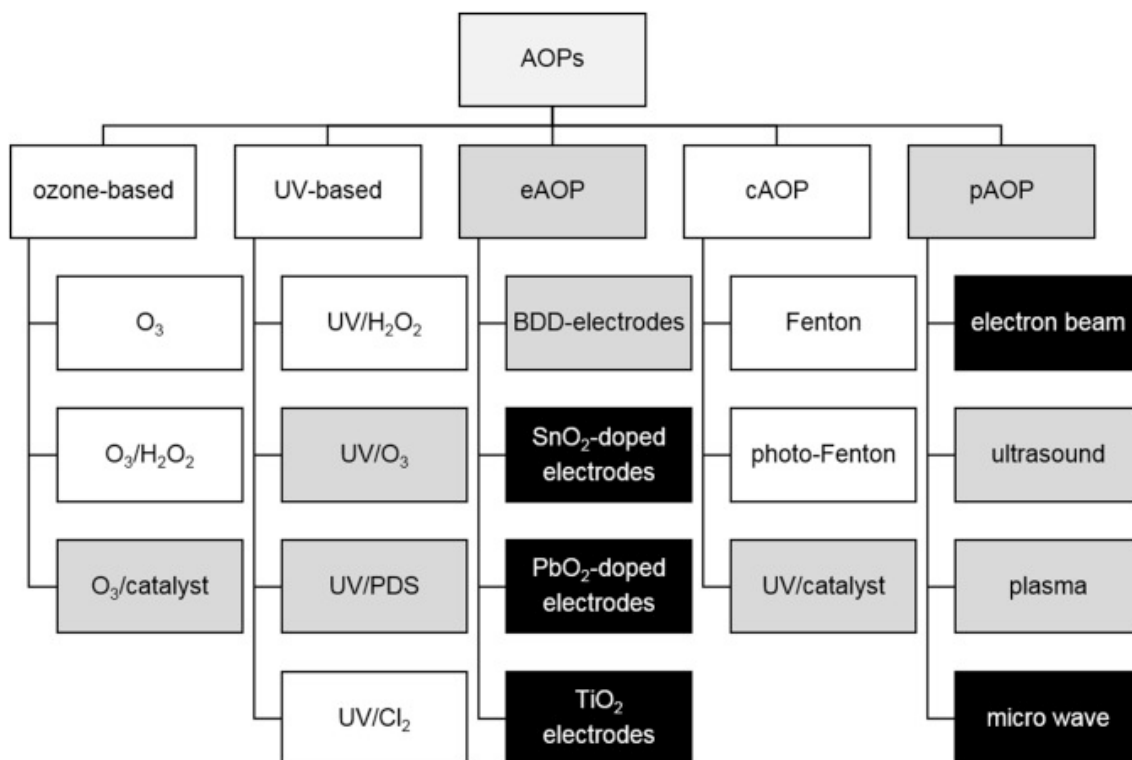
Figure 1.1. Broad overview and classification of different AOPs. Individual processes are marked as established at full-scale (white), investigated at lab- and pilot-scale (grey), and tested at lab-scale (black) (Figure and caption adopted from Miklos et al. (2018))

While AOPs exhibit promising capabilities in effectively eliminating a broad spectrum of CECs, their notable drawback lies in their substantial energy consumption. In a comprehensive analysis conducted by Miklos et al. (2018), the published energy consumption per order (E_{EO}) was compared across various AOPs documented in the literature. The energy efficiency of different AOPs can be seen in Figure 1.2.

Figure 1.2 underscores that ozone and ozone-based AOPs, with a median E_{EO} of less than 1 kWh m^{-3}, emerged as the most energy-efficient AOPs. This noteworthy characteristic, coupled with their ability to efficiently oxidize a diverse range of CECs in both drinking water and wastewater (Bui et al., 2016; de Oliveira et al., 2020; Hansen et al., 2016; Lee et al., 2023; Lim et al., 2022), has made ozone-based AOPs stand out as the top choice for scale-up and gaining more focus in research and practical use.
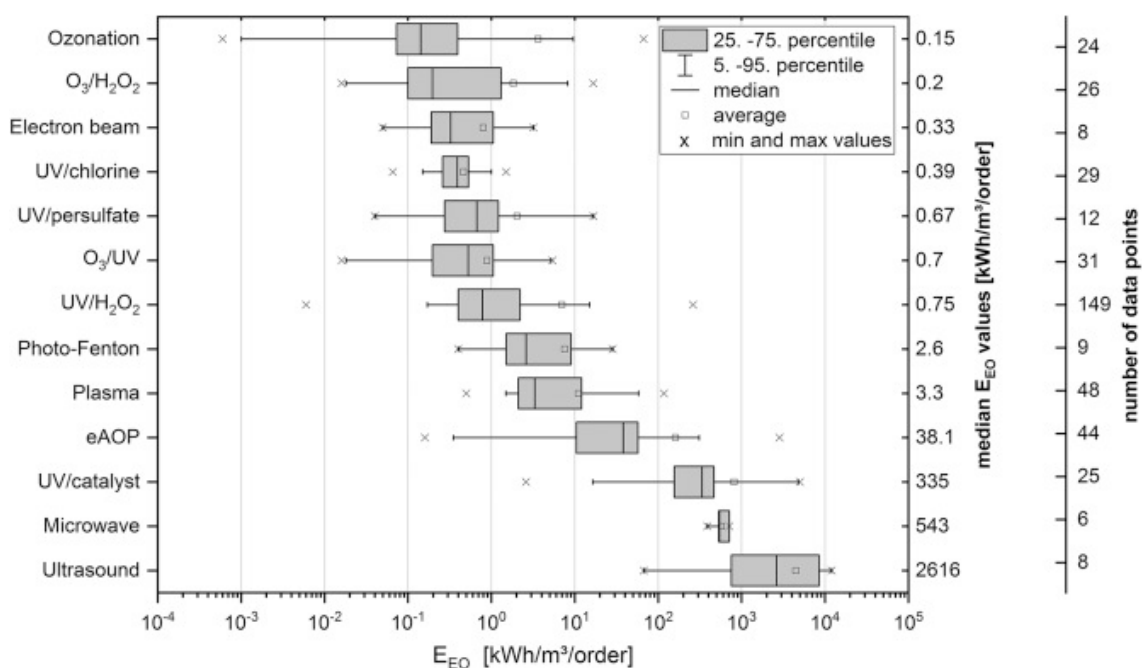
Figure 1.2. Overview of published E$_{EO}$-values of different AOPs sorted according to median values (Figure and caption adopted from Miklos et al. (2018))

1.3 OZONE OXIDATION MECHANISMS

Ozone with a redox potential of 2.07 V can oxidize a wide range of CECs via two mechanisms including direct reaction of molecular ozone and indirect reaction of generated reactive oxidative species (ROS) such as OH$^{\bullet}$ radicals (Miklos et al., 2018). Direct reaction of ozone and CECs occurs through different pathways:

1. Oxidation-reduction pathway via electron transfer process such as reaction with HO$_2^{\bullet}$ or O$_2^{\bullet-}$ (Equations (1.1) and (1.2)) (Wang and Chen, 2020):

$$O_3 + HO_2 \rightarrow O_3^{\bullet-} + HO_2^{\bullet} \qquad (1.1)$$

$$O_3 + O_2^{\bullet-} \rightarrow O_3^{\bullet-} + O_2 \qquad (1.2)$$

2. Electrophilic reaction where ozone attacks the nucleophilic position of the compounds and substitutes one part of them. The –OH-, –NO$_2$ and –Cl groups, have a significant influence on the reactivity of the aromatic ring with ozone as electrophilic agent (Wang and Chen, 2020) .

3. Nucleophilic reaction where ozone molecule can obtain a negative charge in one of the oxygen atoms due to the resonance structure. In this case, ozone shows a nucleophilic

property and tends to attack the electrophilic positions of the molecules, such as carbonyl or double and triple nitrogen carbon bonds. However, this reaction has only been observed in non-aqueous solution systems (Wang and Chen, 2020).

In the indirect mechanism, O_3 decomposition and reaction with hydroxide ions or organic matter forms $OH^\bullet$ radicals that precedes AOPs reactions (Khan et al., 2020). The formation of $OH^\bullet$ is quite slow, and follows a second order kinetic at the constant rate of 70 $M^{-1}s^{-1}$ (Equation (1.3) to Equation (1.7)) (Merényi et al., 2010).

$$O_3 + OH^- \rightarrow HO_4^- \tag{1.3}$$

$$HO_4^- \leftrightarrow HO_2^\bullet + O_2^{\bullet-} \tag{1.4}$$

$$O_2^{\bullet-} + O_3 \rightarrow O_2 + O_3^{\bullet-} \tag{1.5}$$

$$O_3^{\bullet-} \rightarrow O_2 + O^{-\bullet} \tag{1.6}$$

$$O^{-\bullet} + H_2O \rightarrow OH^\bullet + OH^- \tag{1.7}$$

$OH^\bullet$ is a non-selective radical with a higher redox potential (2.8 V) that can react with all organic pollutant (Chen and Wang, 2021; Lim et al., 2022).

However, the generation of $OH^\bullet$ is limited in neutral and acidic environments due to the stability of O_3 (Lee et al., 2013). Furthermore, because of the reaction between O_3 and organic compounds, aldehydes with the functional group of R-CH=O and carboxylic acids with the functional group of R-COOH are formed. These compounds do not further react with O_3 due to the absence of electron-rich sites in their molecular structure. Consequently, ozonation alone cannot achieve complete mineralization of the organic matter (Miklos et al., 2018).

1.4 Hybrid ozone systems- UVOX Redox® technology

To overcome the above-mentioned limitations and increase the efficiency of ozonation, the integration of O_3 with an activation method in a hybrid system have been suggested (Saeid et al., 2018). Among the hybrid ozone systems, the combination of ozone and UV has gained more attention due to its less chemical usage and higher mineralization rate (Farkas et al., 2024). In the presence of UV light, ozone undergoes photolysis with wavelengths (λ) below 300 nm, producing oxygen atoms in an excited state. Subsequently, a rapid reaction between atomic oxygen and water forms H_2O_2, which then decomposes to generate $OH^\bullet$, that has a 10^6 to 10^{12} times higher oxidation capacity than O_3(Miklos et al., 2018; Von Sonntag, 2008). This method has been successfully applied for TOC

removal (Keen et al., 2016; Paucar et al., 2019; Wols and Hofman-Caris, 2012) and the removal of pharmaceutical compounds from wastewater (Khan et al., 2020).

The main drawback of combining UV light and ozone in the hybrid method is the high electricity demand of both the ozone generator and UV source, resulting in increased costs and energy consumption (Miklos et al., 2018).

Recently, a novel UV/O$_3$ system, known as UVOX Redox®, has emerged for further commercial application and advancement of AOPs. The UVOX technology integrates the oxidizing capability of ozone with UV light, initiating a highly efficient AOP within a single system. Utilizing a UV lamp at a wavelength of 185 nm, atmospheric oxygen is converted into ozone (Ekowati et al., 2019). The produced gas mixture is then injected into the water via a Venturi injection system. Subsequently, water and the gas mixture undergo irradiation with UV light at 254 nm, leading to the decomposition of ozone molecules and the generation of OH$^\bullet$ radicals (Ekowati et al., 2019). Therefore, the UVOX technology has the potential to reduce the energy requirements of AOPs, as the specialized UV wavelength can generate ozone without the need for a separate ozone generator. A schematic representation of this system is illustrated in Figure 1.3. This innovative technology has recently been explored for treating water from swimming pools, demonstrating removal of specific micropollutants such as ibuprofen (Ekowati et al., 2019).
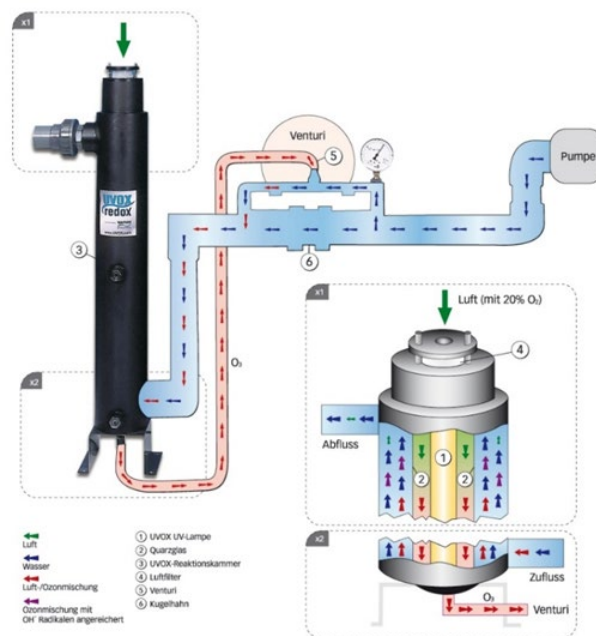
Figure 1.3 The UVOX Redox set-up (UVOX.com)

1.5 CECs REMOVAL FROM DIGESTATE

While ozonation is well-stablished in removing CECs from drinking water and, in some cases, wastewater, a review of the literature revealed a lack of data on its application to treat high- strength water matrix such as liquid digestate. The primary difference between the current ozone practices and ozonation of digestate lies in the characteristics of the liquid digestate and the effect of water matrix on ozone demand. The most recent review papers show the effect of the organic matter on increasing the ozone demand in different wastewater matrix, yet the range of DOC in the studied wastewaters varied between 5 to 48 mg/L (Asghar et al., 2022). Treating the liquid digestate with a reported DOC of between 120 to 3160 mg/L (Akhiar et al., 2017) can significantly increase the ozone dose required. The problem accelerates by considering the presence of carbonate species in digestate supernatant. Carbonate species can scavenge the OH$^•$ radicals (if generated), limiting the exposure of CECs to this oxidant (Asghar et al., 2022). Furthermore, the presence of ammonia in the digestate supernatant can stoichiometrically consume a substantial portion of ozone and produce nitrite and nitrate that have the potential to significantly scavenge the OH$^•$ radicals (Lado Ribeiro et al., 2019). While hybrid ozone systems, such as the combination of UV/O$_3$ (e.g., the innovative UVOX system), is promising in generating more OH$^•$ radicals to drive AOPs reactions, the presence of high concentrations of organic matter in digestate can impede the penetration of UV light into the water matrix, thereby restricting oxidant production, increasing required ozone dose to achieve certain CECs removal.

Understanding the effect of the digestate matrix and the reactions of its components with ozone is crucial to enhance the efficiency of this technology for CECs removal and to predict the required ozone dose and decide on the cost-effectiveness of the technology. To comprehend the complex reactions and interactions involved in ozonation, various models have been developed over time to enhance understanding of the ozonation process, thereby optimizing the process and predicting the removal of CECs.

1.6 OZONATION MODELS

Ozonation models can be categorized into two main types based on their purpose: ozone decomposition models and prediction models for micropollutant removal.

Ozone decomposition models, such as the Staehelin, Hoigné, and Bühler (SHB) model for acidic to neutral pH conditions and the Tomiyasu, Fukutomi, and Gordon (TFG) model for high pH values, were initially developed to focus on ozone kinetic reactions and decomposition rates in pure and drinking water (Bühler et al., 1984; Tomiyasu et al., 1985). The SHB model has been later enhanced by incorporating new reaction pathways and considering water quality characteristics such as pH (Lovato et al., 2009), and dissolved organic matter (DOM) (Audenaert et al., 2013).

The second category comprises models aimed at predicting micropollutant removal and oxidant exposure during ozonation, predominantly kinetic models with a focus on hydroxyl radicals (OH$^\bullet$) formation and the scavenging effect of water matrix components on OH$^\bullet$ radicals. These models assess the efficiency of ozonation in each water matrix using the R_{CT} value (Kim et al., 2020), as described in Equation (1.8)

$$R_{CT} = \frac{\int OH \cdot dt}{\int O_3\, dt} \qquad\qquad (1.8)$$

Where, $\int O_3$ is ozone exposure and $\int OH^\bullet$ is hydroxyl radical exposure (Lado Ribeiro et al., 2019). This approach has been applied to various water matrix to determine R_{CT} and incorporate its value, in addition to kinetic rate constant of CECs, into the prediction equation for the abatement of CECs as per Equation (1.9) (He et al., 2022; Kim et al., 2020; Moradi et al., 2023).

$$-ln\frac{C_t}{C_0} = (k_{O3} + R_{CT}\, k_{OH^\bullet}) \int_0^t O_3 dt \qquad\qquad (1.9)$$

Where, C_t and C_0 are the concentration of certain CECs at time t and time 0, k_{O3} and $k_{OH^\bullet}$ are the kinetic rate constant of certain CECs in reaction with O_3 and OH$^\bullet$, respectively.

While ozone process modeling has seen notable progress, current approaches come with certain limitations. Some models have focused on ozone self-decomposition in a pure water, neglecting impurities to simplify the system. Others have addressed individual contaminants by controlling other variables. Moreover, a notable limitation of prediction models is the variation of the R_{CT} value across different water matrices. Consequently, it is essential to conduct experiments to determine the R_{CT} value in each water matrix before predicting the removal of CECs. This is because the model depends on this value as well as the rate constant values (k_{O3} and k_{OH}), as per Equation (1.9), which are also not known for all CECs (Antoniou et al., 2013).

Furthermore, while ozonation models can aid in understanding the competitive effects of water matrix components on ozone consumption, current models primarily focus on ozone decomposition in low-strength water matrices such as pure and drinking water, or in the presence of a single impurity while controlling other variables. Consequently, these models fail to accurately describe ozonation in digestate matrices where organic and inorganic matter are simultaneously present. Although in some models a high concentration of alkalinity (up to 150 mg/L) was considered (Kim et al., 2020), the organic matter was limited to 5 mg/L. Yet, the model resulted in a complicated prediction equation. Furthermore, to the best of our knowledge, ammonia has not been accounted

for in previous models. Thus, the current approach may not be applicable to describe the effect of digestate matrix on CECs removal.

Therefore, more research is needed to evaluate the feasibility of ozone-based AOPs for CECs removal and the effect of digestate matrix on the efficiency of the process, along with developing prediction model tailored to distinct characterization of digestate.

1.7 PROBLEM STATEMENT

Anaerobic digestion converts organic waste into bioenergy, concurrently yielding nutrient-rich digestate suitable for irrigation. However, the direct application of digestate poses environmental and health risks, including the discharge of contaminants of emerging concerns (CECs) (Yang et al., 2022a). Currently, due to the absence of a cost-effective technology, turning digestate into an environmentally friendly biofertilizer is not an option in many countries. Consequently, the primary alternatives are the direct application of untreated digestate, carrying CECs, or its disposal in landfills, which may not be an ideal solution from an environmental perspective.

Ozone-based AOPs has proven efficacy in removing CECs from water sources, ranging from laboratory to full-scale applications. However, its application for digestate treatment is yet to be addressed. There are challenges associated with its application in high-strength water matrix such as digestate that can affect the ozone efficiency. The significant organic load present in digestate competes for oxidant exposure, thereby increasing the ozone demand for CECs removal during ozonation. Moreover, this organic load can hinder the penetration of UV light in hybrid ozone systems like UVOX Redox, thereby limiting the generation of other reactive oxidative species. Ammonia in digestate exerts both competitive effect in ozone reactions and scavenging effect in radical reactions, with the latter stemming from concurrent nitrification processes. Additionally, carbonate species, traditionally regarded as a scavenger in ozonation, is often overlooked in scenarios where the direct mechanism of molecular ozone is predominant. High alkalinity in digestate, though not directly reactive with molecular ozone, could influence the direct reaction of ozone with other matrix components by creating a buffering capacity that maintains pH.

Besides the potential effect of digestate matrix, the energy consumption in treating digestate with ozonation might be another challenge. Despite offering the lowest E_{EO} among AOPs, ozone generation is still an energy-intensive method. Comprehensive understanding of the ozonation process within distinct water matrices is crucial for predicting ozone consumption and assessing the cost-effectiveness of this process. An ideal solution entails the development of a simple model tailored to predict CECs removal, capturing the unique characteristics of digestate. Existing models primarily describe ozonation in low-strength water matrices such as pure water and drinking water. The main shortcoming of the current models that makes it not applicable for digestate matrix, is the

absence of ammonia in ozone decomposition and consumption rate; along with the overlooking of the effect of alkalinity in scenarios dominated by the direct mechanism of molecular ozone. Furthermore, the CECs prediction models often rely on the parameters such as R_{CT}, necessitating experimental work to determine this parameter prior to predicting the CECs removal.

Considering the aforementioned challenges and the significant cost and energy demands associated with ozone generation, an evaluation of ozone performance and efficiency becomes essential before advocating this technology as a potential post-AD treatment for CECs removal from digestate. This evaluation involves determining the ozone dose required for CECs removal from liquid digestate, assessing the influence of the digestate matrix on CECs removal, and developing a prediction model for the ozonation process in liquid digestate.

1.8 RESEARCH OBJECTIVES

The primary objective of this thesis is to evaluate ozone-based AOPs as a potential post-AD solution for removing contaminants of emerging concern (CECs) from digestate before discharge or land application. This aims to enhance the management and reuse of liquid digestate in line with circular bioeconomy principles. Accordingly, the following are the main research objectives:

1. Assess the effect of the digestate matrix on the kinetic rate removal of CECs from digestate and quantify the required ozone dose for CECs removal.

2. Develop a mathematical model to describe the main reactions involved in digestate ozonation, considering the simultaneous presence of ammonia, alkalinity, and organic matter, and predict the ozone consumption yield by each component.

3. Develop a mathematical model to predict CECs removal in various water matrices regardless of the R_{CT} value.

4. Assess the efficacy of a hybrid ozone/UV pilot (UVOX Redox®) in removing CECs from digestate across different AD plants

1.9 RESEARCH APPROACH

This thesis is structured into six chapters as illustrated in Figure 1.4. Chapter 1 provides an overview about the current practices in digestate handling, compares various methods for CECs removal in other water matrices, and identifies the research gaps and the potential challenges of application of these methods for digestate treatment. In chapter 2, the overall feasibility of O_3-based AOPs for CECs removal from digestate is evaluated.

In this chapter, the general effect of digestate matrix on increasing required ozone dose is discussed. Chapter 3 introduces a mathematical model designed to elucidate the ozonation process within digestate. Key components governing digestate ozonation are discussed, providing the foundation for a comprehensive understanding of digestate ozonation prior to CECs removal prediction. Moving forward to Chapter 4, the model is further developed to predict the removal of CECs from digestate. In Chapter 5, the investigation extends to the application of O_3-based AOPs both independently and in conjunction with an activation method. This pilot-scale study explores the efficacy of these approaches in removing CECs from digestate in two distinct AD plants. Chapter 6 summarizes the key findings of the previous chapters and provides research gap and outlook for future research.
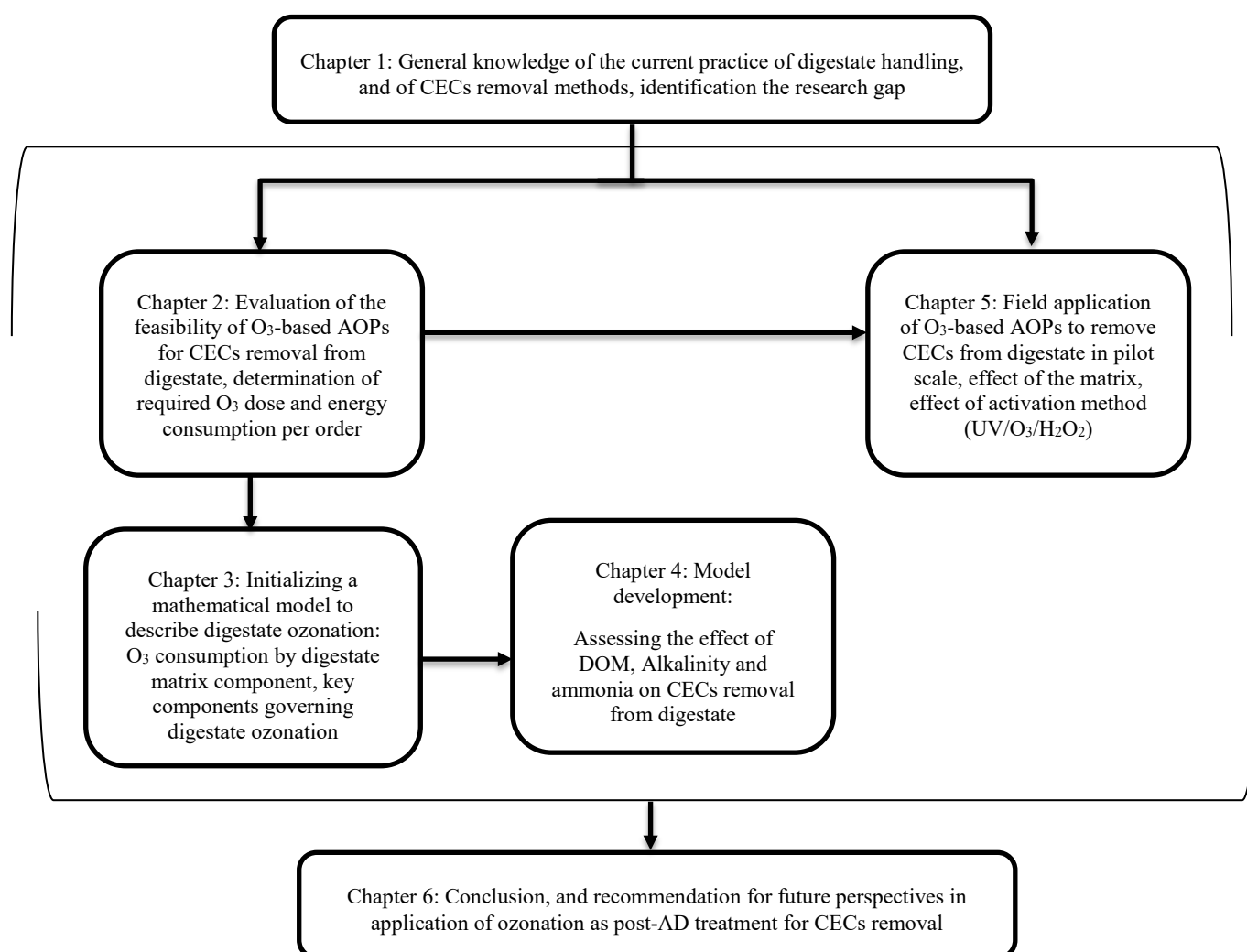
Figure 1.4. Structure of the thesis and link between the chapters

1.10 ANNEX

Annex 1.9.1. Occurrence of CECs in treatment plant effluent and sludge

Table A1.1 Occurrence of the most prescribed pharmaceutical and endocrine disruptive compounds in WWTPs in various countries

Country	Water type	Compound	Class/ family	Concentration (ng/L)	Ref.
Iran-Bushehr-	Septic Tank effluent	Tetracycline, Fluoroquinolones, Macrolides Amoxicillin	Antibiotics	149.63	Kafaei et al. (2018)
	Activated sludge effluent			13.49-198.47	
	Stabilization pond effluent			6.55-16.37	
Greece	Wastewater	B-Lactams	Antibiotics	1243	Kosma et al. (2014)
USA	WWTP (secondary treatment effluent)	Sulfamethoxazole	Antibiotics	3800	Kwon and Rodriguez (2014)
Spain	WWTP (tertiary treatment effluent)	Fluoroquinolones	Antibiotics	341	Cabeza et al. (2012)

Germany	Treated wastewater	Macrolides Sulphonamides	Antibiotics	6000 2000	Hirsch et al. (1999)
Canada	Activated sludge effluent	Macrolides Macrolides Sulphonamides	Antibiotics	7000 270	Guerra et al. (2014)
Algeria	WWTP (treated wastewater)	Ibuprofen, Naproxen, Diclofenac	NSAIDs	155.5–6554	Kermia et al. (2016)
India	WWTP (treated wastewater)	Ibuprofen, Naproxen, Diclofenac	NSAIDs	22000-17000	Thalla and Vannarath (2020)
Iran-Tehran	WWTP (treated wastewater)	Ibuprofen, Naproxen, Diclofenac	NSAIDs	230-1050	Eslami et al. (2015)
Korea	WWTP (treated wastewater)	Ibuprofen, Naproxen, Diclofenac	NSAIDs	7560-19200	Sim et al. (2011)
Iran-Ahwaz	WWTP (treated wastewater)	17β-Estradiol	Endocrine disruptive	57.46-70.60	Hassani et al. (2016)
Iran-Ahwaz	WWTP (treated wastewater)	17β-Estradiol	Endocrine disruptive	57.46–70.6	Hassani et al. (2016)
US-Illinois	WWTP (treated wastewater)	17β-Estradiol	Endocrine disruptive	25.3	Heffron et al. (2016)

Canada - Quebec	WWTP (treated wastewater)	Bisphenol A	Endocrine disruptive	410 (mean)	Mohapatra et al. (2011)
Romania	WWTP (treated wastewater)	Bisphenol A	Endocrine disruptive	75 (max)	Chiriac et al. (2021)
Slovenia	Food processing treated wastewater	Bisphenol A	Endocrine disruptive	3030	Česen et al. (2018)

Table A1.2. Occurrence of the most prescribed pharmaceutical and endocrine disruptive compounds in sludge in selected countries

Country	Matrix	Compound	Class/ family	Concentration (µg/kg DM[1])	Ref.
Morocco	WWTP-primary sludge	Fluoroquinolone	Antibiotics	4.21 and 2.92	Khadra et al. (2019)
USA	Manure-sawdust digestate sludge	Tetracycline	Antibiotics	115000	Arikan et al. (2007)
China	Manure digestate sludge	Tetracycline	Antibiotics	60000	Hu et al. (2011)
China	Primary sludge	Fluoroquinolone	Antibiotics	3064 6037 3074	Zhang and Li (2018)

Taiwan	Sewage sludge	Sulphonamide	Antibiotics	5900 9400 5200	Yang et al. (2016)
Asian countries (average amount)	Raw sludge	Fluoroquinolone Tetracycline Macrolide Sulphonamide	Antibiotics	1000 10 10 10	Ezzariai et al. (2018)
Sweden	WWTP-dried sludge	Ibuprofen, Naproxen, Diclofenac	NSAIDs	39-138	Sagristà et al. (2010)
Spain	Primary sludge Secondary sludge Digested AD sludge	Ibuprofen	NSAIDs	2988 1898 1020	Martín et al. (2012)
Pakistan	WWTP-sludge	Ibuprofen, Naproxen, Diclofenac	NSAIDs	6046-7273	Ashfaq et al. (2017)
Spain	WWTP-primary sludge WWTP-secondary sludge Digestate sludge	Ibuprofen	NSAIDs	1584 2206 1274	Martín et al. (2012)
China	WWTP-sludge	17β-Estradiol	Endocrine disruptive	1-8	Shi et al. (2013)

Spain	WWTP-primary sludge	17β-Estradiol	Endocrine disruptive	25	Martín et al. (2012)
	WWTP-secondary sludge			38	
	Digestate sludge			836	
Paris	WWTP-secondary sludge	17β-Estradiol	Endocrine disruptive	18-20	Muller et al. (2010)
Germany	WWTP-secondary sludge	17β-Estradiol	Endocrine disruptive	5-490	Ternes et al. (1999)
Canada-Quebec	Primary sludge, Secondary sludge	Bisphenol A	Endocrine disruptive	360000,240000	Mohapatra et al. (2011)
Spain	WWTP-treated sludge	Bisphenol A	Endocrine disruptive	579-658	Abril et al. (2020)
Germany	WWTP-treated sludge	Bisphenol A	Endocrine disruptive	4-1363	Fernández et al. (1996)
UK	Digestate sludge	Bisphenol A	Endocrine disruptive	4600-38700	Petrie et al. (2019)

2

REMOVAL OF CONTAMINANTS OF EMERGING CONCERN FROM DIGESTATE SUPERNATANT

In this chapter, the feasibility to remove different CECs from digestate using O_3 and O_3/H_2O_2 was assessed, and the general effect of the matrix in the oxidation was explained. While the lab-scale ozonation provided an ozone dose of 1.49 mg O_3/mg DOC in 5h treatment, almost all the compounds were removed at a lower ozone dose of maximum 0.48 mg O_3/mg DOC; only ibuprofen required a higher dose of 1.1 mg O_3/mg DOC to be oxidized. The digestate matrix slowed down the kinetic ozonation rate to approximately 1% compared to the removal rate in demineralized water. The combined treatment (O_3/H_2O_2) showed the additional contribution of H_2O_2 by decreasing the ozone demand by 59 to 75% for all the compounds. The acute toxicity of the digestate, measured by the inhibition of *Vibrio fisheries* luminescence, decreased by 18.1 % during 5h ozonation, and by 34% during 5h O_3/H_2O_2 treatment. Despite the high ozone consumption, the ozone dose (mg O_3/mg DOC) required to remove all CECs from digestate supernatant was in the range or lower than what has been reported for other (waste-)water matrix, implying that ozonation can be considered as a potential post-AD treatment to produce cleaner stream for agricultural purposes.

2.1 INTRODUCTION

Anaerobic digestion (AD) plants, acting as circular bioeconomic hubs, can recover valuable renewable energy and nutrients from multiple organic waste streams. The AD biological process converts solid organic waste to biogas. The remaining sludge (digestate) is further dewatered and the digestate supernatant, due to its high content of nitrogen and phosphorus, can be used as irrigation water (Wang and Lee, 2021). However, the potential presence of contaminants of emerging concern (CECs), could hinder the utilization of digestate supernatant in the agricultural field (Edith et al., 2019; Gurmessa et al., 2020; Minh et al., 2009). Despite the well-established agronomic benefits of digestate (Koszel and Lorencowicz, 2015; Šimon et al., 2015), various research indicated that AD processes do not significantly contribute to CECs removal (Gros et al., 2019; Widyasari-Mehta et al., 2016). The presence of pharmaceutical compounds such as antibiotics, non-steroidal anti-inflammatory drugs (NSAIDs), and also hormones, most of them exhibiting endocrine disrupting properties, have been reported in treated wastewater, sludge, and digestate in municipal/agro-industrial wastewater treatment plants (WWTPs) (Peng et al., 2006; Petrie et al., 2015). In the liquid digestate from several biogas plants, for example, antibiotics were detected in a wide range of concentrations, for instance 38.5 μg/L for oxytetracycline (Yang et al., 2022a), 120 μg/L for tetracycline (Kasumba et al., 2020) and 66,400 μg/L for chlortetracycline (Nurk et al., 2019). The endocrine disrupting effects on living organisms and the development of antibiotic-resistant bacteria (ARBs), among others, are examples of the ecological and hazardous impacts that they may have (Ouda et al., 2021). However, liquid digestate is currently applied to agricultural fields without any post-AD treatment for the removal of CECs. As such, an increasing attention must be put on their removal before the liquid digestate is applied to soils.

Ozone-based AOPs have been successfully applied to remove CECs from drinking water and as an advance treatment in WWTPs (Asghar et al., 2022; Bui et al., 2016; de Oliveira et al., 2020; Hansen et al., 2016; Qu et al., 2015). Ozone can oxidize most of the organic contaminants either by directly attacking electron-rich sites of the target compounds or by indirectly producing hydroxyl radicals (OH$^{\bullet}$) (Miklos et al., 2018) that will later oxidize the target compound. Wang et al. (2023) showed an increase in indirect mechanism and an enhance in micropollutant removal from biotreated landfill leachate by adding H_2O_2 to the ozonation treatment (Wang et al., 2023a). In another study, Lee et al. (2023) indicated that the combination of O_3/H_2O_2 in treating wastewater effluent improves the removal of ozone-resistance micropollutant, and prevents the formation of some toxic by-product including bromate (Lee et al., 2023).

Yet, the application of ozone-based AOPs to treat water samples with high load of organic matter such as digestate supernatant is rather limited. The possible challenges in treating digestate supernatant with ozonation in compare with the above-mentioned (waste-)water matrix may include both the high load of dissolved organic matter (DOM), as well as the

presence of carbonate species competing for the OH$^\bullet$ radicals (Asghar et al., 2022; Buffle et al., 2006b). In a study to track the matrix effects on the oxidation of pharmaceuticals during ozonation, it was observed that the removal of pharmaceutical varied in different water matrices. For instance, the residual concentration of phenacetin, at an initial concentration of 1μM and after dosing 1 mg/L of ozone was 0.71 μM for a wastewater sample with TOC of 13.2 mg/L, and 0.9 μM for a wastewater with TOC of 22.9 mg/L. The same pattern was observed for different ozone dose ranging between 0.5 to 5 mg/L. Thus, it was concluded that the higher the load of organic matter, the lower the amount of oxidant available for the target micropollutant; i.e., necessitating higher oxidant concentration for achieving the target removal efficiency (Javier Benitez et al., 2009). Cruz-Alcalde et al. (2020) showed a competitive effect exhibited by the organic matter on the micropollutant removal during ozonation of wastewater at different concentrations of organic matter. According to their study, the amount of ozone needed to remove refractory micropollutants from wastewater increased from 19 mg/L in the sample with DOC of 6.6 mg/L to 48 mg/L in the sample with DOC of 21.3 mg/L (Cruz-Alcalde et al., 2020).

Research Gap: Digestate supernatant is currently applied in agricultural field without further treatment for CECs removal. Adsorption, filtration, and AOPs are just a few of the technologies used to remove CECs. Nevertheless, AOPs are favoured since adsorption and filtering do not degrade CECs but rather transfer them from one phase to another. Regarding the AOPs, although ozonation is a potential technology for removing CECs, a review of the literature revealed a lack of data on its application to treat digestate supernatant. The most recent review papers show the effect of the organic matter on increasing the ozone demand in different wastewater matrix, yet the range of DOC in the studied wastewaters varied between 5 to 48 mg/L (Asghar et al., 2022). Treating the current digestate supernatant in this research with a DOC around 1200 mg/L can significantly increase the ozone dose required. The problem accelerates by considering the high load of carbonate species in digestate supernatant (1950 mg CaCO$_3$/L), that can scavenge the OH$^\bullet$ radicals, limiting the exposure of CECs to oxidants. Furthermore, the high load of ammonia in the digestate supernatant (700 mg/L) can stoichiometrically consume a substantial portion of ozone and produces nitrite and nitrate that have the potential to significantly scavenge the OH$^\bullet$ radicals (Lado Ribeiro et al., 2019). Having mentioned these challenges and considering the high cost and energy required for ozone generation, it is important to determine the ozone dose required for CECs removal from digestate supernatant before considering ozonation as a potential post-AD treatment to remove these compounds.

As such and with the main goal of contributing to improve the potential handling and reuse of the treated digestate supernatant, it is essential to assess how the physicochemical characteristics of the digestate (the water matrix) can affect or interfere with the removal of CECs. Therefore, this study aimed to assess (i) the removal of certain CECs present in

digestate supernatant, (ii) the specific ozone dose required to achieve a target removal of CECs, (iii) the potential effects of the digestate matrix on the removal of CECs, (iv) the comparison of the CECs removal performance when using O_3 versus O_3/H_2O_2, and (v) the toxicity removal of the digestate supernatant during O_3 and O_3/H_2O_2 oxidation.

Based on the type of the digestate, the most consumed veterinary antibiotics for food processing animals was chosen to assess in this study. Furthermore, NSAIDs and bisphenol A (a known endocrine disruptive compound) have been added to the selected list of compounds. This selection has been made considering their frequent occurrence in different types of sludge and their threat to the environment.

2.2 MATERIALS AND METHODS

2.2.1 Chemicals

Doxycycline hyclate (DOX), tetracycline (TCN), chlortetracycline hydrochloride (CTC), oxytetracycline (OTC), sulfamethoxazole (SMX), sulfamethazine (SMN), 17β-Estradiol (17-β-EST), ibuprofen (IBU), naproxen (NPX), bisphenol A (BPA), and diclofenac sodium (DIC) were purchased from Sigma Aldrich, Chemie GmbH, Germany. A stock solution of each compound was prepared in methanol (HPLC Grade) at a concentration of 4 g/L. Thereafter, to conduct each ozonation test, a working solution was prepared in demineralized water (DW) reaching a final concentration of 10 mg/L of each compound. Before each experiment, the working sample (prepared either in a DW matrix or in the digestate supernatant matrix) was spiked with the working solution reaching a concentration of 100 µg/L of each target compound.

2.2.2 Digestate collection and sample preparation

Grab samples of the digestate (20 L) were collected from the outflow valve of a digester in a biogas plant located in Kozani, Greece. The biogas plant with an annual energy generation of 854 MWh is situated near the town of Servia in Kozani. The feedstock of the plant is composed of animal faeces, urine and manure (including spoiled straw) and corn silage. Generally, the feedstock consists of 50 m^3 (tonnes) of pig waste and 2 tonnes of corn silage. The digester is operated at mesophilic condition, and the digestate is currently used in land application by local farmers who provide the corn silage feedstock. Prior to each experiment, the collected digestate was pasteurized at 70 °C for 3 h and separated using a centrifuge at 4800 rpm for 20 min followed by a series of sieves and vacuum filtration with 1.2 µm (GFC, Whatman), and 0.45 µm pore size filters (Whatman). Later, the maximum transferred ozone in the laboratory-scale ozone set-up was determined during set-up calibration, and since the ozone transferred was limited, the digestate supernatant was diluted to reach a dissolved organic carbon (DOC)

concentration of approximately 275 mg/L. With the applied dilution, it was possible to supply the ozone dose around 1 mg O_3/mg DOC, and track the removal process in the short-term experiment (5h). The working sample (Table 2.1) was spiked with CECs up to a final concentration of 100 µg/L of each compound. Prior to the experiments with digestate, no more chemicals including buffering compounds were added to the sample, and pH were tracked throughout the experiments. As for demineralized water, the initial pH was increased to 8.5 by adding NaOH (1M).

Table 2.1. Physicochemical characterization of the working sample

Parameter	Dimension	Value	std
COD	mg/L	987	11.8
DOC	mg/L	275	8.6
TN	mg TN-N/L	212	6
TKN	mg TKN-N/L	208	9.7
Ammonia	mg NH_4-N/L	172	7.1
Nitrite	mg NO_2-N/L	n.d*	-
Nitrate	mg NO_3-N/L	n.d	-
Alkalinity	mg $CaCO_3$/L	489	11.2
pH	-	8.5	-

* not detected

2.2.3 Set-up and ozone experiment

Ozone experiments were conducted using a bubble column reactor in a semi-continuous mode. The set-up consisted of an ozone generator with activated alumina air DSC dryer (Trailigaz LABO, France), a PVC reactor made of transparent acrylate with a 2.6 L (51.75 cm height and 8 cm inner diameter) capacity equipped with a humidifier (DH3b, BMT MESTECHNIK, Berlin, Germany), and a diffuser with 5 cm diameter, which was installed at the bottom of the reactor occupying 40% of the bottom area of the reactor (Figure 2.1). The off-gas was continuously captured by the humidifier and destructed in a catalytic ozone destruction equipment. Prior to the experiment, the gaseous ozone concentration in the inlet was adjusted to 20.5 ± 0.2 mg/L and kept constant throughout

the experiments. The inlet and off-gas ozone concentrations were monitored and recorded by an online sensor (Ozone analyser BMT 964, BMT MESTECHNIK GmbH, Stanhnsdorf, Germany). The flowrate of the air was set at 350 L/h, and the given pressure, current and voltage were 0.78 bar, 0.7 A, and 210 V (Power= 0.132 kW), respectively, to maintain a steady ozonated air flowrate of 51 ± 2 L/h throughout the experiments. The resulting ozone stream was introduced in the reactor via the coarse bubble diffuser located at the bottom of the reactor. The dissolved O_3 concentration in the liquid phase was monitored by an online sensor (Krypton KO_3 ozone in water analyzer, Dr. A. Kuntze GmbH Meerbusch, Germany); in addition, the ozone concentration was also monitored by taking regular samples and conducting the Indigo method (Bader and Hoigné, 1981). A minimum of 2.5 L of the sample (either with the DW matrix or with the digestate supernatant) was introduced into the reactor to minimize the headspace in the reactor, and the experiment was carried out in ambient temperature (20 °C). To assess the kinetic of the oxidation process, samples were withdrawn at different contact times (0, 0.25, 0.5, 0.75, 1, and after 5 h); after the samples were taken, the residual oxidant was quenched using $Na_2S_2O_3$ (at a final concentration of 80 mg/L), and kept refrigerated at -18 °C before the analyses.
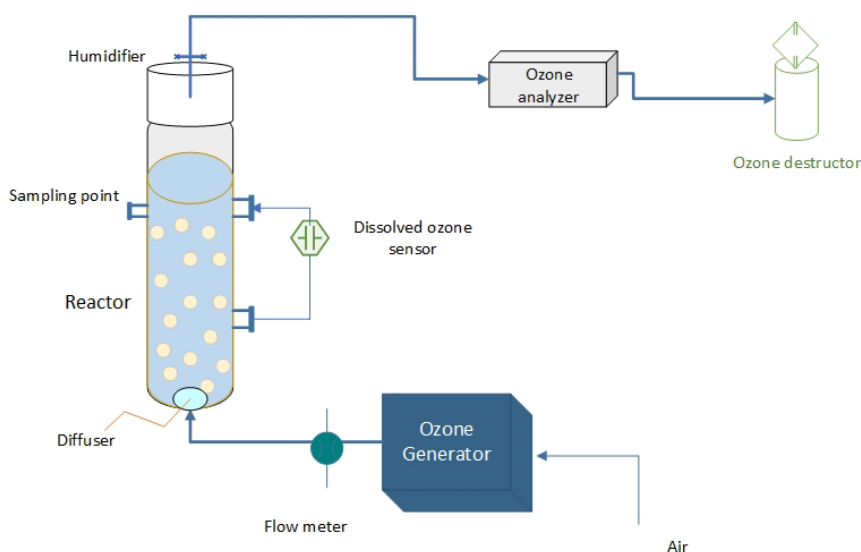
Figure 2.1. Schematic of ozone set-up

2.2.4 Ozone mass balance and data treatment

To evaluate the ozone mass balance and ozone mass transfer, three parameters including the Applied Ozone Dose (AOD), the Transferred Ozone Dose (TOD), and the Utilized Ozone Dose (UOD), were determined using Equation (2.1) to Equation (2.3).

$$AOD \left(\frac{mg\ O_3}{h}\right) = Q_g \left(\frac{L}{h}\right) \cdot C_{O3-g-in}(\frac{mg}{L}) \qquad (2.1)$$

$$TOD \left(\frac{mg\ O_3}{h}\right) = Q_g \left(\frac{L}{h}\right) \cdot \left(C_{O3-g-in} \left(\frac{mg}{L}\right) - C_{O3-g-out} \left(\frac{mg}{L}\right)\right) \qquad (2.2)$$

$$UOD \left(\frac{mg\ O_3}{h}\right) = TOD - \left(\left(C_{O3-l}\left(\frac{mg}{L}\right) \cdot V_l(L)\right)/t(h)\right) \qquad (2.3)$$

Where, *AOD* represents the applied ozone mass into the reactor in a fraction of time, Q_g is the flow rate of the ozonated gas, $C_{O3-g-in}$ is the ozone concentration in the gas phase entering the reactor recorded by the online sensor. *TOD* is the cumulative transferred ozone dose into the liquid in a fraction of time, $C_{O3-g-out}$ is the concentration of the ozone in the off-gas recorded by the online sensor before the off-gas goes to the ozone destructor, *UOD* is the utilized (consumed) ozone mass in the reactions, C_{O3-L} is the dissolved ozone concentration that is recorded by online liquid sensor, and V_L is the volume of the liquid in the reactor.

To compare the CECs removal efficiency from the digestate with the CECs removal efficiency from other (waste-)water matrices, the O_3 dose required for at least 90% removal of the target compounds was determined as per Equation (2.4) and Equation (2.5) (Antoniou et al., 2013). By dividing the O_3 dose per the initial DOC of each sample, the obtained specific ozone dose (mg O_3/mg DOC) can be compared across different (waste-)water samples.

$$\log \frac{C}{C_0} = -\frac{DO_3}{DDO_3} \leftrightarrow C = C_0 \times 10^{-\frac{DO_3}{DDO_3}} \qquad (2.4)$$

Where,

$$DO_3 = \frac{UOD}{V_l} \qquad (2.5)$$

25

Equation (2.4) describes the ratio of each compound to its initial concentration (C and C_0) after certain O_3 concentration (DO_3) was consumed during the ozonation time. By data fitting to Equation (2.4), DDO_3 was determined for each compound. DDO_3 is the decadic ozone dose required for 90% removal of each compound, and it is a compound specific parameter in each water matrix which is independent of CECs concentration and depends on the ozone decomposition in each water matrix (Hansen et al., 2016).

For the specific DDO_3, the DDO_3 obtained from Equation (2.4) was divided by the initial DOC. This dimensionless term specifies the O_3-degradability of the compounds as follows: if $\frac{DDO_3}{DOC} < 0.7$ then the compound is easily degradable, if $0.7 < \frac{DDO_3}{DOC} < 1.4$ then the compound is moderately degradable, and if $\frac{DDO_3}{DOC} > 1.4$ then the compounds is O_3-recalcitrant (Antoniou et al., 2013; Hansen et al., 2010; Hansen et al., 2016).

Furthermore, since AOPs are electric-energy-intensive (Miklos et al., 2018), for economic purposes, it is crucial to assess the operational energy consumption (Yang et al., 2021a). The treatment efficiency was evaluated using electrical energy per order (E_{EO}) recommended by IUPAC and described by Bolton et al. (2001). E_{EO} (kWh/m^3) is defined as the electrical energy consumption to remove the contaminant by one order of magnitude (90%) in 1 m^3 of water (Equation (2.6)).

$$E_{EO} = \frac{1000 \times W \times t}{V \times log\left(\frac{C_0}{C_t}\right)} \qquad (2.6)$$

Where, W is the power of the system (kW), t is the treatment time (h), V is the volume of the water (L), C_0 and C_t are the concentration (mg/L) of the target contaminant at time 0 and time t, respectively.

2.2.5 Analytical methods

The following equipment and methods were applied for the analytical determination of the parameters of interest: ammonia (NH_4-N) based on Standard Methods (NEN 6742) (APHA, 1992) using a spectrophotometer (Perkin Elmer, UV-Vis Lambda 365, the Netherlands), Total Kjeldahl Nitrogen (TKN) by a TKN apparatus equipped with a Kjeldtherm digester (Gerhardt, Germany) and a distiller (Gerhardt, Vapodest, Germany), and the dissolved organic nitrogen (DON-N) by deducting the concentration of the background ammonia from TKN. Total dissolved nitrogen (TN) and dissolved organic carbon (DOC) were measured by TOC analyser (Shimadzu, the Netherlands), alkalinity (mg CaCO$_3$/L) was measured by automatic titration (Metrohm, 848 Titriano plus, Applicon, the Netherlands), and NO_3-N was measured by ion chromatography (ICS-1000, Dionex, the Netherlands).

The CECs analysis was subcontracted to Laboratorios Tecnológicos de Levante, Valencia, Spain (Certificate nº 121/LE1782) where the following methods were applied: For BPA, the internal standard Bisphenol A D16 was added to the 10 times diluted sample, and the derivatization was done in basic medium (pH>9 with NaOH) with acetic anhydride. The analytes were extracted using the SBSE (twister) technique (12 h, 1500 rpm). The twister was collected and analysed by thermal desorption in GC-QQQ (GC chromatograph, Agilent 7890) equipped with Triple Quadrupole Mass Spectrometer (QQQ Agilent 7000C), with MPS Autosampler Gerstel, using a Sapiens Column 5-MS (30 m 0.25 mm 0.25 um), with the flow of 1.2 mL/min. The sample linear range was between 0.1 to 10 µg/L with detection limit of 0.1 µg/L.

For antibiotics, the sample was stirred and filtered by filter of 13 mm PTFE Hydrophilic, 0.45 um Teknokroma (Ref TR-F1-0021). The filtrate was collected in vial and analysed by direct injection into high-performance liquid chromatography (Agilent HPLC Agilent 1260), equipped with triple quadrupole-mass spectrometer (Agilent QQQ Agilent 6460). The applied column was Eclipse plus C18 (2.1 × 100 mm, 1.8 um) with mobile Phase A: Water 0.1% formic acid, and mobile Phase B: acetonitrile 0.1% formic acid with the flow of 0.3 mL/min. The linear range for CIP, ERY, SMX and SMN was between 0.1 to 100 ppb, and for TCN, CTC, DOX, and OTC between 0.5 to 500 ppb with detection limit of 0.5 µg/L.

For NSAIDs and hormone, the sample was stirred and filtered by filter of 13 mm PTFE Hydrophilic, 0.45 um Teknokroma (Ref TR-F1-0021), and the filtrate was collected in vial and analysed by direct injection into the same HPLC-QQQ but equipped with Poroshell 120 Phenyl-Hexyl column (3.0 × 100 mm, 2.7 mm) with mobile phase A: Water 0.1 mM ammonium fluoride, mobile phase B: methanol 0.1 mM ammonium fluoride with the flow of 0.4 mL/min. The linear range for 17-β-EST, DIC, NPX and IBU was between 0.1 to 100 ppb with detection limit of 0.1 µg/L. All the target CECs were detected with analysis recovery between 86-110%.

2.2.6 Kinetic studies

Previous studies have applied the chemical kinetic method based on Equation (2.7) to predict the removal of a variety of CECs during O_3 treatment (Gomes et al., 2017).

$$-\frac{dC}{dt} = k_{O3}[O_3][C] + k_{OH\cdot}[OH\cdot][C] \qquad (2.7)$$

Where, C is the concentration (M) of the target compounds and k_{O3} and $k_{OH\cdot}$ are the apparent rate constant of the reaction of each compound with ozone, and OH$\cdot$, respectively. Since OH$\cdot$ is produced from the ozone decomposition in the liquid, its

concentration is proportional to the concentration of O_3, thus, the simplified and integrated form of Equation (2.7) can be shown as Equation (2.8) for comparison purposes

$$-ln\frac{C_t}{C_0} = k_{obs} \int_0^t O_3 dt \qquad\qquad (2.8)$$

Where, k_{obs} is $k_{O3}+R_{CT}\, k_{OH.}$ and R_{CT} is $\int_0^t C_{OH}.dt/ \int_0^t O_3\, dt$ (He et al., 2022).

$\int_0^t O_3 dt$ was determined by integrating DO_3 in Equation (2.5) to the ozonation time, and k_{obs} was calculated by fitting the data to Equation (2.8).

2.2.7 MicroTox® test

MicroTox® test with *Vibrio fisheries* is a highly sensitive, reproducible, and internationally accepted method which has been standardized as ISO (2007) for measuring toxicity (Libralato et al., 2010). The test is based on the luminescence light emission of the marine organism *Vibrio fisheries*. The osmotic adjustment solution, diluent, and solo reagent shot vials containing the organism were purchased from MicroLAN b.v. (the Netherlands). The organism was exposed to the untreated and treated samples and the acute toxicity assay was carried out by measuring the inhibition of the light emission after 5, 15 and 30 min exposure time via Toxicity-meter (MicroTox M500, SDI, MicroLAN, the Netherlands).

2.2.8 Research approach

In this study, digestate supernatant was treated with O_3 and O_3/H_2O_2 in a continuous ozonation bubble column reactor. To determine the ozone dose required for removal of the target CECs, kinetic rate, effect of the matrix, effect of the chain initiator (H_2O_2), and toxicity, five experiments were conducted (Table 2.2).

Table 2.2. Outline of the Experiments

Experiment	Sample	Treatment	O_3 Mass balance	CECs analysis	Toxicity (*Vibrio fisheries*)	Objective
Exp. 1	Demineralized water spiked with CECs	O_3	+	+	-	Comparing CECs removal

Exp. 2	Digestate supernatant spiked with CECs	O_3	+	+	+	from DW and digestate to assess the effect of the matrix
Exp. 3	Digestate supernatant	$O_3 +$ different ratio of H_2O_2:O_3	+	-	-	Optimization the ratio of H_2O_2/O_3
Exp. 4	Demineralized water spiked with CECs	O_3/H_2O_2	+	+	-	Comparing Exp.4 and Exp.5 for the effect of the matrix, Comparing Exp. 2 and Exp. 5 for the effect of H_2O_2
Exp. 5	Digestate supernatant spiked with CECs	O_3/H_2O_2	+	+	+	

To achieve the objectives of this study, the ozonation of the CECs in DW was conducted to obtain the removal rate of the target compound without the effect of interferences such as organic matter (Exp. 1). Then, under the same operational condition, the ozonation was conducted to treat digestate supernatant spiked by the same CECs (Exp. 2). By comparing the kinetic rate and ozone consumption in Exp. 1 and 2, it was possible to determinate the competition effect of the digestate matrix on the removal. Thereafter, the optimum dosage of H_2O_2 was determined in Exp. 3, and the experiments were repeated under the same operational condition by adding hydrogen peroxide to the reactor to treat demineralized water spiked with CECs (Exp. 4) and digestate supernatant spiked with CECs (Exp. 5), and the potential effect of hydrogen peroxide on the removal of the CECs was assessed. During digestate supernatant treatment in Exp. 2 and 5, the changes in the matrix component such as alkalinity, DOC and organic/inorganic nitrogen was determined to study the potential competition of the matrix component on ozone consumption. At the end, the toxicity of the treated and untreated digestate in Exp. 2 and Exp. 5 was determined using the Microtox® test.

2.3 RESULTS AND DISCUSSION

2.3.1 Ozone mass balance and mass transfer in demineralized water and digestate

The O_3 profile in the gas and liquid phase as a function of treatment time and the ozone mass balance during ozone treatment for demineralized water (Exp. 1) and digestate supernatant (Exp. 2) is depicted in Figure 2.2. The same profile for O_3/H_2O_2 treatment applying for demineralized water (Exp. 4) and digestate supernatant (Exp. 5) is shown in Figure 2.3. The dissolved O_3 was observed only in the DW treated by O_3, but for the digestate it remained zero throughout the entire treatment.

b   —— AOD   ------ TOD

    ✳ UOD   ------ Transfer yield

c   —— · O$_3$- inlet (gas)

    - - -   O$_3$- outlet (gas)

    ●   O$_3$- disloved (liquid)

d —— AOD   ---- TOD
× UOD   ---- Transfer yield
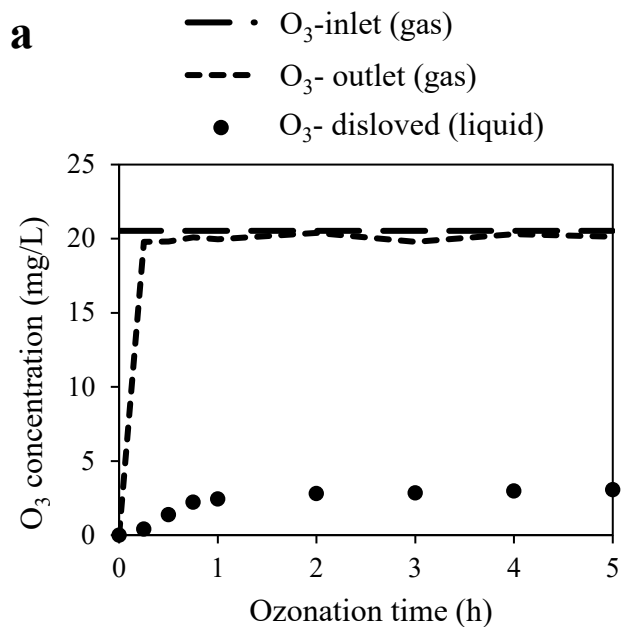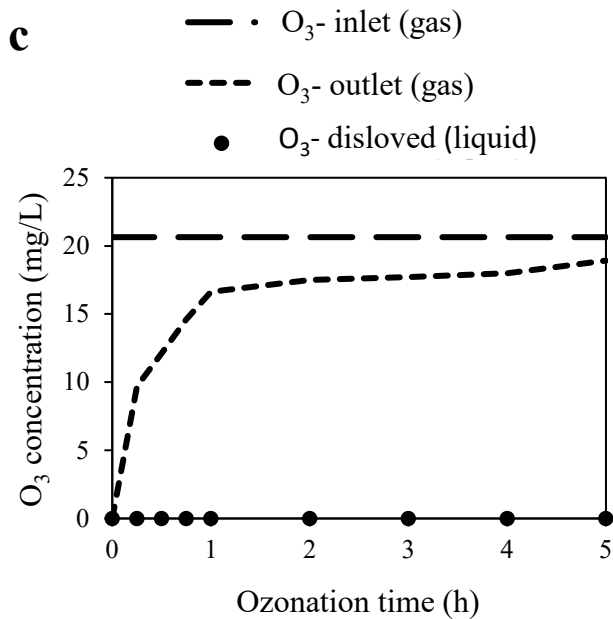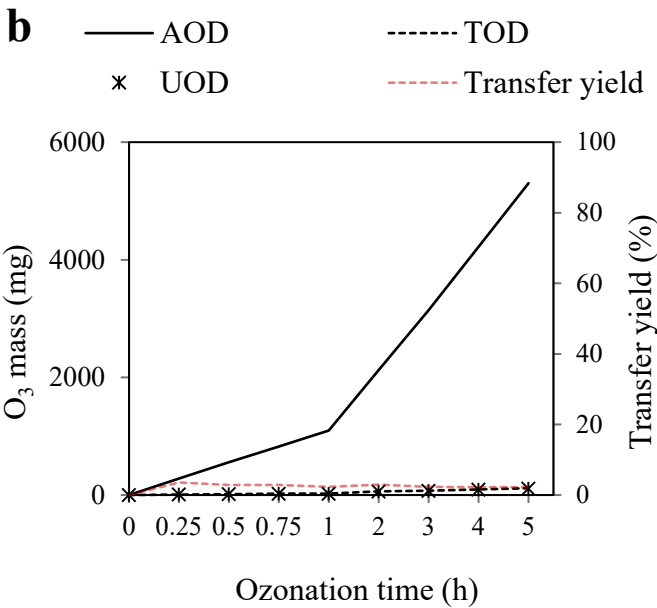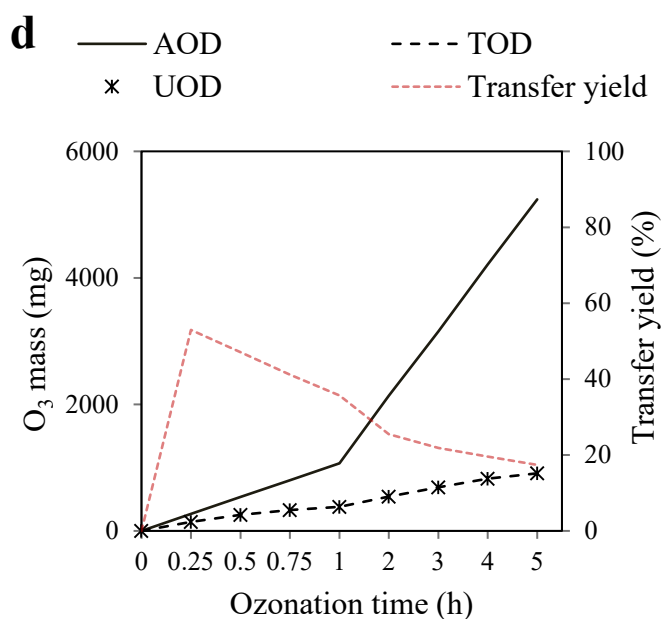
Figure 2.2. Gaseous and liquid O₃ profile, mass balance and mass transfer during 5h O₃ treatment; (a) O₃ profile in DW spiked with contaminants of emerging concern (Exp. 1), (b) mass balance in DW spiked with contaminants of emerging concern, (c) O₃ profile in digestate spiked with contaminants of emerging concern (Exp. 2), and (d) mass balance in digestate spiked with contaminants of emerging concern. (Initial ozone concentration: 20.5 ± 0.2 mg/L, ozone flow rate: 51±2 L/h, Sample volume: 2.6 L)

a —— O₃- inlet (gas)
---- O₃- outlet (gas)
● O₃- disloved (liquid)

b

c
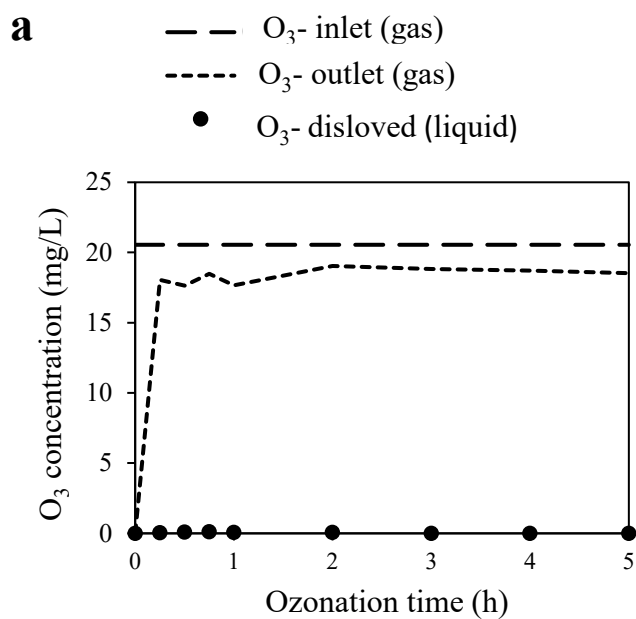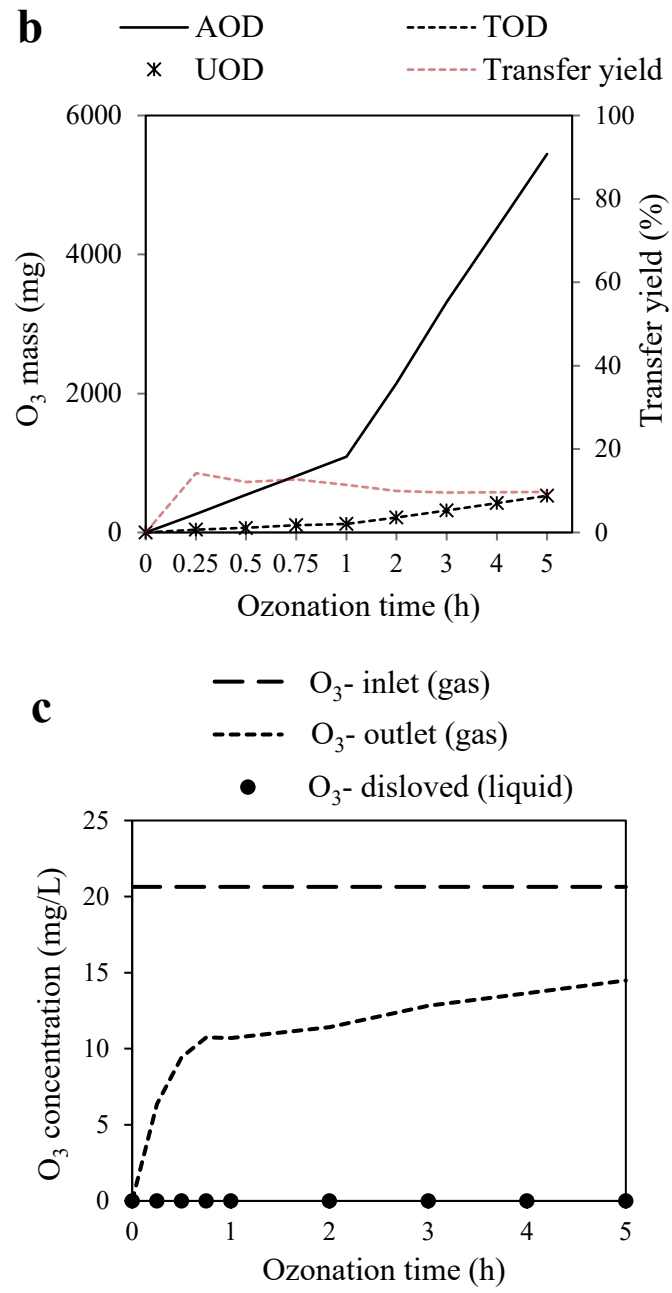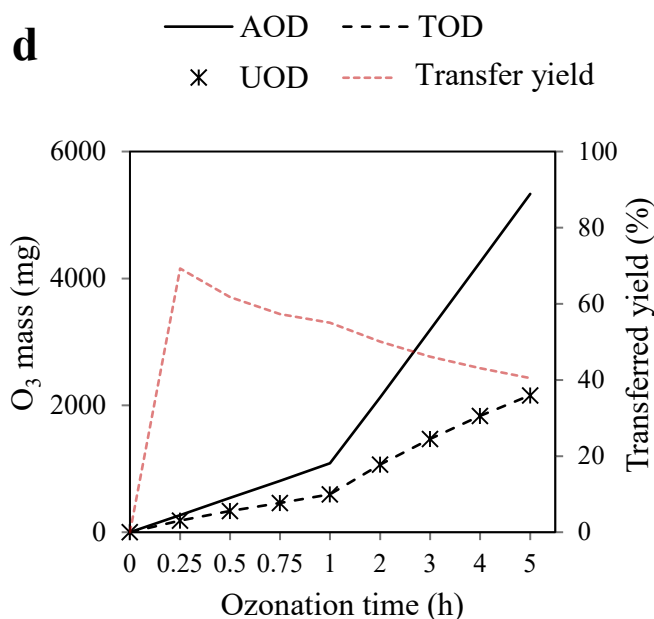
Figure 2.3. Gaseous and liquid O₃ profile, mass balance and mass transfer during 5h O₃/H₂O₂ treatment; (a) O₃ profile in DW spiked with contaminants of emerging concern (Exp. 4), (b) mass balance in DW spiked with contaminants of emerging concern, (c) O₃ profile in digestate spiked with contaminants of emerging concern (Exp.5), and (d) mass balance in digestate spiked with contaminants of emerging concern. (Initial ozone concentration: 20.5 ± 0.2 mg/L, ozone flow rate: 51 ± 2 L/h, Sample volume: 2.6 L)

While treating DW (Exp. 1), since no other chemicals besides CECs was in the sample, the dissolved O₃ was detectable before 15 minutes (Figure 2.2.a). In the rest of the experiments (Exp. 2, 4 and 5) however, the dissolved O₃ remained zero or was negligible during the 5h ozonation, indicating that all the transferred ozone was consumed in ozone reaction with target compounds or organic material in general. Considering the negligible concentration of dissolved ozone, the ozone transfer yield (TOD/AOD) is the main parameter to characterize the behaviour of each water matrix (either DW or digestate) towards ozone and to show the reactivity of the matrix components. The transfer yield in Figure 2.2 and Figure 2.3 shows that; (i) a two-phase of ozonation can be identified in all the O₃ profiles in Figure 2.2 and Figure 2.3, with the first phase up to 15 min that the transfer yield increased, and the second phase after 15 min that the transfer yield gradually dropped until the end of the ozonation time; (ii) comparing Figure 2.2.b and Figure 2.2.d shows a higher transfer yield in digestate (53%) in 15 min, in compare to the maximum transfer yield in DW (3.5%) that implies more reactions of ozone in the digestate matrix due to the high load of organic and inorganic material competing for ozone consumption. The same trend can be observed by comparing Figure 2.3.b and Figure 2.3.d; (iii) the transfer yield in O₃/H₂O₂ treatment (Figure 2.3) is higher than in O₃ treatment (Figure 2.2)

both in DW (transfer yield: 14%) and digestate supernatant (transfer yield of 70%), which can be explained by more reaction of ozone with H_2O_2.

2.3.2 Removal of contaminants of emerging concern by O_3 and O_3/H_2O_2

Dividing the ozone consumption (DO_3) by the DOC content of digestate supernatant, the specific ozone dose was calculated, and the CECs removal as a function of the specific ozone dose was determined and shown in Figure 2.4 for both O_3 and O_3/H_2O_2 treatment. Applying O_3 and O_3/H_2O_2 treatment on DW with a DOC of 11.2 mg/L (Exp. 1 and Exp. 4), all the CECs except IBU were removed from DW in the first 15 min at a specific O_3 dose of 0.26 mg O_3/mg DOC by O_3 treatment, and in the first 5 min at a specific O_3 dose of 0.16 mg O_3/mg DOC by O_3/H_2O_2 (ratio of H_2O_2/O_3: 2.5) treatment (data not shown). Applying the same operational conditions like for DW, the complete removal of all the studied CECs from the digestate supernatant matrix occurred in a 45 min period at a specific ozone dose of 0.51 mg O_3/mg DOC (Exp. 2). IBU showed the lowest removal efficiency, requiring a 5h treatment with specific ozone dose of 1.11 mg O_3/mg DOC for 90% removal. Nevertheless, by adding hydrogen peroxide (Exp. 5), the removal efficiencies below the detection limits were observed in less than 15 min at specific ozone dose of 0.27 mg O_3/mg DOC. Also, for IBU, the removal efficiency increased, and 96% removal was achieved in 0.5h at specific O_3 dose of 0.51 mg O_3/mg DOC.
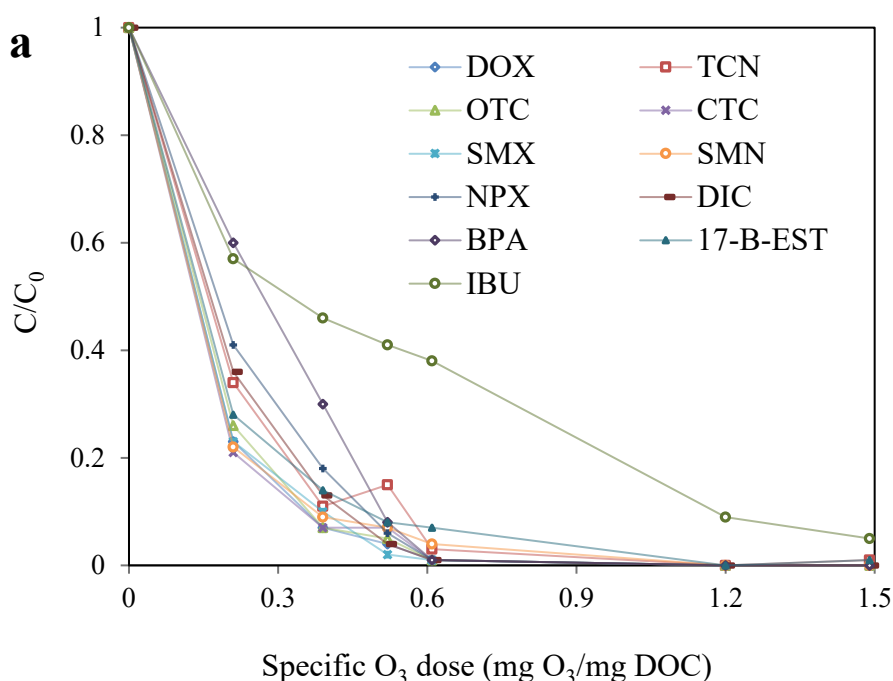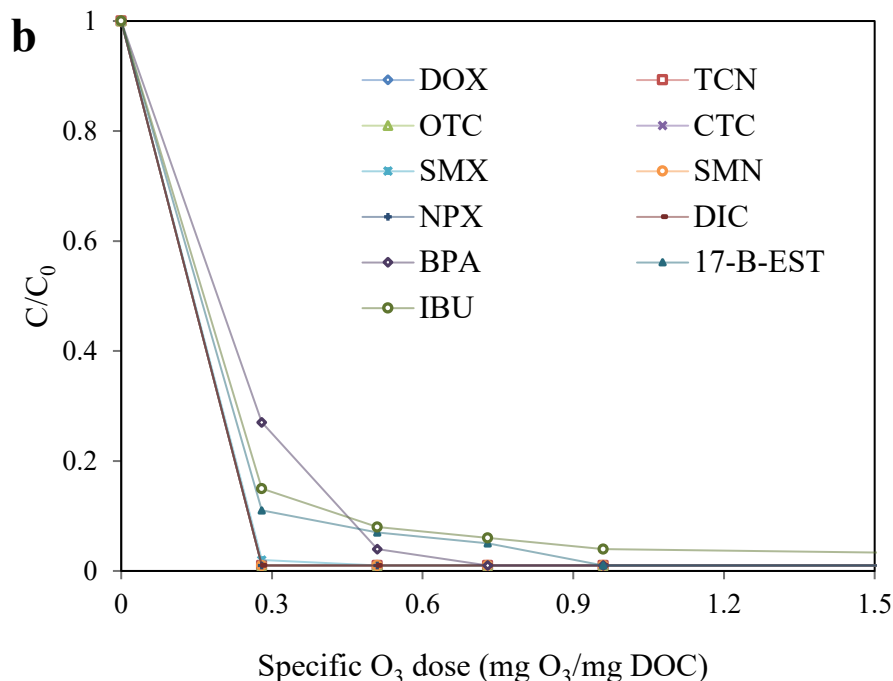
Figure 2.4. Removal of various contaminants of emerging concern from digestate supernatant in different specific ozone dose in (a) O_3 and (b), O_3/H_2O_2 treatment (H_2O_2/O_3: 2.5) (C_0 and C refers to the initial concentration of each compound and its concentration when a specific O_3 dose was applied within the 5h experiment)

To compare the CECs removal efficiency from digestate with other (waste-)water matrix in previous studies, the DDO_3 and specific DDO_3 for 90% removal was determined by fitting the data for each CECs to Equation (2.4). Furthermore, the E_{EO} to remove each compound was calculated by using Equation (2.6). As it can be observed in Table 2.3, the interference of the digestate component on the removal efficiency in ozone treatment significantly (p-value= 0.0002 <0.05) increased the specific ozone dose for all the compounds (e.g.; from 0.26 to 0.32 mg O_3/mg DOC for DOX, and from 0.52 to 1.11 mg O_3/mg DOC for IBU) compared to DW. Besides, the energy consumption to achieve the same removal in digestate increased (e.g.; from 7.9 to 18.5 kWh/m^3 for DOX, and from 57.3 to 132 kWh/m^3 for IBU). Adding H_2O_2 decreased the O_3 demand for the removal of the target compounds, for instance, for the most recalcitrant CECs in this study, IBU, the specific ozone dose for 90% removal, decreased to 0.46 mg O_3/mg DOC, which was 41.5% less than the ozone dose required in ozone treatment alone. The same trend was observed for all CECs where the specific ozone dose was significantly, with a p-value of 10^{-4} <0.05, lower than the one in ozone treatment.

Table 2.3. O_3 dose required for 90 % removal of the target compounds from digestate supernatant

O_3	DW				Digestate			
	DO_3 (mg/L)	DDO_3 (mg/L)	DDO_3/DOC (mg O_3/mg DOC)	E_{EO} (kWh/m³)	DO_3 (mg/L)	DDO_3 (mg/L)	DDO_3/DOC (mg O_3/mg DOC)	E_{EO} (kWh/m³)
DOX	3.56	3	0.26	7.9	106	89.6	0.32	18.5
TCN	3.56	3.7	0.32	7.9	106	110.7	0.4	27.5
OTC	3.56	3.2	0.28	5.3	106	93.8	0.34	18.5
CTC	3.56	3.1	0.27	14.3	106	92.1	0.35	18.5
SMX	3.56	3.5	0.31	5.3	106	105.4	0.38	26.4
SMN	3.56	3.5	0.31	4.8	106	103.1	0.37	25.2
NPX	3.56	2.8	0.25	4.8	142	112.9	0.41	31.7
DIC	3.56	2.5	0.22	4.8	142	98.1	0.35	29
BPA	3.56	3.3	0.29	4.8	142	132.6	0.48	36.1
17-β-EST	3.56	3.3	0.29	4.8	142	130.6	0.47	34.3
IBU	7.84	5.9	0.52	57.3	410	305.9	1.11	132

O_3/H_2O_2	DW				Digestate			
	DO_3 (mg/L)	DDO_3 (mg/L)	DDO_3/DOC (mg O_3/mg DOC)	E_{EO} (kWh/m³)	DO_3 (mg/L)	DDO_3 (mg/L)	DDO_3/DOC (mg O_3/mg DOC)	E_{EO} (kWh/m³)
DOX	1.86	1.6	0.11	2.1	76	29.2	0.11	13.2
TCN	1.86	1.9	0.13	2.1	76	33.5	0.12	13.2
OTC	1.86	1.6	0.11	2.1	76	29	0.11	13.2
CTC	1.86	1.6	0.11	3.2	76	30.6	0.11	13.2
SMX	1.86	1.9	0.13	2.1	76	39.3	0.14	15.8
SMN	1.86	1.8	0.12	2.1	76	33.5	0.12	13.2
NPX	1.86	1.5	0.10	2.1	76	24.5	0.09	13.2
DIC	1.86	1.3	0.09	2.1	76	23.2	0.08	13.2
BPA	1.86	1.7	0.12	3.7	76	58.2	0.21	18.5
17-β-EST	1.86	1.7	0.12	2.1	76	73.4	0.27	13.2
IBU	5.16	3.9	0.27	14.9	141	125	0.46	24.1

The specific DDO_3 can be applied to compare the oxidation of each compound in other water matrix (like drinking water or wastewater) (Buffle et al., 2006; Hansen et al., 2016), and to categorize the compounds as easily degradable, moderately degradable and

persistent (Antoniou et al., 2013). Based on the data obtained from Table 2.3, all the evaluated compounds are O_3-degradable except for IBU. Although no data is available for removing CECs from digestate supernatant, comparing the data in Table 2.3 to previous studies shows that in spite of the complex matrix of the digestate supernatant, the specific DDO_3 is comparable with previously reported data in the literature for wastewater, surface, and groundwater. Antoniou et al. (2013) reported a specific O_3 dose of 0.55 to 0.77 g O_3/g DOC for easily degradable compounds including diclofenac and sulfamethoxazole in secondary effluent wastewater (Antoniou et al., 2013). For the removal of the same compounds in an WWTP upgraded with post-ozonation, Hollender et al. (2009) reported a specific ozone dose of 0.47 g O_3/g DOC (Hollender et al., 2009). In the current study, the specific DDO_3 for diclofenac and sulfamethoxazole was 0.35 and 0.38 mg O_3/mg DOC, respectively. For more refractory compounds, such as ibuprofen a specific DDO_3 higher than 1 g O_3/g DOC for secondary effluent treatment was reported (Bahr et al., 2007). For ibuprofen removal from hospital wastewater, a specific ozone dose of 1.3 g O_3/g DOC (Hansen et al., 2016), and from secondary effluent 1.61 g O_3/g DOC (Antoniou et al., 2013) were also reported. In our study, ibuprofen was removed using a specific DDO_3 of 1.11 mg O_3/mg/DOC. The specific ozone dose for the removal of the target CECs in our study compared with other studies was either in the range or slightly lower although the digestate supernatant contains higher concentrations of organic matter rather than the previous studies (e.g. of between 5.2 and 18 mg DOC/L reported by Hansen et al. (2016), Antoniou et al. (2013), and Bahr et al. (2007)).

The E_{EO} value for 90% removal of CECs from DW was between 4.8 to 57.3 kWh/m^3 which was significantly lower (p-value=0.001 <0.05) than the E_{EO} in digestate (25.2 to 132 kWh/m^3). The higher E_{EO} in digestate shows the effect of the matrix component that most likely compete with the target compounds for ozone consumption. Adding H_2O_2 decreased the E_{EO} required to achieve the same removal (e.g. from 27.5 to 13.2 kWh/m^3 for TCN, and from 132 to 24.1 kWh/m^3 for IBU) due to the contribution of OH$^•$ radical that increases the CECs removal by more oxidation. Since E_{EO} value depends on various variables including the efficiency and power of ozone generator, water matrix, and pH among others, the reported E_{EO} in the literature varies widely by several order of magnitude (between 0.001 to 10 kWh/m^3 (Miklos et al., 2018)). For instance, an E_{EO} between 0.14-1.1 kWh/m^3 for removing 17-B-EST from biologically treated sewage was reported by Hansen et al. (2010). Pisarenko et al. (2012) reported an E_{EO} range between 0.022 kWh/m^3 for DIC to 0.393 kWh/m^3 for IBU in O_3 treatment of MBR-filtrate wastewater. In another study a range of 1.4 to 5.4 kWh/m^3 for removing the trace organic contaminants from water was reported (Yang et al., 2021a). The E_{EO} in the current study both in DW and digestate was higher in compare with reported values in the literature which could be explained by the mechanism of ozone generation as well as the matrix effect. The ozone generation mechanism in the current study was less efficient than the mentioned studies since the ozone was produced from air while in those studies the ozone was produced from pure oxygen. Furthermore, the higher organic matter content (e.g.

DOC of 275 mg/L in this study in compare with DOC of 6 mg/L for MBR-filtrate wastewater (Pisarenko et al., 2012)) increases the ozone dosage, necessitating a higher E_{EO} to achieve the same removal. However, although the E_{EO} value for digestate was higher than the one reported for other (waste)water in the literature, it is still less energy demanding in compare with other technologies applied for removing CECs for example photocatalysis with E_{EO} of 335 kWh/m^3 and ultrasound with E_{EO} of 2616 kWh/m^3 (Miklos et al., 2018). As such it has been reported that the AOPs with E_{EO} value between 1-100 kWh/m^3 might still provide solution for full-scale applicability (Miklos et al., 2018).

Nevertheless, the higher ozone consumption (DO$_3$ in Table 2.3) in digestate supernatant in compare with other water matrix including DW in this study, implies the inhibition of the digestate supernatant matrix that can affect the kinetic rate of the removal. By fitting the CECs concentration over the ozonation time to Equation (2.8), the observed reaction rate constant (k_{obs}) for each compound in DW and digestate supernatant in the presence and the absence of H$_2$O$_2$ was determined (Table 2.4).

Table 2.4. Kinetic removal rates of the target compound in demineralized water (DW) and in the digestate supernatant

Compounds	O$_3$		O$_3$/H$_2$O$_2$	
	k_{obs}_DW $(M^{-1}s^{-1})$	k_{obs}_digestate $(M^{-1}s^{-1})$	k_{obs}_DW $(M^{-1}s^{-1})$	k_{obs}_digestate $(M^{-1}s^{-1})$
Doxycycline	62.9	0.63	361.1	4.2
Tetracycline	59.4	0.52	341.5	3.6
Oxytetracycline	64.4	0.6	370	4.2
Chlortetracycline	31.7	0.6	182.2	4
Sulfamethoxazole	102.4	0.52	588.2	3.1
Sulfamethazine	103.5	0.53	594.2	3.6
Naproxen	106.2	0.34	598.4	5
Diclofenac	108.6	0.39	623.7	5.2
Ibuprofen	9.8	0.09	18.3	0.48
Bisphenol A	81.2	0.29	455.4	1.08
17-β-Estradiol	99.5	0.27	571.5	1.5

In ozone treatment, the observed kinetic rate in digestate supernatant was between 0.09 $M^{-1}s^{-1}$ ($R^2= 0.88$) for ibuprofen to 0.63 $M^{-1}s^{-1}$ ($R^2= 0.91$) for doxycycline, which is 1 % of the transformation rate obtained from the test in demineralized water. By adding H_2O_2, however, the rate increased; for instance, to 4.2 $M^{-1}s^{-1}$ ($R^2= 0.94$) for doxycycline and to 1.08 $M^{-1}s^{-1}$ ($R^2= 0.96$) for ibuprofen. The acceleration and improvement of CECs removal by adding H_2O_2 has been reported in previous studies (Katsoyiannis et al., 2011; Lado Ribeiro et al., 2019; Miao et al., 2015). Lin et al. (2009) reported that adding H_2O_2 at a H_2O_2/O_3 ratio of 5.0 resulted in complete removal of pharmaceuticals from wastewater in 5 min, while, by ozonation alone, the complete removal occurred in 20 min (Lin et al., 2009).

In contrast, in a study for ozonation of pharmaceuticals in hospital wastewater, no observed effect by adding H_2O_2 at a H_2O_2/O_3 ratio of 0.1 was reported (Hansen et al., 2016). The difference can be explained by the applied pH and H_2O_2 dose added to the system. First of all, the applied pH in our study was in the neutral to alkaline range which favours the decomposition of O_3 and generation of $OH^{\bullet}$. In contrast, with the applied pH in their study (5.0-6.25), the decomposition of O_3 is hampered, and the dominant removal mechanism for the target CECs is via the reaction with molecular O_3. The second reason is the higher ratio of H_2O_2 in our study compared to their study. Stoichiometrically, one molecule of H_2O_2 is needed for two molecules of O_3, while in their study the ratio of H_2O_2/O_3 was 0.1, which makes the H_2O_2 the limiting factor in $OH^{\bullet}$ generation reactions.

2.3.3 Potential effect of the molecular structure on CECs removal

The molecular structure of the compounds affects their reaction with ozone, removal efficiency and ozone demand. Ozone selectively reacts with the electron moieties of the compounds. For such reaction, a functional group in the target compound provides the electron dense moieties for electrophilic reaction of molecular ozone. The electron-rich functional group for the CECs of study includes tertiary amines and phenol group in DOX, TCN, OCT, CTC, secondary amine in SMX, secondary amines and aniline group in SMN, phenol group in BPA and 17-β-EST, and methoxy group in NPX. In contrast, IBU, composed of only one ring bound to a carboxyl group. The carboxyl group has the inhibitory effect on electrophilic substitution reaction because it acts as a withdrawal functional group and decreases the density of negative charge on the ring. The carboxylic group can be also seen in DIC structure on the phenolic ring, yet the ozone consumption for DIC removal and the reaction rate, categorizes this compound as a fast-degradable CECs. The oxidation of DIC is due to the secondary amine surrounded by the two rings and the electronegativity of the halogens (Cl^-) on one of the rings. Antoniou et al. (2013) has reported the same effect in the removal of poorly degradable compounds (including IBU), suggesting that the contribution of $OH^{\bullet}$ radicals can improve the removal rate of this compound (Antoniou et al., 2013). In a pilot study for removing pharmaceuticals

from municipal wastewater effluent via ozonation, Huber et al. (2005) also reported that the lack of an electron-rich functional group is the main reason of recalcitrance of IBU towards O_3 treatment, which supports the result of this study regarding the slow reaction of ibuprofen with ozone (Huber et al., 2005).

2.3.4 Transformation of the matrix components during ozonation of digestate supernatant

The slower removal kinetic rate and higher O_3 demand in the digestate supernatant in compare with DW suggests the potential inhibition/competition effect of the different component in the digestate supernatant. The inhibition effect of the matrix could be due to the O_3 consumption by the matrix components in the direct mechanism, or hampering the formation of $OH^{\bullet}$ radical and scavenging the generated $OH^{\bullet}$ in the indirect mechanism.

The removal of DOC as an indicator for organic matter mineralization turned to be 7% and 29% in O_3 and O_3/H_2O_2 treatment, respectively (data not shown). Despite the low mineralization, Figure 2.5 shows that 65% of the dissolved organic nitrogen (DON-N) was removed during ozonation of the digestate supernatant which suggests a fast reaction of O_3 with the nitrogen fraction present in the organic matter.
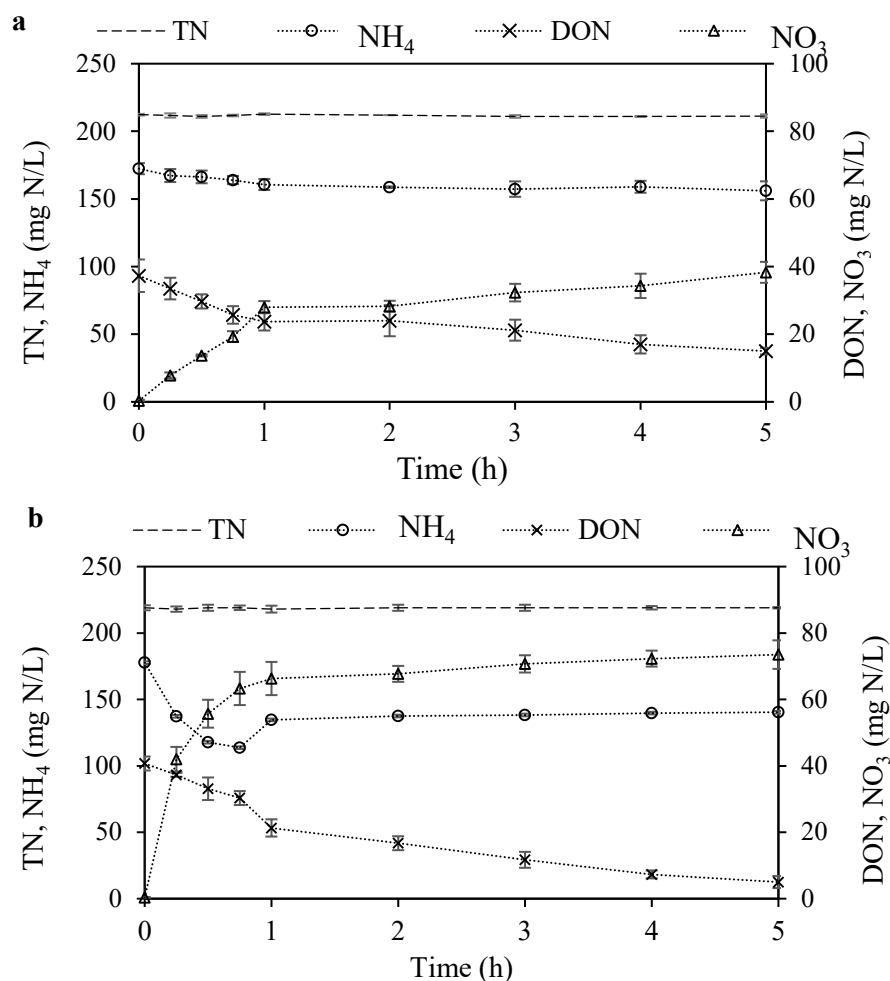
Figure 2.5. Oxidation of organic and inorganic nitrogen in digestate supernatant during 5h (a) O₃ treatment, and (b) O₃ /H₂O₂ treatment (Initial ozone concentration: 20.5 ± 0.2 mg/L, ozone flow rate: 51±2 L/h, sample volume: 2.6 L)

The low mineralization (DOC removal) can be explained by the mechanism of the reaction of molecular O_3 with organic compounds. Molecular O_3 reacts selectively with electron rich compounds in an electrophilic reaction by a cycloaddition mechanism, with unsaturated double bond or electron donors' compounds, such as aromatic ring and amines. The decomposition of organic matter may form smaller organic matter and by-product with a lack of double bonds, aromatic groups, and other electron moieties. Thus, in spite of the depletion of the parent compounds, mineralization cannot be expected during ozonation (Gomes et al., 2017). Nevertheless, during 5h ozonation 38.3 mg NO_3-N/L was formed (Figure 2.5.a). The formation of NO_3-N during non-catalytic ozonation can be due to the oxidation of inorganic and organic nitrogen. Comparing the NO_3-N yield with the converted NH_4-N (16 mg/L) suggests that stoichiometrically, 42 % of the NO_3-N yield could have been originated from the oxidation of ammonia. As such, the rest

42

of the NO_3-N (58 %) was produced from the oxidation of N-contained organic matter (DON-N), that shows the competition of DON-N with the target compounds for ozone consumption via NO_3-N formation mechanism. In a study for ozonation the wastewater effluent containing 1400 µM NH_4-N and low concentration of NO_3-N (0.5 µM) and DOC of 6.7 mg/L, the contribution of NH_4-N to nitrate production showed a range between 20 to 43 % in different O_3 doses, with an average reported value of 32 ± 7 %, while DON contributed to production of 68% of the generated NO_3-N (de Vera et al., 2017), which is in line with this study. By adding H_2O_2 to the system, the generated NO_3-N during 5h ozonation was 73.5 mg/L (Figure 2.5.b), which is 1.9 times higher than in ozone treatment alone. This can be explained by the contribution of $OH^\bullet$ radicals in oxidation of DON and NH_4-N. $OH^\bullet$ is a non-selective oxidant that attacks all the organic and inorganic compounds, while ozone selectively attacks only to the electron-rich compounds.

The total alkalinity (mg $CaCO_3$/L) decreased by only 3.6 and 6.4 % for O_3 and O_3/H_2O_2, respectively, and the pH remained constant at (8.5±0.2) during the 5h experiment (data not shown). However, the alkalinity effect on ozonation could be via the indirect mechanism by scavenging the $OH^\bullet$ radicals. During the indirect mechanism in ozonation process, formation of $OH^\bullet$ radical and the effect of the scavengers could affect the CECs removal efficiency. It has been reported, for instance, that carbonate species and nitrite inhibit radical-based reactions in ozonation and affect the removal of the compounds that have a low reaction rate with molecular ozone (Asghar et al., 2022; Feng et al., 2016). Previous research showed that the main $OH^\bullet$ scavengers are DOM (measured as DOC), HCO_3^-, CO_3^{2-}, and nitrite with an apparent reaction rate constant of 8.1×10^4 ((mg C/L)$^{-1}$s^{-1}), 8.5×10^6 (M^{-1} s^{-1}), 3.9×10^8 (M^{-1} s^{-1}), and 1.0×10^{10} (M^{-1} s^{-1}), respectively (Lee et al., 2013; Yang et al., 2021c). Furthermore, a high load of ammonia in the digestate matrix has also scavenging effect on $OH^\bullet$ radical with a rate constant of 2.3×10^6 (M^{-1} s^{-1}) for protonated form at pH < 7, and 1.8×10^8 M^{-1} s^{-1} for natural form at pH > 7 (Yang et al., 2021b). These compounds interfere the conversion rate of O_3 to $OH^\bullet$ and consume the $OH^\bullet$. The total scavenging rate of each water matrix is usually determined by multiplying these apparent rates to the concentration of the scavengers in each matrix (Yang et al., 2021c). In our study, nitrite was not found during the experiments; based on the pH, the majority of alkalinity was in the form of bicarbonate with molar concentration of 0.0489 M, and the carbonate was negligible; and ammonia was in its natural form (NH_3-N). As such, given the concentration of DOC, alkalinity (in the form of bicarbonate), and ammonia (Table 2.1), the total $OH^\bullet$ scavenging rate turned to be 2.49×10^7 s^{-1}, with the contribution of DOC 89% (2.3×10^7 s^{-1}), alkalinity (HCO_3^-) 1.67% (4.16×10^5 s^{-1}), and ammonia 8.88% (2.2×10^6 s^{-1}). Due to the lack of information in the literature, comparing the $OH^\bullet$ scavenging rate in different digestate supernatants was not possible. However, the effect of scavengers in other wastewater streams on CECs removal have been widely reported. For instance, a total scavenging rate of 1.9×10^5 s^{-1} was reported during the ozonation of municipal effluent (DOC= 9.6 mg C/L, alkalinity 2.5 mg $CaCO_3$/L, Nitrate= 0.24 mg N/L) (Liu et al., 2020), which is lower than the scavenging

rate determined in digestate supernatant, implying the higher inhibition of the matrix in digestate in compare with the wastewater effluent.

2.3.5 Toxicity (Microtox®)

The inhibition of luminescence emission by organism *Vibrio fisheries* were compared for the samples taken from the reactor in O_3 and O_3/H_2O_2 treatment in Figure 2.6.
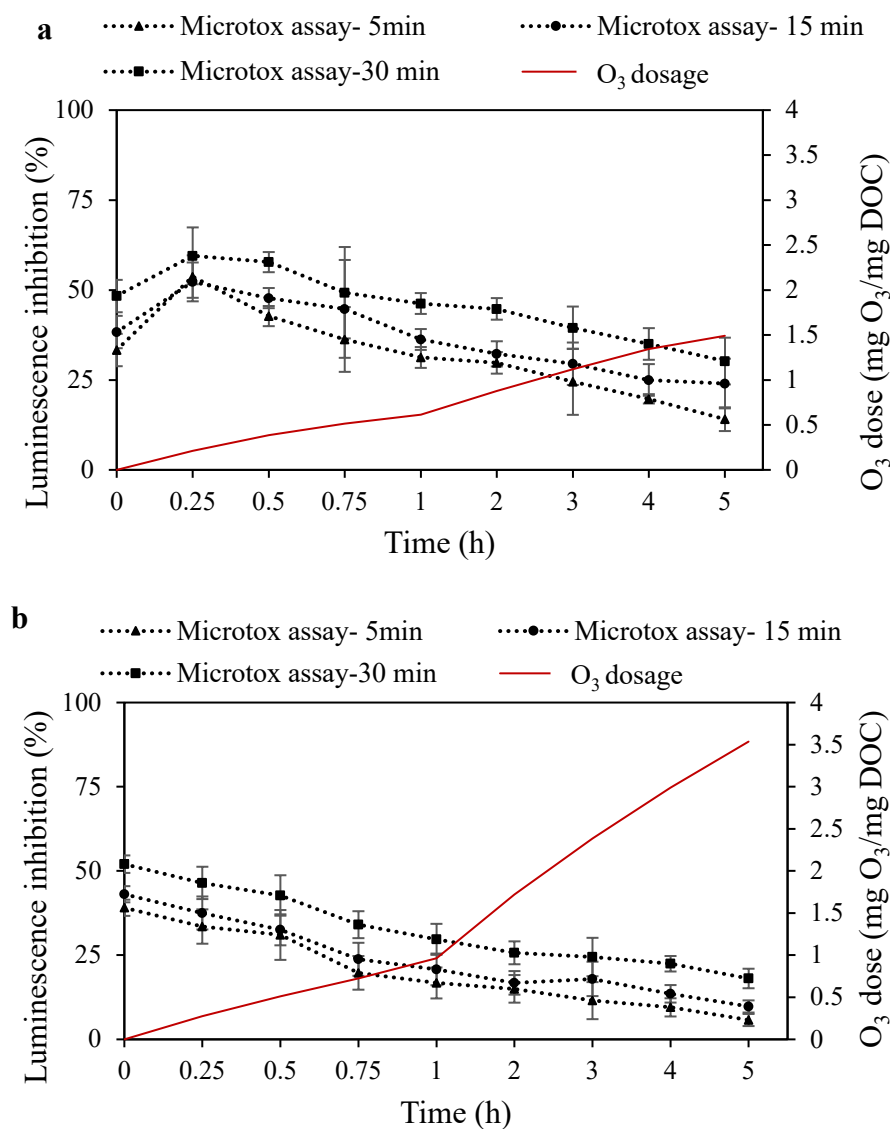
Figure 2.6. Comparison the acute toxicity with assay time of 5,15, and 30 min for organism Vibrio fisheries in 5h (a) O_3 and (b) O_3/H_2O_2 treatment in different O_3 dose

By increasing the assay time from 5 to 15 and 30 min, the acute toxicity, measured as inhibition of the luminescence emission, increased by an average of 4.9 and 13.5 % for O_3 treatment and by an average of 3.75 and 12.6 % for O_3/H_2O_2 treatment. In 5h ozone treatment, the inhibition decreased by 17.3, 14.3, and 18 % for assay exposure time of 5, 15, and 30 min. However, the highest inhibition (52-59%) was observed in 0.25 h with the ozone dose of 0.2 mg O_3/mg DOC. A possible explanation is that in lower ozone dose, high toxic transformation by-products might have been formed while with more ozone exposure they were removed. O_3/H_2O_2 treatment was more effective in toxicity removal. As for toxicity assay of 5 min, the inhibition decreased from 39 to 5.7 %, which is 1.7 times more than in O_3 treatment. It can be explained by more mineralization in compare to ozone treatment, and as a result less toxic compounds for the organism, i.e. formaldehyde, acetate, and carboxylic acid which are the end by-product of ozonation (Antoniou and Andersen, 2012). In a study for ozonation of biologically treated hospital wastewater with ozone dose between 2.4 to 18 mg/L, an increase in luminescence inhibition of *Vibrio fisheries* was reported at ozone dose of 10 mg/L and then the toxicity decreased by dosing more ozone up to 18 mg/L (Tang et al., 2019), which supports the result of the current study. The same increasing pattern was observed for ozonation of biologically treated municipal wastewater when the toxicity measured by the same organism increased at ozone dose of between 0.38 to 0.47 mg O_3/mg DOC (Tang et al., 2020). Yet, a full acute toxicity removal was reported in continuous ozonation of sewage treatment plant effluent by ozone dose of up to 150 mg/L without any observed increase in toxicity (Carbajo et al., 2015). By screening the inhibition of *Vibrio fisheries* in different matrix, Wang et al. (2021), reported that the acute toxicity towards this organism is not easily comparable in different matrix. Since the organism is sensitive to the variety of organic and inorganic pollutants, by-products and pH, the acute toxicity measured by luminescence emission of *Vibrio fisheries* differs in different matrix (Wang and Wang, 2021). It can explain the difference in toxicity pattern and also the different ozone dose in which an increasing pattern was observed in this study, and in the reported ozonation of municipal and hospital wastewater (Carbajo et al., 2015; Tang et al., 2020).

2.4 PRACTICAL APPLICATIONS AND FUTURE RESEARCH PROSPECTS

This study was to evaluate the feasibility of CECs removal from digestate supernatant with high load of organic and inorganic material and to determine the ozone dose required for CECs removal from digestate supernatant. The digestate from AD plant with manure feedstock was applied in this research due to the presence of pharmaceutical regarding the animal growth. Ozone-based AOPs showed the effectivity to remove CECs from digestate supernatant, yet, it is recommended to evaluate the method for other types of digestate for instance municipal with wider range and different concentration of CECs. Furthermore, in this research the focus was to determine the ozone demand and assess the general effect of the matrix. More study is needed to comprehend the individual and

combined effect of various matrix components on CECs removal, as well as an energy and cost analysis. This will help to better understanding the mechanism and efficiency of CECs removal in ozone-based treatments.

2.5 CONCLUSIONS

In this study, to remove the most persistent CECs (ibuprofen) from the digestate supernatant, a specific ozone dose of 1.11 mg O_3/mg DOC was required. The matrix composition affects the CECs removal by decreasing the kinetic rate, increasing the ozone consumption, and potentially scavenging the OH$^\bullet$. Dissolved organic nitrogen (DON-N) showed the highest affinity for O_3 consumption. Adding hydrogen peroxide, decreased the O_3 demand to 0.46 mg O_3/mg DOC achieving full CECs removal including ibuprofen. Both O_3 and O_3/H_2O_2 treatment decreased the acute toxicity of digestate supernatant. In general, this study addresses required information regarding ozonation of the digestate supernatant, showing that in spite of the competition effect of the matrix, complete removal of the target CECs was possible in less than 1h in the digestate supernatant with an ozone dose in the same range as for other (waste-)water matrix. Accordingly, this study suggests that ozonation has the potential to be applied as post-AD treatment for cleaner production.

2.6 ANNEXES

Annex 2.6.1. Characterization of the digestate sludge

Table A2.1. Characterization of the digestate sludge (total, solid and liquid fraction) in three consecutive months of sampling

Total		Feb., 2021	March, 2021	April, 2021
Parameter	Dimension	Value	Value	Value
Fraction	%	1	1	1
Density	g/ml	1	0.98	0.91
pH		8	8.6	8.4
Conductivity	ms/cm	16.8	17.6	21.9
COD	mg/L	31967	29166	22858
TSS	mg/L	21230	20036	15616
VSS	mg/L	10564	10151	8383
TS	mg/L	37830	29592	24461
VS	mg/L	24431	17243	17511
TN	mg N/L	3738	3142	3184
TP	mg PO_4-P/L	1071	500	518
Na	mg/L	2528	3660.5	1996
Mg	mg/L	1352	813	370
Al	mg/L	92	423.5	163.8
Fe	mg/L	184	353	69
K	mg/L	3340	3776	4297
Ca	mg/L	2052	1707	509.6
Liquid fraction		Feb., 2021	March, 2021	April, 2021
Parameter	Dimension	Value	Value	Value
Fraction	%	0.96	0.97	0.99
COD	mg/L	9330	8750	6516
DOC	mg/L	2256	3030	1819
TKN	mg NH_4-N/L	2957	2644	1888
NH_4-N	mg NH_4-N/L	1409	2037	1842
NO_2-N	mg NO_2-N/L	n.d	n.d	n.d
NO_3-N	mgNO_3-N/L	n.d	n.d	n.d
TN-N	mg N/L	2192	2710	1944
PO_4	mg PO_4-P/L	62	24	51.6
TIC	mg/L	2498	3857	3213
Alkalinity	mg HCO_3/L	1602	1129	947
Na	mg/L	726	821	465
Mg	mg/L	159	201	142

Al	mg/L	0.151	0.38	0.781
Fe	mg/L	7.2	12.5	8.117
K	mg/L	1164	1400	1363
Ca	mg/L	354	413	61.4
Solid fraction		Feb.,2021	March, 2021	April, 2021
Parameter	Dimension	Value	Value	Value
Fraction	%	0.04	0.02	0.02
COD	g/Kg DM*	575	698	442
TKN	g NH_4-N/Kg DM	22.4	19.5	19
TP	g PO_4-P/Kg DM	25	21	32
Alkalinity	g HCO_3/Kg DM	160	227	292
Na	g/Kg DM	45	69	37
Mg	g/Kg DM	30	21	16
Al	g/Kg DM	18	14	11
Fe	g/Kg DM	4.4	11.5	4
K	g/Kg DM	55	81	104
Ca	g/Kg DM	42	44	31

Annex 2.6.2. Calibration of the ozone set-up with KI test

KI can capture all the ozone delivered to the reactor. To calibrate the set up and to check if the observed values of ozone in, ozone out and excess accumulated ozone gives a valid calculated ozone consumption, the reactor was filled with 2.5 L of KI 20 g/L and ozone experiment was conducted in the same operational condition as for the experiments. At different contact time the ozonated KI was collected and titred with $Na_2S_2O_3 \cdot 5H_2O$ (0.1 M). In principle KI is oxidized to I_2 during ozonation in alkaline solution. By titration the acidified ozonated solution, the reacted O_3 can be stoichiometrically determined as follow:

$O_3 + 2KI \rightarrow I_2 + 2KOH + O_2$ in alkaline condition

$I_2 + 2Na_2S_2O_3 \rightarrow Na_2S_4O_6 + 2NaI$ in acidic condition
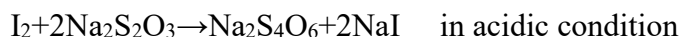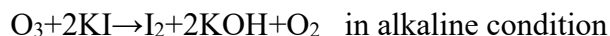
mg O_3= M titrant× V titrant × (O_3 Mw/2)×(V1(ml)/V2)

Where, V1: volume of the sample in the reactor, V2: volume of the sample withdrawn from the reactor for titration. Table A2.2 shows the reacted ozone that practically was obtained after titration.

Table A2.2. Determination of reacted ozone by using KI 20 g/L

Time (min)	pH KI	pH after acidification	V titrant (ml)	Reacted O_3 (mg)
5	10.6	1.9	0.3	71.28
10	11.3	2	0.9	211.68
15	11.6	1.83	1	232.8
20	11.31	1.9	1.5	345.6
30	11.2	2	2.4	552.96
45	11.3	2	3.1	706.8
60	11.35	1.8	4	912

The result obtained from titration was the same as the mass balance obtained from the observed data by the sensors.

Annex 2.6.3. Optimization of H_2O_2/O_3 ratio

The contribution of $OH^•$ and its reaction with organic matter, can improve the mineralization rate. It has been reported that adding an initiator for the decomposition chain reaction, i.e. H_2O_2, can improve the decomposition of O_3 and the efficiency of ozonation. The ratio between H_2O_2/O_3 is critical because overdosing of H_2O_2 generates less oxidative radicals such as $HO_2^•$. The lower H_2O_2 dosage favours the decomposition of O_3 to $OH^•$ radicals while two molecules of O_3 react with one molecule of H_2O_2 to generate two $OH^•$, which suggests a ratio of 0.5 for H_2O_2/O_3. Improving the pharmaceutical removal from water and wastewater with the ratio between 0.3-1.0 has been reported in previous studies, while as for bromate inhibition in treating drinking water, a ratio of 3.5 was reported. To optimize the H_2O_2/O_3 ratio, mineralization in 8 ratios was compared in Figure A2.1.
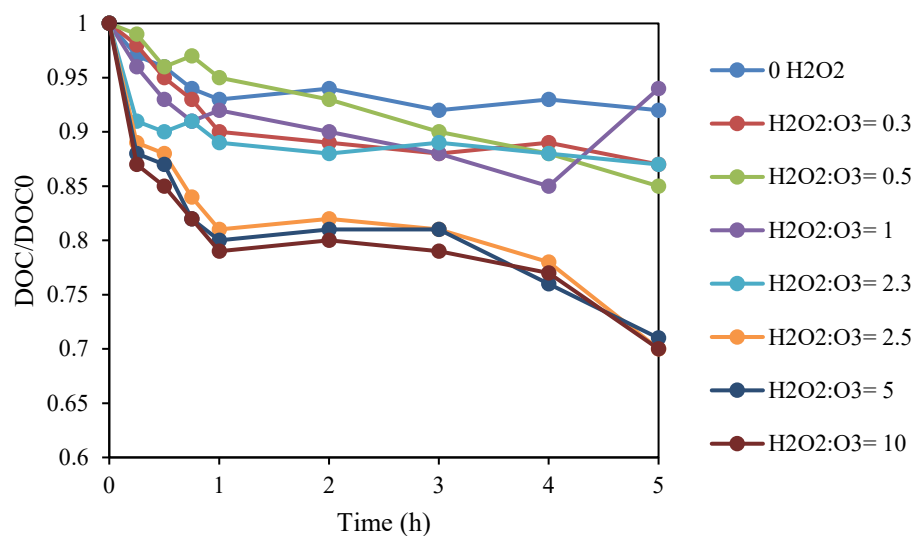
Figure A2.1. Effect of oxidant dosage on DOC removal

The data obtained from Figure A2.1 showed an optimum ratio of 2.5 for H_2O_2/O_3.

3

MATHEMATICAL MODELLING OF OZONATION PROCESS OF HIGH-STRENGTH LIQUID DIGESTATE

The primary objective of this chapter was to develop a mathematical model that describes the key reactions driving the ozonation of high-strength digestate, aiming at enhancing the understanding of such complex process. The model was calibrated using lab-scale experimental data. It includes six mathematical equations that consider various processes: ozone transfer into the liquid, oxidation of dissolved organic carbon (DOC), ammonia (NH_3), and dissolved organic nitrogen (DON). The model effectively represents the transformation of key variables, encompassing DON, DOC, NH_3, and nitrate generation (NO_3), along with alkalinity neutralization and excess dissolved ozone in the liquid. A quantitative assessment using the Normalized Root Mean Square Deviation (NRMSD) revealed a strong agreement between predicted and measured data. Specifically, the deviation between measured and modelled values were 6 % for dissolved ozone, 11 % for dissolved organic carbon, 7 % for alkalinity, 9 % for dissolved organic nitrogen, 5 % for ammonia, and 7 % for nitrate generation. In summary, this model provides a mathematical framework that offers valuable insights into the ozonation process of digestate. It underlines the significant role of key parameters, such as the influence of organic matter in alkalinity generation, which governs other oxidation processes.

3.1 INTRODUCTION

Anaerobic digestion (AD) is a promising process to convert organic waste to bioenergy. Beyond methane production, growing attention has focused on the recycling and reuse of the effluent stream generated by anaerobic digesters, known as digestate. Generally, digestate is initially separated into solid and liquid fractions. The solid fraction can be utilized to produce pyrochars (Monlau et al., 2015), or via enzymatic or thermal pre-treatment to increase the biomethane production (Dietrich et al., 2020). The nutrient-rich liquid fraction is suitable for nutrient recovery or for irrigation and land application (Wang et al., 2023b). Although land application of liquid digestate is considered a straightforward and economic reuse application (Wang et al., 2023b), the presence of contaminants in digestate limits its application due to the potential environmental risk (Yang et al., 2022a). Recently, utilization of ozone-based advanced oxidation processes (AOPs) was suggested as a potential method for further treatment of digestate (Moradi et al., 2023). Nevertheless, the ozonation process of digestate is still a relatively unexplored area, and there is limited knowledge about the inhibition and competition effect of digestate components that can affect the ozone consumption rate. The ozonation process can be optimized to maximize the efficiency and minimize operational costs by understanding the ozone transfer from gas to liquid, and the ozone consumption by different components within the water matrix.

The need to comprehend the complex reactions and interactions involved in ozone-based treatment methods has prompted the evolution of various models throughout the years. Ozonation models were initially developed by focusing on ozone kinetic reactions and decomposition rates in pure and drinking water. Specifically, the Staehelin, Hoigné, and Bühler (SHB) model was utilized for acidic to neutral pH conditions (Bühler et al., 1984), while the Tomiyasu, Fukutomi, and Gordon (TFG) model was applied for high pH values (Tomiyasu et al., 1985). These models served as pioneering contributions in this field. Later, the SHB model has been developed by integrating new reaction pathways and considering the effect of water quality characteristics such as pH (Lovato et al., 2009) and dissolved organic matter (DOM) (Audenaert et al., 2013). Recently, empirical models were also developed to predict micropollutant removal and oxidant exposure (Kim et al., 2020).

Despite the advances in ozone process modelling, there are limitations in the existing approaches. The models have either focused on the self-decomposition of ozone in the absence of impurities to simplify the system or considered individual contaminants by controlling other variables. While these models were beneficial to the estimation of self-decomposition kinetic rates, they are primarily applicable to scenarios involving drinking water or natural water under controlled conditions. Furthermore, the concentrations of organic matter and alkalinity are limited in those models. Although certain models took into consideration a high alkalinity concentration (of up to 150 mg/L) (Kim et al., 2020),

the organic matter was limited to 5 mg/L. Yet, the model resulted in a relatively complicated expression. In addition, to the best of our knowledge, ammonia has not been accounted for in the aforementioned models. Given that digestate contains a substantial amount of ammonia, its presence can potentially influence the ozonation process and the effective utilization of ozone. Therefore, the current models cannot describe the oxidation mechanisms in high-strength water matrices such as digestate.

This research aims to bridge this knowledge gap by developing a mathematical model tailored to the distinctive characteristics of the complex matrix of digestate. Therefore, the objective of this research was to stablish an innovative modelling approach that considers the main processes to describe (i) the ozonation of high-strength digestate, (ii) main reactions driving the ozonation process, (iii) ozone consumption yield by digestate matrix components, and (iv) the key components governing the ozonation of digestate.

3.2 MATERIALS AND METHOD

3.2.1 Experimental

The experimental work was carried out using digestate collected from a pig-manure biogas plant located in Kozani, Greece, fed with animal faeces, urine, manure, and corn silage. Digestate was later separated using a centrifuge and through a series of filtration steps down to 0.45 μm. The liquid digestate contained: 150 mg DOC/L, 180 mg NH_4-N/L, 46 mg N/L as DON, 150 mg $CaCO_3$/L as alkalinity, and pH 8.0.

The ozonation experiments were carried out in a bubble column reactor with a 2.6 L capacity equipped with a humidifier (DH3b, BMT MESTECHNIK, Berlin, Germany), and a diffuser at the bottom of the reactor. The digestate in the reactor was fed continuously with gaseous ozone at an initial concentration of 20.5 ± 0.2 mg O_3 gas/L gas and flow rate of 51 ± 2 L gas/h. The off-gas was continuously captured by the humidifier and destructed in a catalytic ozone destruction equipment. The gaseous ozone (input and output) was recorded with an ozone analyzer BMT 964 (BMT MESTECHNIK GmbH, Stanhnsdorf, Germany). The dissolved ozone concentration was monitored and recorded with a Krypton KO3 ozone analyzer (Dr. A. Kuntze GmbH Meerbusch, Germany). Details about the ozone set-up are illustrated in Chapter 2.

For modeling purposes, the experiments continued until the concentration of dissolved ozone became constant (35h). To assess the oxidation of digestate matrix components, including NH_3-N, DON-N, NO_3-N, DOC, and conversion of total alkalinity (as mg $CaCO_3$/L) during ozonation time, samples were withdrawn at intervals of 1 hour, and the concentration of the above-mentioned compounds was determined in accordance with Standard Methods (Moradi et al., 2023). The ozonation experiment in digestate was repeated three times, and the measured data for dissolved ozone, and the conversion of

53

NH_3-N, DON-N, NO_3-N, DOC, and total alkalinity (as mg $CaCO_3$/L) during ozonation time was used for model calibration.

For internal validation of the model, another set of experiments was conducted with digestate from the same biogas plant with different initial concentrations of DOC, DON-N, ammonia and alkalinity (Table 3.1). The ozone experiment with each water matrix was conducted under the same operational conditions as explained earlier. Each experiment was repeated three times, and the obtained data for dissolved ozone and conversion of DOC, DON-N, NH_3-N, and total alkalinity in this set of experiments were used for internal validation of the model.

For external validation, the same ozonation experiment was conducted on a distinct digestate collected from sewage treatment plant in Malta. This liquid digestate contained: 220 mg DOC/L, 200 mg NH_4-N/L, 65 mg N/L as DON, 250 mg $CaCO_3$/L as alkalinity and pH 8.2. All the experiments were repeated three times and the observed data was used for model validation. Table 3.1 shows the experimental work for model calibration and validation.

Table 3.1. Experimental work for calibration and validation of digestate ozonation model. (Initial ozone concentration: 20.5 ± 0.2 mg/L, ozone flow rate: 51±2 L/h, sample volume: 2.6 L)

	Digestate Source	DOC (mg/L)	DON-N (mg N/L)	NH_3-N (mg N/L)	Total alkalinity (mg $CaCO_3$/L)
Exp.1 (Model calibration)	Pig-manure digestate	150	46	180	150
Exp.2 (Internal validation)	Diluted Pig-manure digestate (first dilution)	70	25	90	80
Exp.3 (Internal validation)	Diluted Pig-manure digestate (second dilution)	40	14	43	36
Exp.4 (Internal validation)	Diluted Pig-	14	5.5	17	16

	manure digestate (third dilution)				
Exp.5 (External validation)	Sewage treatment plant digestate	220	65	200	250

3.2.2 Model development

The ozonation process was simulated using the Aquasim software version 2.1d (win/mfc) (Reichert, 1994). The model describes the ozone transfer into the liquid phase until reaching a saturation concentration. Additionally, the model considers the consumption of ozone by various components present in the digestate matrix and describes the conversion and removal of individual components. The model includes modified second order kinetic conversion rates for each component. A Monod-type switch functions, as later described in section 3.3.2., was integrated to the kinetic reaction rates to describe how the conversion rates slow down and stop when a defined limiting compound started to become limiting or was fully oxidized. The interlinked mathematical expressions of the ozonation process were defined considering different underlying assumptions, including:

1. Ideal Mixing: The liquid inside the reactor was continuously exposed to well-mixing conditions during the whole ozonation tests to avoid any gradients and, consequently, the concentrations of all the compounds were homogenous inside the entire reactor.

2. Incomplete DOC oxidation: Supported by literature (Gomes et al., 2017), in the ozonation tests it was observed that the ozonation of DOC in digestate did not result in complete mineralization, leaving a residual fraction of refractory DOC (f_{DOC_r}). Through parameter estimation, based on observed data, the DOC refractory fraction corresponded to approximately 1/3 of the initial DOC concentration (on a stochiometric ratio basis).

Following these assumptions, the model was developed considering the ozone transfer and ozone consumption as per Equation (3.1) (Presumido et al., 2022).

$$\frac{dS_{O_3}}{dt} = k_L a \left(S_{O_3^*} - S_{O_3} \right) - k_c S_{O_3} \qquad (3.1)$$

Where $\frac{dS_{O_3}}{dt}$ is the dissolved ozone changes over the time, $k_L a$ is the mass transfer coefficient, $S_{O_3^*}$ is the liquid ozone concentration in equilibrium, S_{O_3} is the ozone concentration in the liquid, and k_c is the sum of all the ozone consumption rates by different components in digestate matrix, described in section 3.2.3.

3.2.3 Model calibration

The model calibration was performed following a step-wise approach: (i) first, the values of $k_L a$ and $S_{O_3^*}$ were estimated using the parameter estimation tool of Aquasim and fitting the measured dissolved ozone concentrations obtained from Exp.1 to the value described by the S_{O_3} state variable; (ii) in the second step, the kinetic rate constant of the reaction between DOC and ozone (k_{DOC}) was determined in order to describe the measured concentrations of dissolved organic carbon (state variable S_{DOC}) taking into consideration the generation of refractory DOC (f_{DOC_r} in assumption 2); afterwards, (iii) the alkalinity generated by the DON oxidation process (i_{CO3_NH3}) was determined based on the mass/charge relation between the production of ammonia and alkalinity and the concentrations of dissolved organic nitrogen (S_{DON}) were satisfactorily described by estimating the kinetic rate constant of the reaction between DON and ozone (k_{DON}); (iv) in the fourth step, the concentrations of ammonia (S_{NH3}) and total alkalinity (T_{Alk}) were fitted to the measured data of Exp.1 taking into account a two-step alkalinity conversion with two different kinetic rates and estimating the values of k_{HCO3}, k_{CO3}, and k_{NH3} (the kinetic rate constants of bicarbonate, carbonate and ammonia, respectively); finally, (v) a slight deviation between the predicted S_{O3} (concentration of dissolved ozone) and the measured data, occurred during the calibration, was corrected by estimating the values of Y_{O3_DOC}, Y_{O3_DON}, and Y_{O3_NH3} (the ozone consumption yields by DOC, DON, and NH_3, respectively).

After calibration, the model successfully predicted the generation of the nitrate (S_{NO3}) observed in experimental work. Table 3.2 shows the state variables, kinetic and stoichiometry parameters introduced to the model. Table 3.3 shows the Gujer-Petersen matrix describing the ozonation process in this study.

Table 3.2. State variables, kinetic parameters and stochiometric coefficients applied in the mathematical model

Symbol	Description	Unit
State variables		
S_{O3}	Dissolved O_3 concentration	mg O_3 L^{-1}
S_{DOC}	Dissolved organic carbon concentration	mg DOC L^{-1}
S_{DON}	Dissolved organic nitrogen concentration	mg DON-N L^{-1}
S_{NH3}	Ammonia-nitrogen concentration	mg NH_3-N L^{-1}
$S_{CO3}{}^{2-}$	Alkalinity concentration in the form of carbonate	mg L^{-1}
$S_{HCO3}{}^{-}$	Alkalinity concentration in the form of bicarbonate	mg L^{-1}
S_{H+}	Generated hydrogen ions	mg L^{-1}
S_{NO3}	Nitrate-nitrogen concentration	mg NO_3-N L^{-1}
S_{DOC_r}	Refractory DOC concentration	mg DOC L^{-1}
T_{Alk}	Total alkalinity concentration	mg L^{-1}
Kinetic parameters		
k_La	Volumetric mass transfer coefficient of ozone into water	h^{-1}
k_{DOC}	Kinetic rate constant of DOC conversion	L mg^{-1} h^{-1}
k_{DON}	Kinetic rate constant of DON conversion	L mg^{-1} h^{-1}
k_{NH3}	Kinetic rate constant of NH_3 conversion	L mg^{-1} h^{-1}
k_{CO3}	Kinetic rate constant of $CO_3{}^{2-}$ conversion	L mg^{-1} h^{-1}
k_{HCO3}	Kinetic rate constant of $HCO_3{}^{-}$ conversion	L mg^{-1} h^{-1}
K_{DOC}	Half-saturation DOC concentration	mg DOC L^{-1}

K_{DON}	Half-saturation DON concentration	mg DON-N L^{-1}
K_{NH3}	Half-saturation NH_3 concentration	mg NH_3-N L^{-1}
K_{O3}	Half-saturation O_3 concentration	mg O_3 L^{-1}
K_{TAlk}	Half-saturation T_{Alk} concentration	mg L^{-1}

Stochiometric parameters

Y_{O3_DOC}	Stoichiometric yield coefficient of ozone consumption for DOC conversion	mg O_3 mg DOC^{-1}
Y_{O3_DON}	Stoichiometric yield coefficient of ozone consumption for DON conversion	mg O_3 mg DON-N^{-1}
Y_{O3_NH3}	Stoichiometric yield coefficient of ozone consumption for NH_3 conversion	mg O_3 mg NH_3-N^{-1}
I_{CaCO3}	Switch function of alkalinity	-
i_{CO3_NH3}	Alkalinity generation in the DON-conversion process	mg CO_3^{2-} mg NH_3-N^{-1}
f_{DOC_r}	Fraction of refractory DOC	mg DOC L^{-1}

Table 3.3. Gujer-Petersen matrix describing ozonation process in this study

Process	Equations	S_{O3}	S_{CO3}	S_{HCO3}	S_{H2CO3}	S_{H+}	S_{DOC}	S_{NH3}	S_{NO3}	S_{DON}	S_{DOC_r}	Equation
	Delivered O_3											
r1	Transfer	1										$k_La(S_{O3}^* - S_{O3})$
	DOM (organic C, organic N)											
r2	$DOC+O_3 \rightarrow$ mineralization product+ DOC_r	$-Y_{O3\_DOC}$					-1				f_{DOC_r}	(3.2)
r3	$DON+O_3 \rightarrow CO_3^{2-}+NH3$	$-Y_{O3\_DON}$	i_{CO3_NH3}					1		-1		(3.3)
	Inorganic C, N											
r4	$NH_3+O_3 \rightarrow H^++NO_3+H_2O$	$-Y_{O3\_NH3}$				1		-1	1			(3.4)
r5	$CO_3^{2-}+H^+ \rightarrow HCO_3^-$		-1	1		-1						(3.5)
r6	$HCO_3^-+H^+ \rightarrow H_2CO_3$ $\rightarrow H_2O+CO_2$			- 1	1	-1						(3.6)
	N		i_{CO3_NH3}					1				
	charge		-2					1/14				

In Table 3.3, $k_L a (SO_3{}^* - SO_3)$ represents the rate of ozone transfer into the liquid. The remaining reaction equations, presented from Equation (3.2) to Equation (3.6), elucidate the volumetric conversion of DOC, DON, NH_3, and alkalinity during ozonation. These equations exhibit second-order kinetic reaction with some modification regarding the switch functions to regulate the process based on the corresponding limiting compounds, as defined in Table 3.2 and explained in section 3.3.2.

$$r_{DOC} = k_{DOC} \times \left(\frac{S_{DOC}}{(S_{DOC}+K_{DOC}}\right) \times \left(\frac{S_{O_3}}{S_{O_3}+K_{O_3}}\right) \tag{3.2}$$

$$r_{DON} = k_{DON} \times \left(\frac{S_{DON}}{(S_{DON}+K_{DON}}\right) \times \left(\frac{S_{O_3}}{S_{O_3}+K_{O_3}}\right) \tag{3.3}$$

$$r_{NH3} = k_{NH_3} \times \left(\frac{S_{NH3}}{(S_{NH3}+K_{NH3}}\right) \times \left(\frac{S_{O_3}}{S_{O_3}+K_{O_3}}\right) \times I_{CaCO3} \tag{3.4}$$

$$r_{CO3} = k_{CO_3} \times \left(\frac{S_{CO3}}{(S_{CO3}+K_{CO3}}\right) \tag{3.5}$$

$$r_{HCO3} = k_{HCO_3} \times \left(\frac{S_{HCO3}}{(S_{HCO3}+K_{HCO3}}\right) \times \left(\frac{S_{HCO3}}{(T_{Alk}+K_{TAlk}}\right) \tag{3.6}$$

Where, I_{CaCO3} is the switch function showing the effect of total alkalinity based on mg $CaCO_3/L$ on NH_3-N removal:

$$I_{CaCO3} = \frac{T_{Alk}}{T_{Alk}+K_{T_{Alk}}} \tag{3.7}$$

Where,

$$T_{Alk} \left(\frac{mg\ CaCO_3}{L}\right) = \left(\left(\frac{S_{CO_3^{2-}}}{60}\right) + \left(\frac{S_{HCO_3^-}}{61}\right) + \left(\frac{S_{H_2CO_3}}{62}\right)\right) \times 100 \tag{3.8}$$

The switch function, I_{CaCO3}, was incorporated into the ammonia removal reaction due to the observation that the ammonia reaction ceases when total alkalinity levels $\left(\frac{mg\ CaCO_3}{L}\right)$ decrease.

60

3.2.4 Error analysis and model validation

The agreement between measured and predicted data was quantified by Normalized Root Mean Squared Deviation (NRMSD) as shown by Equation (3.9) (Oehmen et al., 2010).

$$NRMSD = \frac{\sqrt{\frac{\sum_{i=1}^{n}(x_{meas,i}-x_{pred,i})^2}{n}}}{x_{meas,max}-x_{meas,min}} \qquad (3.9)$$

Where, x_{meas} and x_{pred} are measured and predicated variables (for instance S_{O3}), $x_{meas,max}$ and $x_{meas,min}$ are the maximum and minimum measured concentration of the variable, and n is the number of data points for each variable. Furthermore, as for internal validation, an assessment was conducted to determine the range of concentrations for which the model retained its applicability, especially for less concentrated water matrices. This evaluation involved using detailed measured data from the ozonation process with further dilutions of the digestate matrix while altering only the initial input values for the model.

For external validation of the calibrated model, the same simulation process was applied for a distinct digestate with different characteristics. For this purpose, the simulation was conducted for municipal digestate collected from biogas plant located in Malta sewage treatment plant. The liquid digestate used for validation contained 250 mg $CaCO_3$/L, 200 mg NH_3-N/L, and 65 mg DON-N/L, and DOC of 220 mg/L.

3.3 RESULTS AND DISCUSSION

3.3.1 Experimental

The ozonation treatment for digestate continued until the dissolved ozone reached a constant value and showed no change afterwards. Up to 25 h of ozonation, no dissolved ozone was recorded by the online sensor, or the concentration was negligible (Figure 3.1.a), implying that all the transferred ozone was consumed by the digestate matrix component. Between 25 to 29 h, the pH dropped from 8.5 to 3.7 and the total alkalinity (150 mg $CaCO_3$/L) was consumed completely (Figure 3.1.b). In this phase, oxidation of DOC and ammonia ceased (Figure 3.1.b and 3.1.c), and the dissolved ozone increased reaching a constant concentration of 5.5 to 6.0 mg O_3/L.

During 25 h ozonation, 157 mg NO_3-N/L were generated from the oxidation of ammonia and DON. After 25 h, when the oxidation of ammonia stopped and the DON was fully oxidized, the nitrate production did not increase further.
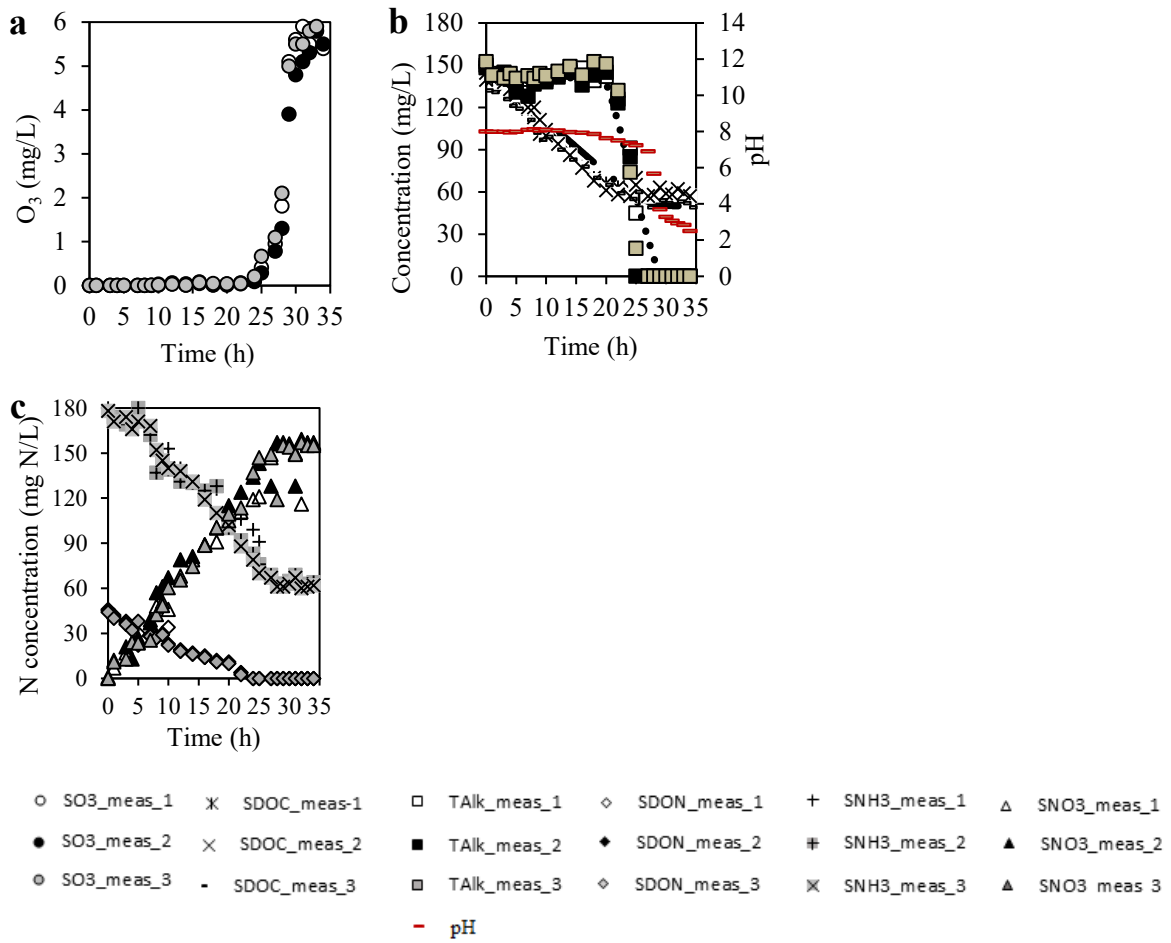
Figure 3.1. Long-term digestate ozonation in the bubble column reactor displaying the concentrations of (a) dissolved O₃ (S_O3), (b) DOC (S_DOC) and total alkalinity (T_Alk), and (c) ammonia (S_NH3), DON (S_DON), and nitrate (S_NO3)

3.3.2 Model approach

Prior to model calibration, the observed data for DOC removal over 35 hours of ozonation were fitted to zero-order, first-order, and second-order kinetic equations. As depicted in Figure 3.2, the second-order kinetic rate demonstrated the highest fit for DOC removal, yielding an R^2 value of 0.93. Consistently, ammonia and DON removal also exhibited the highest agreement with second-order kinetics, suggesting the suitability of second order kinetic rate in modeling the oxidation reaction of digestate components with ozone.
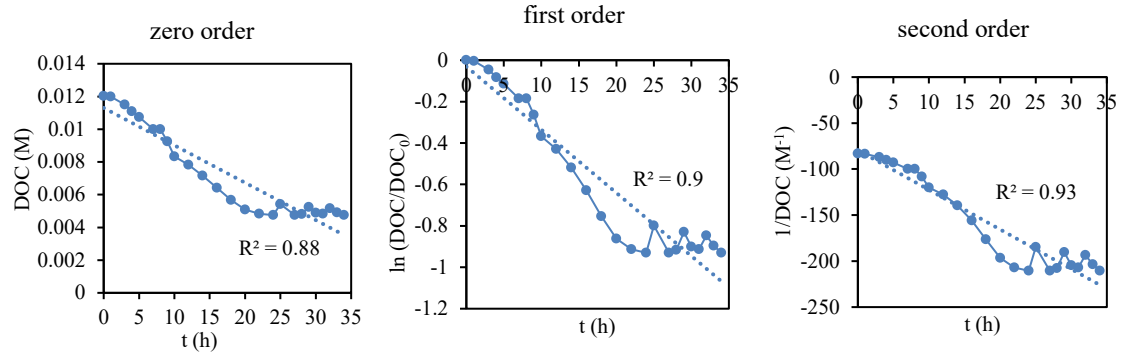
Figure 3.2 Comparison of kinetic rate equations for DOC removal during 35-hour ozonation

Previous studies have also applied the second-order chemical kinetic method, as described by Equation (3.10), during O_3 treatment (Gomes et al., 2017).

$$rate = (k_{O3} \times S_{O3} \times S_x) + (k_{OH} \times S_{OH} \times S_x) \tag{3.10}$$

Where, S_x is the concentration (M) of target compound (such as DOC) and k_{O3} and k_{OH} are the rate constant of the reaction of each compound with ozone, and $OH^\bullet$, respectively. Since $OH^\bullet$ is produced from the ozone decomposition in the liquid, its concentration is proportional to the concentration of O_3, thus, the simplified and integrated form of Equation (3.10) can be shown as Equation (3.11)

$$rate = k \times S_{O3} \times S_x \tag{3.11}$$

Where, k is $k_{O3} + R_{CT} k_{OH}$ and R_{CT} is $\frac{\int_0^t S_{OH^\bullet} \, dt}{\int_0^t S_{O3} \, dt}$ (He et al., 2022).

By integrating the second-order kinetic rate for each component (Equation (3.11)) into the Aquasim software, the model failed to accurately simulate the removal of components, particularly after 25 hours when the oxidation of compounds ceased. Therefore, the removal rates of DOC and other components were modified to include the phase of ozonation when all reactions stop. To achieve this, the approach of the ASM model (Henze et al., 2000) was adopted, and a Monod-type switch function ($\frac{S_{DOC}}{K_{DOC} + S_{DOC}}$), with the parameters defined in Table 3.2., was introduced to the concentration of DOC to

regulate the reaction based on the corresponding limiting compounds. The same approach was applied for other compounds, and the modified rates, as previously showed in Equation 3.2 to Equation 3.6, along with the variables and stoichiometry ratios were integrated into Aquasim software.

The k_La and S_{O3*} values were determined using the parameter estimation tool of Aquasim (26.09 h^{-1} and 6.09 mg/L, respectively) during 35h simulation. The model showed a good agreement between the measured and predicted dissolved O_3 (Figure 3.3.a). The NRMSD for dissolved O_3 was 0.06, indicating that the model prediction deviates by approximately 6 % from the actual data and, therefore, the predicted and measured data have an agreement of around 94%. Furthermore, as shown in Figure 3.3.b, the modified rates successfully described the conversion of total alkalinity (measured as mg $CaCO_3$/L) after considering a two-step alkalinity conversion as a function of the carbonate species with kinetic dissociation rates of 7 L mg^{-1} h^{-1} for k_{CO3} and 24 L mg^{-1} h^{-1} for k_{HCO3}.

The measured data showed that the DOC concentration decreased to one third of its initial value and remained constant until the end of the tests. Based on this observation and reported low mineralization during ozonation (Miklos et al., 2018; Nawrocki and Kasprzyk-Hordern, 2010; Wang and Chen, 2020), it was assumed that DOC oxidation produced an equivalent of 1/3 of its molar ratio as a refractory or non-removable DOC (f_{DOC_r}). Based on this assumption, the predicted DOC value had an agreement of 87% with the measured data (Figure 3.3.b). The ozone consumption yield (Y_{O3_DOC}) determined by the parameter estimation tool was 1.5 mg O_3/mg DOC.

Regarding the N concentrations, the DON transformation was well-described by the model (with an 91% agreement). The ammonia values showed the best fit with the measured data (95%) after a switch function dependent on total alkalinity $(I_{CaCO3} = T_{Alk}/(T_{Alk}+K_{TAlk}))$ was added into the model (Figure 3.3.c). The parameter estimation determined the ozone consumption yield by the conversion of DON (Y_{O3_DON}) and the oxidation of ammonia (Y_{O3_NH3}) as 1.5 mg O_3/mg DON and 6 mg O_3/mg NH_3, respectively.
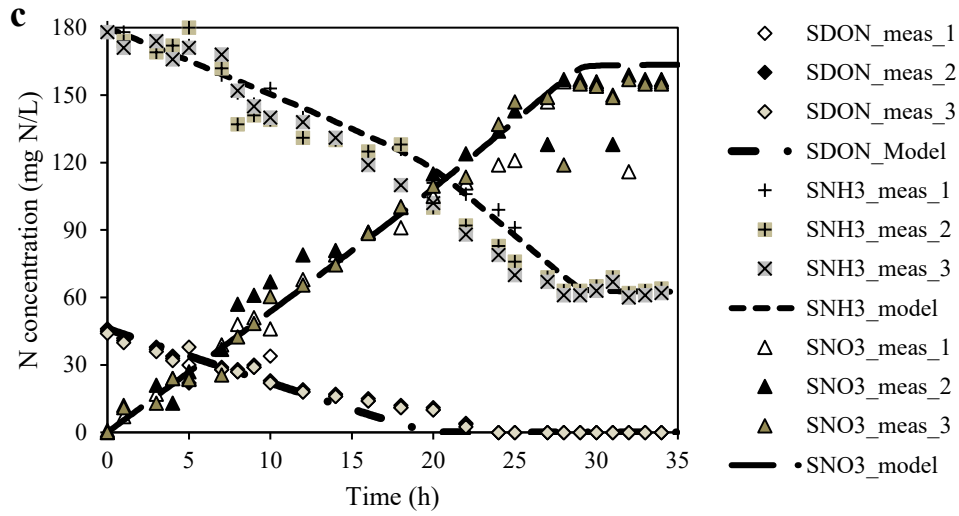
a

b
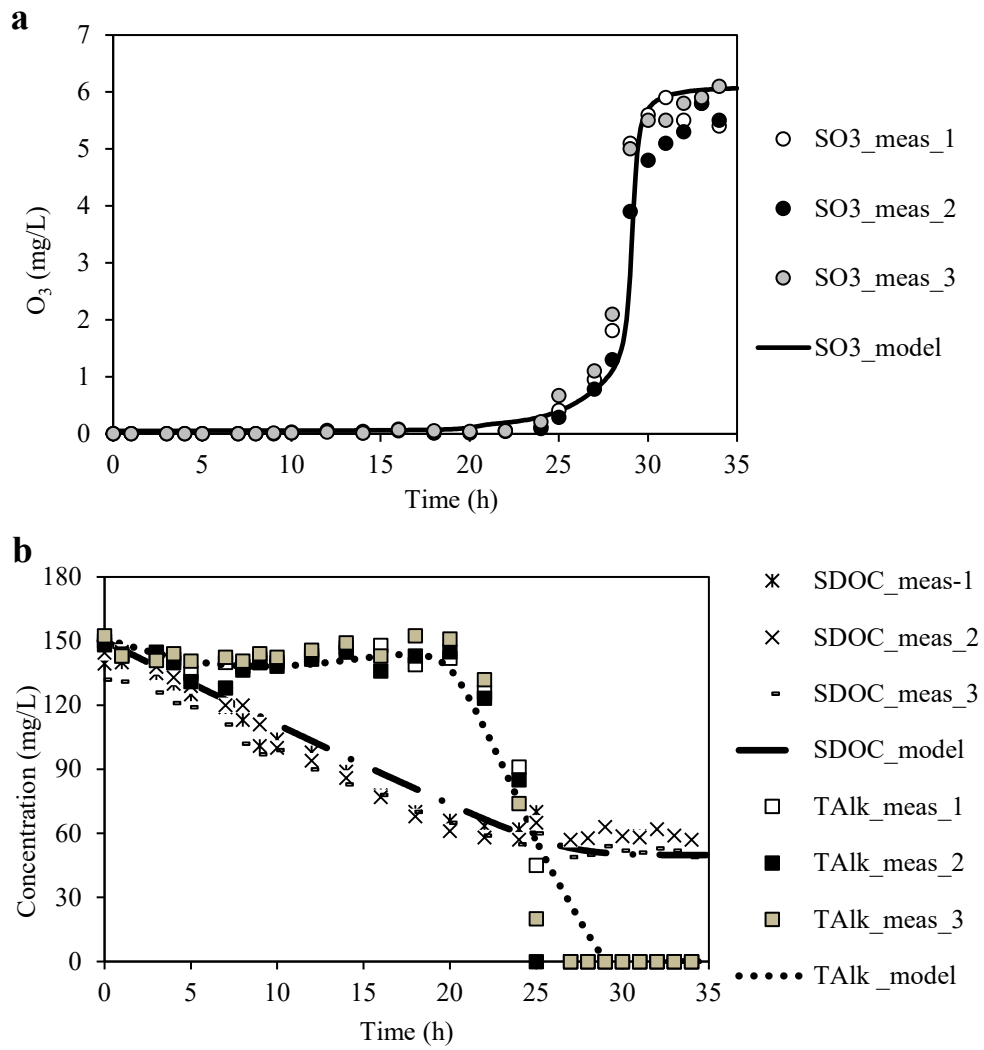
Figure 3.3. Model calibration describing the concentration profiles of (a) dissolved ozone (S_{O3}), (b) DOC (S_{DOC}) and total alkalinity (T_{Alk}), and (c) ammonia (S_{NH3}), DON (S_{DON}), and nitrate (S_{NO3}) during a 35h ozonation test of digestate. Lines indicate the predicted values by model while the markers indicate the measured values.

3.3.3 Describing digestate ozonation with the calibrated model

The experimental data showed that after 25 h ozonation, the ammonia oxidation process ceased despite that the concentration of ammonia was still as high as 70 mg NH_3-N/L. Ammonia oxidation is highly pH dependent (Yang and Liu, 2022), thus, when the buffer capacity of the water matrix was consumed and the pH dropped (Figure 3.2.b), the concentration of ammonia remained rather constant (Figure 3.2.c). In aqueous solution, the two forms of NH_3/NH_4 are in a dynamic equilibrium as per Equation (3.12):

$$NH_3 + H_2O \leftrightarrow NH_4^+ + OH^-$$
(3.12)

The percentage of each species at specific pH can be determined by Equation (3.13) (Kuo et al., 1997).

$$\frac{[NH_3]}{[NH_3]+[NH_4^+]} = \frac{10^{(pH-14)}}{K_b+10^{(pH-14)}}$$
(3.13)

Where, K_b is the ammonia ionization constant with a value of 1.774×10^{-5} (Singer and Zilli, 1975).

Up to 25 h, the buffer capacity, provided by 150 mg CaCO$_3$/L, kept the pH rather constant with a slight decrease from 8.5 to 7.8 (Figure 3.2.b). However, from 25 to 29 h, the pH dropped to 3.7. At this pH, based on Equation (3.13), more than 99% of ammonia was present as NH_4^+. Ammonia can be oxidized by ozonation only in its neutral form, while the ionized specie (NH_4^+) does not react with ozone or even the OH· radical generated during ozonation (Yang and Liu, 2022). Yang and Liu (2022) showed that in the absence of a buffer to keep at least a neutral pH, only 6.7% of ammonia was oxidized with an ozone concentration of 0.105 mM within 1 h ozonation. Their finding supports the result of this study regarding the effect of the buffer capacity on ammonia removal.

After 25 h, the DON was fully oxidized and the DOC removal stopped when one third of the initial DOC concentration remained. Yet, ammonia removal continued up to 29 h, and it stopped after the alkalinity was consumed. This removal pattern shows that the oxidation of all the components are interlinked, and the ozone consumption rate cannot be explained by only the kinetic; instead, the effect of each component on other compounds oxidation should be considered.

The calibrated model successfully described the ozonation process. Overall, the major role of alkalinity on the oxidation of ammonia was considered in the model calibration by adding a switch function (I_{CaCO3}) to the ammonia oxidation rate (Equation 3.4). By adding this switch function, an acceptable description between measured and predicted data was obtained, supporting the validity of the inhibition effect of alkalinity on ammonia removal.

Up to 25 h, all the oxidable organic matter (DOC and DON) was oxidized, and the produced carbonate along with the background alkalinity was consumed by the H^+ generated by the ammonia oxidation process. Then, after 25 h no further conversion of the organic matter (DON and DOC) occurred; therefore, the production of carbonate stopped. Up to 29 h, the remaining alkalinity was neutralized by H^+, and after 29 h, alkalinity declined completely. Since the pH dropped accordingly, all the ammonia was present as tetrahedral (NH_4) form and ammonia oxidation also stopped.

de Vera et al. (2017) showed that at lower ozone doses, the oxidation of DON, particularly amines, increases the concentration of ammonia in aqueous solution, while at higher ozone concentration, DON might be oxidized directly to nitrate via oxygen transfer mechanism. In this research; however, the ammonia concentration decreased constantly even at very low ozone concentrations at the early stage of the ozonation process, and nitrate was constantly generated. This can be explained by the model. The second order kinetic rate estimated by the model for DON oxidation to ammonia was 10 L mg^{-1}h^{-1}, which is much lower than the ammonia oxidation rate (22 L mg^{-1}h^{-1}),

implying that the consumption rate of ammonia is higher than the generation rate and therefore, no increasing pattern of ammonia was observed throughout the long-term experiment.

Furthermore, the model was able to satisfactorily predict the generation of nitrate with a high agreement of 93%. In addition, the measured final concentration of nitrate (157 mg N/L) and the predicted nitrate concentration (163 mg N/L) after 35 h of ozonation were only slightly different (Figure 3.3.c). This is particularly important considering that nitrate formation rate is not explicitly defined within the model but it is determined from the stoichiometry and rates defined for other reactions. The accurate prediction of nitrate; therefore, can support the validity of the model and the assumptions. The capability of the model to predict the nitrate formation is also important for further possible applications. For instance, recently the formation of nitrate during ozonation is considered as a surrogate parameter for different purposes. Song et al. (2017) showed that nitrate formation and the abatement of micropollutant during ozonation of water matrix containing natural organic matter (NOM) are correlated. de Vera et al. (2017) suggested that nitrate formation can be a surrogate for the determination of an oxidant exposed to ozonation. As such, accurately prediction of nitrate formation during ozonation in the current study could contribute to understanding the level of treatment by ozonation prior to the experimental work.

3.3.4 Further evaluation of the model

Initially, the model was calibrated to describe the ozonation process for a high-strength water matrix. Then, the model applicability was further evaluated by simulating the ozonation process in three digestate matrix from the same biogas plant with different digestate characteristics. The ozonation process was simulated using the previously calibrated parameters, rates, and stoichiometry values, as shown in Figure 3.4. The simulated ozonation process for the first and second digestate matrix showed a high agreement (> 90%) between the predicted and measured data for all variables except for alkalinity that had an agreement of 85% and 83% in the first and second digestate matrix. The lowest agreement was observed in the lowest concentrated digestate matrix, with an agreement of 70% for NO_3, 72% for O_3 and 75% for DOC, indicating the model's sensitivity to the initial concentrations (Figure 3.4.g, 3.4.h, 3.4.i).
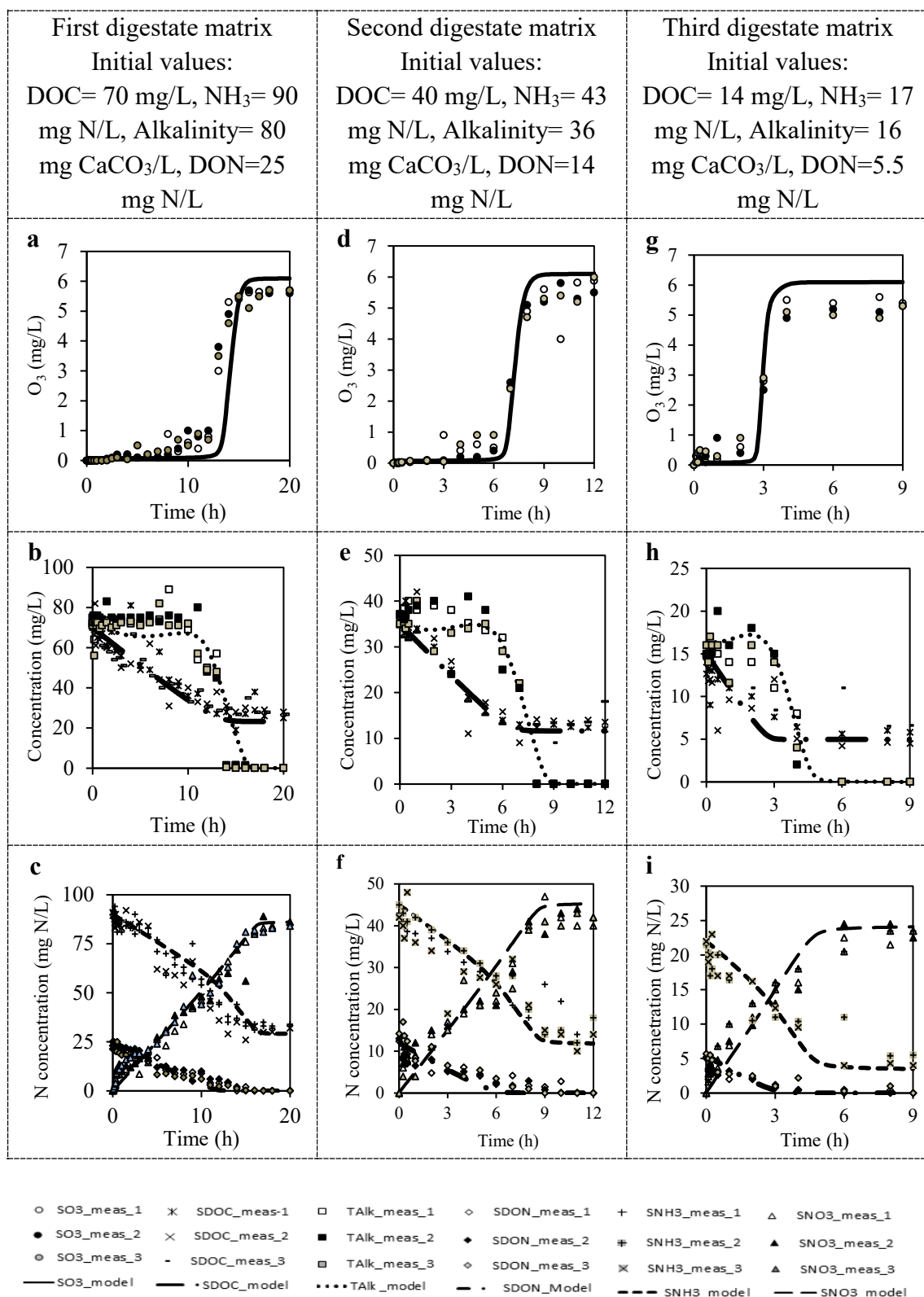
| First digestate matrix Initial values: DOC= 70 mg/L, NH$_3$= 90 mg N/L, Alkalinity= 80 mg CaCO$_3$/L, DON=25 mg N/L | Second digestate matrix Initial values: DOC= 40 mg/L, NH$_3$= 43 mg N/L, Alkalinity= 36 mg CaCO$_3$/L, DON=14 mg N/L | Third digestate matrix Initial values: DOC= 14 mg/L, NH$_3$= 17 mg N/L, Alkalinity= 16 mg CaCO$_3$/L, DON=5.5 mg N/L |

Figure 3.4. Model description of the ozonation of the diluted digestate matrix displaying the concentration profiles of: (a) dissolved ozone (S$_{O3}$), (b) DOC (S$_{DOC}$) and total

alkalinity (T_{Alk}), and (c) ammonia (S_{NH3}), DON (S_{DON}), and nitrate (S_{NO3}) in the first diluted digestate sample. Figures 3.4.d,3.4.e and 3.4.f show the results of the ozonation tests for the second diluted sample and Figures 3.4.g, 3.4.h and 3.4.i for the third dilution.

3.3.5 Model validation

The long-term ozonation process was applied to a different digestate matrix than that one used for the model development and calibration. Thus, the calibrated model was applied to simulate the ozonation process of a municipal liquid digestate by only adjusting the initial concentrations of alkalinity, DOC, DON and ammonia. Despite being a different digestate sample with different initial characteristics, the model effectively described the ozonation process. The simulation results for the new digestate matrix can be seen in Figure 3.5.

An error analysis showed a level of agreement of 88% for O_3, 78% for alkalinity, 97% for DON, 89% for DOC, and 91% for NH_3. This agreement between measured and predicted data confirms the validity of the model to describe the ozonation process in different digestate matrices. Furthermore, the predicted nitrate generation achieved a comparable agreement of 93%, validating the precision of the model.
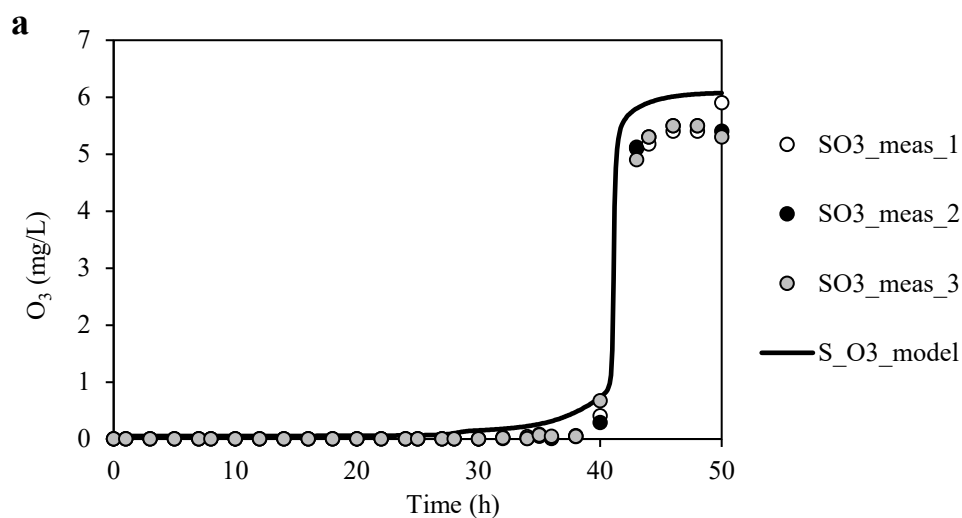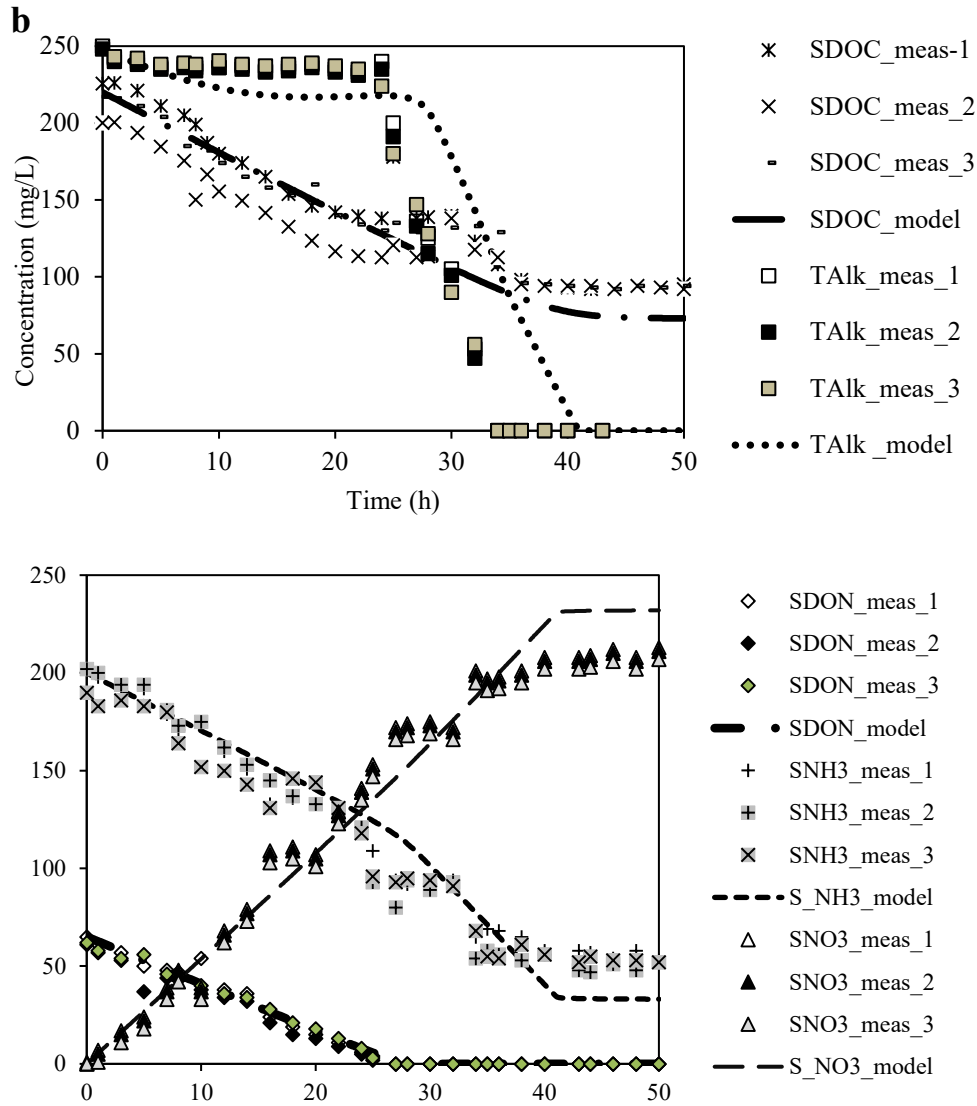
Figure 3.5. Model validation using the results of a 35h ozonation of municipal digestate in the bubble column reactor showing the concentrations of (a) dissolved ozone (S_{O3}), (b) DOC (S_{DOC}) and total alkalinity (T_{Alk}), and (c) ammonia (S_{NH3}), DON (S_{DON}), and nitrate (S_{NO3}).

3.3.6 Distinct feature of the model

This chapter introduced a simplified mathematical model to elucidate the ozonation process in digestate, thereby providing a foundational framework for subsequent model development aimed at predicting the CECs removal from high-strength water matrices (as elaborated in Chapter 4). The differences between the current model and previous models, enabling it to describe the ozone process in digestate matrices are as follows:

This model captures the distinct characteristics of digestates by incorporating ammonia reactions with ozone within the Gujer-Petersen matrix, which were previously irrelevant in traditional models applied to pure water and drinking water reported by Audenaert et al. (2010); Bühler et al. (1984); Tomiyasu et al. (1985).

Moreover, while previous ozone models were confined to a DOC concentration of up to 5 mg/L in the presence of alkalinity (Kim et al., 2020; Lei and Snyder, 2007), this model explores the interactions among high concentrations of DOC, alkalinity, and ammonia present in the digestate matrix, elucidating their simultaneous impact on ozone consumption.

Furthermore, as detailed in the next chapter, previous ozone models for CECs removal prediction rely on R_{CT} values and exposure to hydroxyl radicals (OH·) (Merkus et al., 2023; Yang et al., 2021c). However, due to variations in ozone decomposition and OH· exposure across different water matrices, experimental determination of OH· exposure prior to model application is required in previous models. To overcome this challenge, this model considered that OH· exposure is inherently linked to ozone exposure, as they arise intrinsically from the reactions of ozone with organic matter and water. Significantly, the result demonstrated that by integrating the OH· reaction implicitly into ozone exposure, the model effectively describes the ozonation of digestate and the subsequent oxidation of DOC, DON, ammonia, and alkalinity conversion. This allows for the development of a model for CECs removal independent of experimental work to determine R_{CT}, and OH· exposure.

3.4 CONCLUSIONS

This chapter provides fundamental knowledge on the ozonation process in a complex water matrix such as digestate. The main conclusions of this study are:

1. The model is able to describe the ozone consumption profiles in digestate.

2. The model describes the oxidation of the main components in digestate by ozone, their interaction with other components, and the effect of buffer capacity on the ozonation process.

3. The model was successfully validated with different high-strength digestate samples. Additionally, it proved to be highly effective to describe the ozonation of lower-strength water matrices, down to concentrations as low as 14 mg DOC L^{-1}.

4

MODEL DEVELOPMENT FOR PREDICTING REMOVAL OF CONTAMINANTS OF EMERGING CONCERN

This chapter builds upon the calibrated model from the previous chapter to develop its application to predict removal of persistent CECs. In this chapter, the model was developed by incorporating the removal of ibuprofen (IBU) as a representative for persistent CECs. To assess the individual and combined effect of matrix components on IBU removal, the ozonation process was carried out in nine various water matrices. In single-component water matrix, DON-N showed the most inhibitory effect; with 32% less removal compared to demineralized water (DW). In a dual-component water matrix, the combination of DON-N and alkalinity demonstrated the highest inhibition with only 45% of IBU removal. In a multi-component water matrix, the interaction of matrix component showed a positive effect in comparison with a dual-component water matrix, resulting in 90% IBU removal within 1-h treatment. The inhibition constant of each matrix component on IBU removal was estimated by the parameter estimation tool in Aquasim software. The result of parameter estimation in the model was correlated with the experimental data, showing that DON-N has the highest inhibitory effects ($K\_i\_DON = 0.23$ mg NL^{-1}). The model provides a robust tool for predicting CECs in various water matrices, fostering advances in ozone treatment optimization.

4.1 INTRODUCTION

Anaerobic digestion (AD) is a promising biological process to produce bioenergy from organic waste (Wang et al., 2023b). Additionally, the liquid effluent of AD, known as digestate, represents a valuable source of nutrients with significant agronomic potential. However, the direct application of digestate is restricted in several countries regarding the potential harm to the environment including the presence of contaminants of emerging concern (CECs) (Yang et al., 2022a).

To mitigate the potential environmental hazards associated with CECs, an O_3-based advanced oxidation process (AOPs) was recently applied to remove these contaminants from digestate (Moradi et al., 2023). Notably, while O_3-based AOPs have shown promising result in removing CECs from liquid digestate, a significant difference in removal efficiency was observed when comparing the removal pattern in water and digestate matrix. It implies the influence of the matrix on CECs removal. For instance, the removal of ibuprofen in water required an ozone dose of 0.52 mg O_3/mg DOC, while the presence of the digestate matrix components increased the O_3 required dose to 1.11 mg O_3/mg DOC.

The impact of the water matrix on CECs removal during ozonation in various water systems has been extensively reported (Asghar et al., 2022; Lim et al., 2022). For example, Cruz-Alcalde et al. (2020) reported a competitive effect of organic matter in increasing the ozone demand in wastewater. Also, Merkus et al. (2023) highlighted the promoting effect of alkalinity in degradation of certain micropollutants.

With ozone being an expensive treatment, it is important to estimate the impact of water matrix on the CECs removal prior to the experimental work. It helps to determine ozone dose required for CECs removal and decide about the cost-effectiveness of the process. The current approach to assess the effect of the water matrix on ozonation mainly focuses on the formation of hydroxyl radicals (OH$^\bullet$) and the scavenging effect of water matrix component on OH$^\bullet$ radicals. In this approach, the impact of the water matrix is characterized by the R_{CT} value, as described in Equation (4.1)

$$R_{CT} = \frac{\int OH \cdot dt}{\int O_3 \, dt} \qquad\qquad (4.1)$$

Where, $\int O_3$ is ozone exposure and $\int OH^\bullet$ is hydroxyl radical exposure (Lado Ribeiro et al., 2019). O_3 and OH$^\bullet$ exposures are determined by specific methods, such as mass balance in continuous ozone reactors or the indigo method in batch reactors, as well as application of indicator compounds like pCBA (Merkus et al., 2023). This approach has been applied to various water matrix to determine R_{CT} and incorporate its value, in addition to kinetic

rate constant of CECs, in prediction the abatement of CECs as per Equation (4.2) (He et al., 2022; Kim et al., 2020; Moradi et al., 2023).

$$-ln\frac{C_t}{C_0} = (k_{O3} + R_{CT}\ k_{OH^{\cdot}}) \int_0^t O_3 dt \qquad\qquad (4.2)$$

Where, C_t and C_0 are the concentration of certain compound at time t and time 0, k_{O3} and $k_{OH^{\cdot}}$ are the kinetic rate constant of certain CECs in reaction with O_3 and $OH^{\cdot}$, respectively.

The limitation with this approach to predict the abatement of certain CECs is that R_{CT} value is different in various water matrix. Therefore, an experiment to determine R_{CT} in each water matrix is needed prior to predicting the CECs removal. Furthermore, the rate constant values (k_{O3} and $k_{OH^{\cdot}}$) are not known for all the CECs (Antoniou et al., 2013). Besides, this approach has been applied for lower-strength water matrix, in compare to digestate. According to the recent review papers (Asghar et al., 2022), the impact of water matrix on CECs removal limits to a DOC range of 5 to 48 mg L^{-1}. In high-strength water matrix such as digestate, the ozone exposure for CECs removal depends on not only the kinetic rate, but also to the interactions between matrix components and their ozone consumption yield, as described in previous chapter. Furthermore, research revealed that concentration of scavengers in water matrix might affect the estimation of R_{CT} (Merkus et al., 2023). Therefore, the current approach might not be applicable to predict the effect of water matrix on CECs removal from digestate. More research is needed to explore the availability of ozone for CECs removal, along with the individual and synergistic effects of different matrix components on CECs removal from high-strength water matrix.

Ideally, the development of a model should aim to predict the removal of CECs across diverse water matrices without the necessity of determining any parameters, such as R_{CT}. In pursuit of this objectives, the previous chapter described the interaction of different digestate components with ozone during long-term ozonation. The model revealed a strong dependency of ozone consumption on the concentration of key variables, including NH_3-N, DON-N, DOC, and alkalinity. However, it did not address CECs removal and the effects of individual compounds on the removal process. To bridge this gap, this chapter aims to (i) develop the model by incorporating CECs removal, to predict CECs abatement in various water matrix only by introducing the concentrations of organic and inorganic carbon and nitrogen to the model, (ii) assess the individual and combined effects of each matrix component on CECs removal and mathematically determine the inhibition factor of each matrix component on removal rate.

4.2 MATERIALS AND METHODS

4.2.1 Chemicals

Doxycycline hyclate (DOX), tetracycline (TCN), chlortetracycline hydrochloride (CTC), oxytetracycline (OTC), sulfamethoxazole (SMX), sulfamethazine (SMN), 17β-Estradiol (17-β-EST), ibuprofen (IBU), naproxen (NPX), bisphenol A (BPA), and diclofenac sodium (DIC) were purchased from Sigma Aldrich, Chemie GmbH, Germany. $NaHCO_3$, Na_2CO_3, NH_4Cl, and Tetramethylethylenediamine (TEMDA), all HPLC grade, were purchased from Sigma Aldrich, Chemie GmbH, Germany.

4.2.2 Experimental

To assess the individual and combined effect of the water matrix on CECs removal, 9 experiments were conducted in the absence and presence of alkalinity, ammonia, and DON/DOC. These water matrixes are as following:

No-competitor water matrix: Demineralized water (DW) was spiked only by CECs.

Single-compound water matrix: DW was spiked by CECs and one of the studied matrix components including ammonia, alkalinity, DON/DOC.

Dual-compound water matrix: DW was spiked by CECs and two of the studied matrix components.

Multi-compound water matrix: DW was spiked by CECs and all the studied matrix component. Also, an experiment was conducted with liquid digestate matrix collected from a pig-manure biogas plant located in Kozani, Greece, and filtered down to 0.45 micron.

The concentration of each component was chosen to be in the same range as for real digestate matrix. To prepare these synthetic water matrixes, a mixture of $NaHCO_3$ and Na_2CO_3 were applied as a source for alkalinity to reach a concentration of 200 mg $CaCO_3$/L at pH=8. NH_4Cl was used as a source for ammonia to reach a concentration of 100 mg N/L. TEMDA was used as a source for DON-N to reach a final concentration of 50 mg N/L. The concentration of CECs was 100 μg/L in each water sample. A summary of experimental work is illustrated in Table 4.1.

Table 4.1. Experimental design for pharmaceutical removal during ozonation of single-compound, dual-compound, and multi-compound water matrix

Exp.	Alkalinity (mg L^{-1})	NH$_3$-N (mg L^{-1})	DON-N (mg L^{-1})
1	-	-	-
2	200	-	-
3	-	100	-
4	-	-	50
5	200	100	-
6	-	100	50
7	200	-	50
8	200	100	50
9	Real digestate (CaCO$_3$: 200 mg L^{-1}, NH$_3$-N: 100 mg L^{-1}, DON-N: 50 mg L^{-1})		

Ozone treatment was conducted in a bubble column reactor, where a constant supply of gaseous ozone with an initial concentration of approximately 20.5 mg L^{-1} and a flow rate of around 51 L/h was provided. Further information regarding the ozone setup can be found in chapter 2.

4.2.3 Analytical method

Ammonia (NH$_3$-N) was measured based on Standard Methods (NEN 6742) (APHA 1992) using a spectrophotometer (Perkin Elmer, UV-Vis Lambda 365, the Netherlands). Total Kjeldahl Nitrogen (TKN) was analysed by a TKN apparatus equipped with a Kjeldtherm digester (Gerhardt, Germany) and a distiller (Gerhardt, Vapodest, Germany), and the dissolved organic nitrogen (DON-N) by deducting the concentration of the background ammonia from TKN. DOC was measured by TOC analyser (Shimadzu, the Netherlands), and alkalinity (mg CaCO$_3$/L) was measured by automatic titration (Metrohm, 848 Titriano plus, Applicon, the Netherlands). Nitrate was measured by ion chromatography (ICS-1000, Dionex, the Netherlands). The CECs analysis was subcontracted to Laboratorios Tecnológicos de Levante, Valencia, Spain (Certificate nº 121/LE1782). The applied protocol for CECs analysis can be seen in detail in Chapter 2.

4.2.4 Model development

In order to develop the mathematical model for predicting CECs removal under the influence of various water matrix components, the initial calibrated model containing six mathematical equations was applied.

To assess the effectiveness of the model in predicting the removal of CECs, and determine the individual and combined effect of each matrix component on CECs removal,

ibuprofen (IBU) was selected to study within the model. IBU was chosen due to its persistency, proved by experimental work, that allows for precise monitoring across various ozonation time intervals. The kinetic removal of IBU was added to the initial model. This addition involved certain adjustments to account for the impact of different water matrix components on IBU removal. Notably, these adjustments include the incorporation of an inhibition factor, I_min, which characterizes the inhibitory effect of the water matrix components. The variables and stochiometric parameter used in the model can be seen in Table 4.2, and the Petersen matrix in Table 4.3.

Table 4.2. State variables, kinetic parameters and stochiometric coefficients applied in the mathematical model

Symbol	Description	Unit
State variables		
S_{O3}	Dissolved O_3 concentration	mg O_3 L^{-1}
S_{DOC}	Dissolved organic carbon concentration	mg DOC L^{-1}
S_{DON}	Dissolved organic nitrogen concentration	mg DON-N L^{-1}
S_{NH3}	Ammonia-nitrogen concentration	mg NH_3-N L^{-1}
$S_{CO3}{}^{2-}$	Alkalinity concentration in the form of carbonate	mg L^{-1}
$S_{HCO3}{}^{-}$	Alkalinity concentration in the form of bicarbonate	mg L^{-1}
S_{H+}	Generated hydrogen ions	mg L^{-1}
S_{NO3}	Nitrate-nitrogen concentration	mg NO_3-N L^{-1}
S_{DOC_r}	Refractory DOC concentration	mg DOC L^{-1}
T_{Alk}	Total alkalinity concentration	mg $CaCO_3$ L^{-1}
Kinetic parameter		
k_La	Volumetric mass transfer coefficient of ozone into water	h^{-1}
k_{DOC}	Kinetic rate constant of DOC conversion	L mg^{-1} h^{-1}
k_{DON}	Kinetic rate constant of DON-N conversion	L mg^{-1} h^{-1}
k_{NH3}	Kinetic rate constant of NH_3-N conversion	L mg^{-1} h^{-1}

k_{CO3}	Kinetic rate constant of CO_3^{2-} conversion	L mg^{-1} h^{-1}
k_{HCO3}	Kinetic rate constant of HCO_3^- conversion	L mg^{-1} h^{-1}
k_{IBU}	Kinetic rate constant of IBU conversion	L mg^{-1} h^{-1}
K_{DOC}	Half-saturation DOC concentration	mg DOC L^{-1}
K_{DON}	Half-saturation DON-N concentration	mg DON-N L^{-1}
K_{NH3}	Half-saturation NH_3-N concentration	mg NH_3-N L^{-1}
K_{O3}	Half-saturation O_3 concentration	mg O_3 L^{-1}
K_{TAlk}	Half-saturation T_{Alk} concentration	mg L^{-1}
$K_{\_i\_DOC}$	Inhibition constant of DOC on IBU removal	mg L^{-1}
$K_{\_i\_NH3}$	Inhibition constant of ammonia on IBU removal	mg L^{-1}
$K_{\_i\_DON}$	Inhibition constant of DON-N on IBU removal	mg L^{-1}
$K_{\_i\_TAlk}$	Inhibition constant of alkalinity on IBU removal	mg L^{-1}
I_{CaCO3}	Switch function of alkalinity	-
$I_{\_F\_DOC}$	Inhibition factor of DOC in IBU removal rate	-
$I_{\_F\_DON}$	Inhibition factor of DON-N in IBU removal rate	-
$I_{\_F\_NH3}$	Inhibition factor of NH_3-N in IBU removal rate	-
$I_{\_F\_TAlk}$	Inhibition factor of TAlk in IBU removal rate	-
$I_{\_min\_TAlk\_DOC}$	Min function to identify maximum inhibition of T_{Alk} and DOC	-
$I_{\_min\_DON\_NH3}$	Min function to identify maximum inhibition of DON-N and NH_3-N	-
I_{min}	Inhibition function of matrix components on IBU removal	-

Stochiometric parameters

Y_{O3_DOC}	Stoichiometric yield coefficient of ozone consumption for DOC conversion	mg O_3 mg DOC^{-1}
Y_{O3_DON}	Stoichiometric yield coefficient of ozone consumption for DON-N conversion	mg O_3 mg DON-N^{-1}
Y_{O3_NH3}	Stoichiometric yield coefficient of ozone consumption for NH_3-N conversion	mg O_3 mg NH_3-N^{-1}
Y_{O3_IBU}	Stoichiometric yield coefficient of ozone consumption for IBU conversion	mg O_3 mg IBU^{-1}
i_{CO3_NH3}	Alkalinity production in the DON-N oxidation process	mg CO_3^{2-} mg NH_3-N^{-1}
f_{DOC_r}	Fraction of refractory DOC	mg DOC L^{-1}

Equations	S_{O3}	S_{CO3}	S_{HCO3}	S_{H2CO3}	S_{H+}	S_{DOC}	S_{NH3}	S_{NO3}	S_{DON}	S_{DOC_r}	S_{IBU}	Eq.
Delivered O₃												
Transfer	1											(4.1)
DOM (organic C, organic N)												
$DOC+O_3 \rightarrow$ mineralization product+ DOC_r	$-Y_{O3\_DOC}$					-1				f_{DOC_r}		(4.2)
$DON+O_3 \rightarrow CO_3^{2-}+NH_3$	$-Y_{O3\_DON}$	i_{CO3_NH3}					1		-1			(4.3)
Inorganic C, N												
$NH_3+O_3 \rightarrow H^++NO_3+H_2O$	$-Y_{O3\_NH3}$				1		-1	1				(4.4)
$CO_3^{2-}+H^+ \rightarrow HCO_3^-$		-1	1		-1							(4.5)
$HCO_3^-+H+\rightarrow H_2CO_3 (H_2O+CO_2)$			- 1	1	-1							(4.6)
$IBU+O_3 \rightarrow$ product	$-Y_{O3\_IBU}$										-1	(4.7)
N		i_{CO3_NH3}					1					
charge		-2						1/14				

In Table 4.3, Equation (4.1) to Equation (4.6) describe the initial model as discussed in Chapter 3. Equation (4.7) was added to the model to define the IBU removal.

$$k_L a \left(S_{O_3^*} - S_{O_3} \right) \tag{4.1}$$

$$r_{DOC} = k_{DOC} \times \left(\frac{S_{DOC}}{(S_{DOC} + K_{DOC})} \right) \times \left(\frac{S_{O_3}}{S_{O_3} + K_{O_3}} \right) \tag{4.2}$$

$$r_{DON} = k_{DON} \times \left(\frac{S_{DON}}{(S_{DON} + K_{DON})} \right) \times \left(\frac{S_{O_3}}{S_{O_3} + K_{O_3}} \right) \tag{4.3}$$

$$r_{NH3} = k_{NH_3} \times \left(\frac{S_{NH_3}}{(S_{NH_3} + K_{NH_3})} \right) \times \left(\frac{S_{O_3}}{S_{O_3} + K_{O_3}} \right) \times I_{CaCO3} \tag{4.4}$$

$$r_{CO3} = k_{CO_3} \times \left(\frac{S_{CO_3}}{(S_{CO_3} + K_{CO_3})} \right) \tag{4.5}$$

$$r_{HCO3} = k_{HCO_3} \times \left(\frac{S_{HCO_3}}{(S_{HCO_3} + K_{HCO_3})} \right) \times \left(\frac{S_{HCO_3}}{(T_{Alk} + K_{TAlk})} \right) \tag{4.6}$$

$$r_{IBU} = k_{IBU} \times \left(\frac{S_{IBU}}{S_{IBU} + K_{IBU}} \right) \times \left(\frac{S_{O_3}}{S_{O_3} + K_{O_3}} \right) \times I_{min} \tag{4.7}$$

Where, I_{CaCO3} is the switch function showing the effect of total alkalinity on NH_3-N removal:

$$I_{CaCO3} = \frac{T_{Alk}}{T_{Alk} + K_{T_{Alk}}} \tag{4.8}$$

Where,

$$T_{Alk} \left(\frac{mg\ CaCO_3}{L} \right) = \left(\left(\frac{S_{CO_3^{2-}}}{60} \right) + \left(\frac{S_{HCO_3^-}}{61} \right) + \left(\frac{S_{H_2CO_3}}{62} \right) \right) \times 100 \tag{4.9}$$

To determine the inhibition factor of each matrix component on IBU removal, the following steps were conducted:

1. Kinetic removal of IBU was added to the initial model to include the removal of CECs, as per Equation (4.7).

2. An inhibition constant was defined for each matrix component as $K_{\_i\_DOC}$, $K_{\_i\_DON}$, $K_{\_i\_NH3}$, $K_{\_i\_TAlk}$.

3. An inhibition factor for each component was added to the model as formula variables (Equation (4.10) to Equation (4.13)):

$$I_{\_F\_NH_3} = \frac{K_{\_i\_NH_3}}{S_{NH_3} + K_{\_i\_NH_3}} \qquad (4.10)$$

$$I_{\_F\_DOC} = \frac{K_{\_i\_DOC}}{S_{DOC} + K_{\_i\_DOC}} \qquad (4.11)$$

$$I_{\_F\_DON} = \frac{K_{\_i\_DON}}{S_{DON} + K_{\_i\_DON}} \qquad (4.12)$$

$$I_{\_F\_TAlk} = \frac{K_{\_i\_TAlk}}{T_{Alk} + K_{\_i\_TAlk}} \qquad (4.13)$$

4. The "min" function in Aquasim was applied to determine the compound with highest inhibition effect on IBU removal. This function was applied for each pair including inorganic/organic nitrogen (Equation (4.14)), and inorganic/organic carbon ((Equation (4.15))

$$I\_min_{\_DON\_NH_3} = min(I_{\_F\_NH_3}, I_{\_F\_DON}) \qquad (4.14)$$

$$I\_min_{\_TAlk\_DOC} = min(I_{\_F\_TAlk}, I_{\_F\_DOC}) \qquad (4.15)$$

5. An inhibition factor (I_{min}) was added to the kinetic removal rate of IBU (Equation (4.7)), as per Equation (4.16)

$$I_{min} = min(I\_min_{\_DON\_NH_3}, I\_min_{\_TAlk\_DOC}) \qquad (4.16)$$

4.2.5 Error Analysis

An Error analysis was conducted to determine the agreement between measured and predicted concentration of IBU over the time. This agreement was determined by Normalised Root Mean Squared Deviation (NRMSD) as shown by Eq. (4.17) (Oehmen et al., 2010).

$$NRMSD = \frac{\sqrt{\frac{\sum_{i=1}^{n}(x_{meas,i} - x_{pred,i})^2}{n}}}{x_{meas,max} - x_{meas,min}} \qquad (4.17)$$

Where, x_{meas} and x_{pred} are measured and predicated IBU, $x_{meas,max}$ and $x_{meas,min}$ are the maximum and minimum measured concentration of IBU, and n is the number of data points.

4.3 RESULTS AND DISCUSSION

4.3.1 Model development

Experimental work revealed that all CECs were removed from demineralized water within 5 min (data not shown), except for IBU, which required 60 min to be completely removed. This persistent behaviour led to a comprehensive comparison of IBU removal in nine different water matrices, with IBU serving as a representative for persistent CECs. Therefore, IBU removal Equation was integrated into the previous derived model (Equation (4.7)).

The incorporation of Equation (4.7) into the initial model enabled accurate prediction of IBU removal across all the 9 studied water matrices. The agreement between predicted and observed data surpassed 91 %, with the NRMSD less than 0.09 for all the studied water matrices. Figure 4.1 illustrates the predicted and observed removal patterns for IBU, along with changes in water matrix components during 1 hour of ozonation.
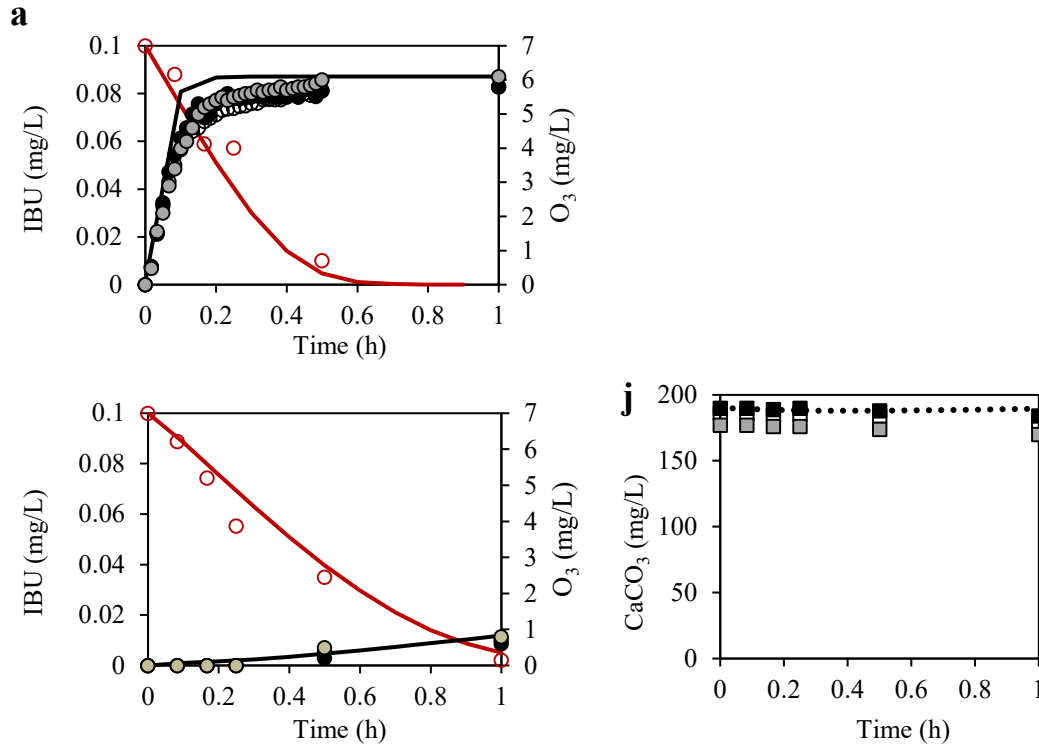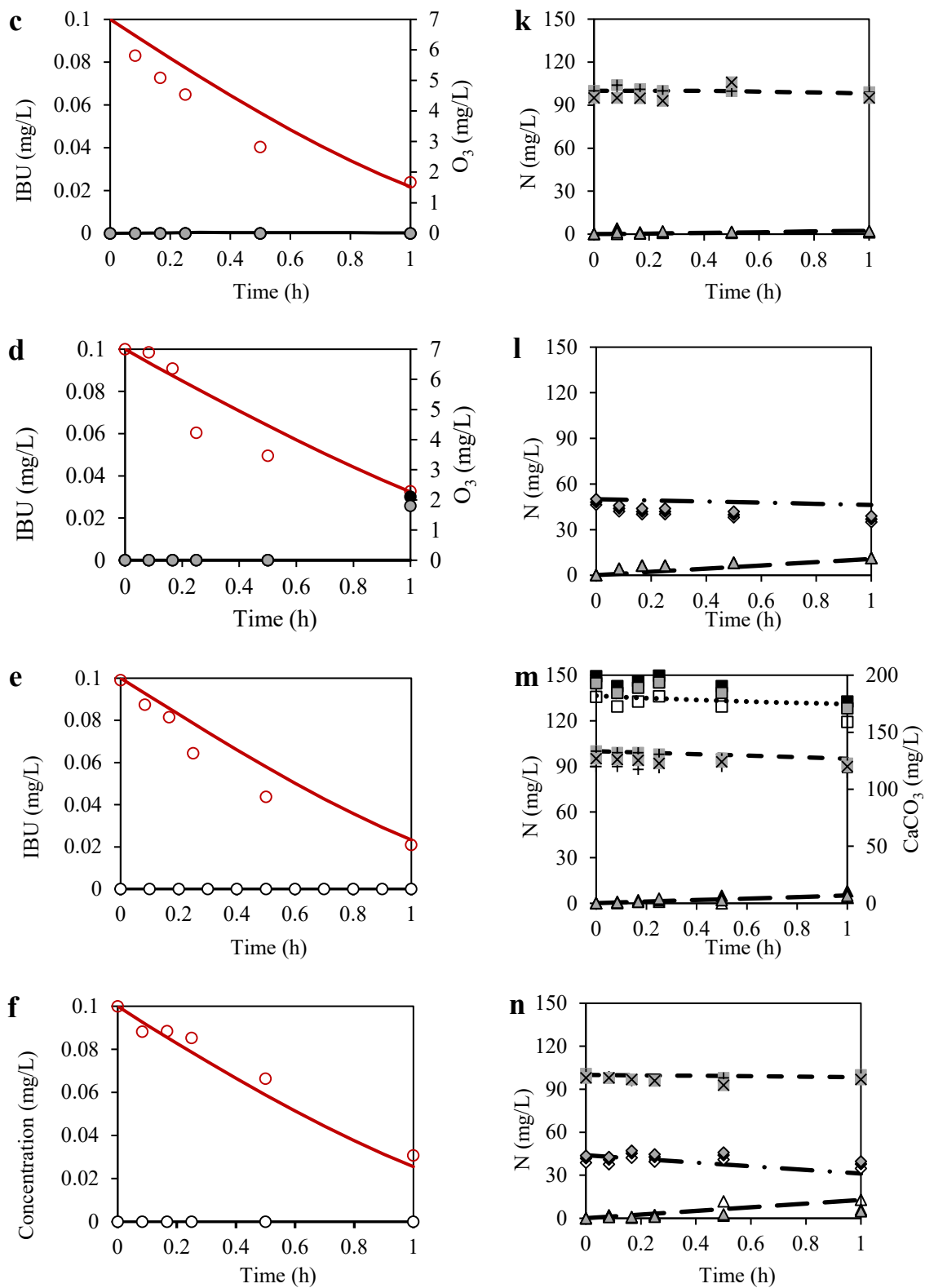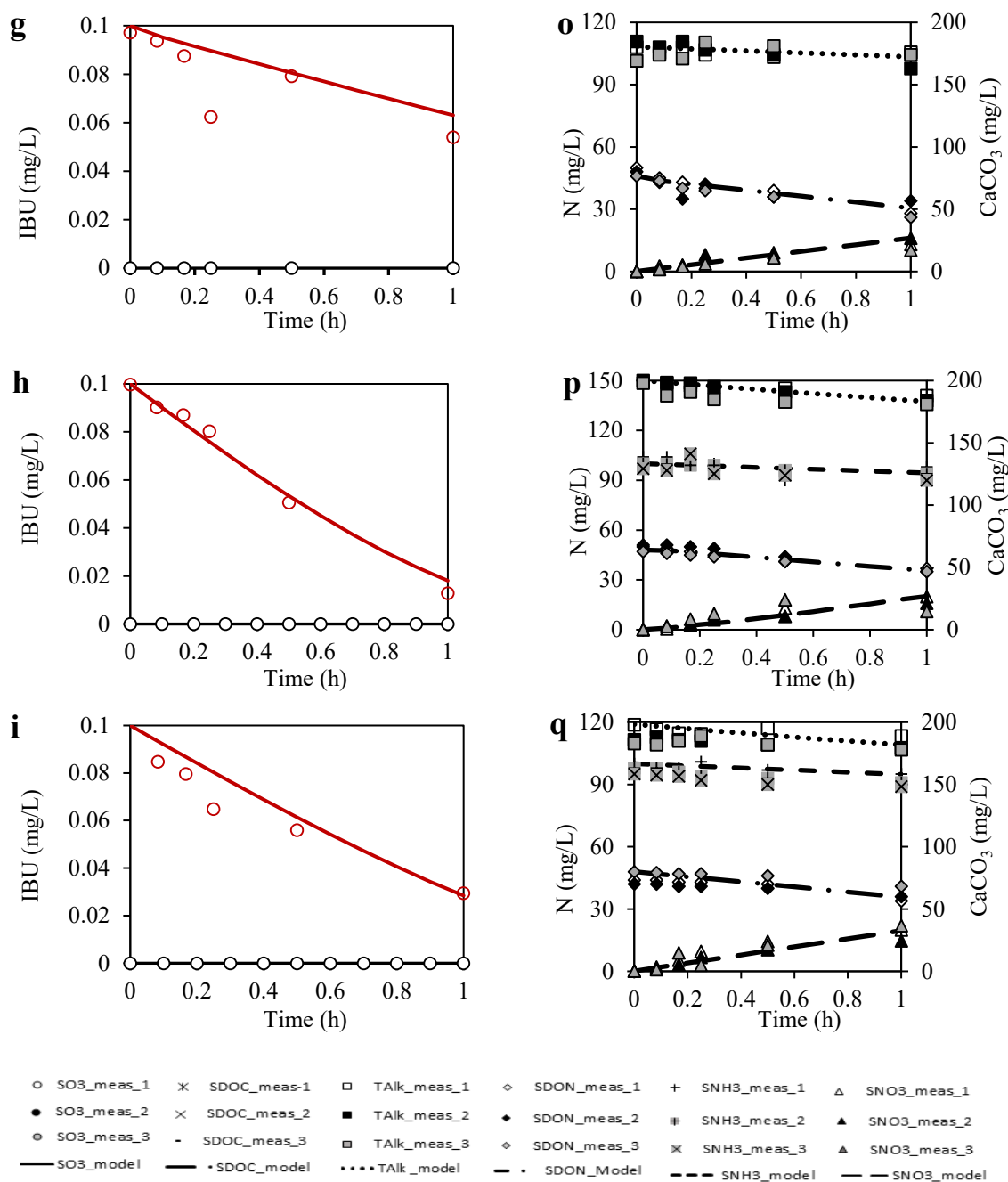
Figure 4.1 Predicted and observed data for IBU removal in (a) DW, single-compound water matrix including (b) alkalinity, (c) ammonia, (d) DON-N, dual-compound water matrix including (e) alkalinity + ammonia, (f) DON-N + ammonia, (g) alkalinity + DON-N, and multi-compound water matrix including (h) DON + ammonia + alkalinity, and (i) liquid digestate, and (j, k, l, m, n, o, p, q) transformation of DON-N, alkalinity and ammonia during 1-h ozonation of the same water matrix. (Alkalinity: 200 mg CaCO$_3$/L, Ammonia: 100 g NH$_3$-N/L, DON-N: 50 mg DON-N/L)

4.3.2 Individual and combined effect of water matrix component on IBU removal

In the single-compound water matrices, DON-N showed the strongest inhibitory effect on IBU removal, resulting in an IBU net removal of only 68% after 1 hour. Ammonia and alkalinity displayed lower inhibition, allowing for an 80%, and 98 % IBU removal within the same timeframe. In the dual-compound water matrix, the combined presence of DON-N and alkalinity exhibited the highest inhibitory effect, resulting in a 45% net removal of IBU after 1 hour. In multi-component water matrix containing DON-N, alkalinity, and ammonia, IBU net removal after 1 hour reached 90%, and in real digestate matrix, IBU net removal was 82%.

The model successfully predicted IBU removal and quantified the effect of each matrix compound on IBU removal, by incorporating the inhibition factor as "min" function (I_{min}) into the IBU removal rate (Equation (4.7)). This factor relates the removal rate of IBU to the concentrations of organic/inorganic carbon and nitrogen. The inhibition constants for each parameter were estimated using parameter estimation tool in Aquasim. Consistent with experimental findings, the model indicated that DON-N poses the highest inhibition on IBU removal with the lowest value of inhibition constant K_{i_DON} of 0.23 mg NL^{-1}, followed by ammonia (0.47 mg NL^{-1}), DOC (0.53 mg DOC L^{-1}) and alkalinity (0.84 mg $CaCO_3L^{-1}$).

The high inhibitory effect of DON-N is attributed to the presence of active electron-dense functional groups in its molecular structure, such as amines or aromatic rings, providing active sites for molecular ozone reactions (Moradi et al., 2023; Sharma and Graham, 2010). Further support for these findings comes from the work of de Vera et al. (2017), demonstrating that DON-N consumes ozone through an oxygen transfer mechanism, leading to nitrate production. This aligns with the observed nitrate production in our research in the presence of DON-N (Figure 4.1.d, 4.1.f, 4.1.g, 4.1.h and 4.1.i).

The model and experimental data indicated that alkalinity has the least impact on IBU net removal. Yet, the IBU removal rate in the presence of alkalinity (0.171 mg $L^{-1}h^{-1}$) was lower than that in DW (0.182 mg $L^{-1}h^{-1}$). The impact of carbonate species on ozonation primarily occurs through an indirect mechanism of ozonation, where ozone decomposes and generates OH$^{\bullet}$ radicals. OH$^{\bullet}$ radicals possess higher oxidation capacity (2.7 V) than ozone (2.08 V) and effectively eliminate a broad spectrum of organic matter (Rekhate and Srivastava, 2020; Wang and Wang, 2020). The presence of alkalinity scavenges OH$^{\bullet}$ radicals, yielding carbonate radicals with a lower redox potential (1.57 V) (Yan et al., 2019) than that of OH$^{\bullet}$ radicals. Consequently, the reaction of OH$^{\bullet}$ radicals with carbonate species adversely affects the removal of target compounds due to the less availability of OH$^{\bullet}$ radicals (Asghar et al., 2022; Balachandran et al., 2014). This finding is in alignment with the observed decrease in OH$^{\bullet}$ generation reported by Balachandran et al. (2014) in the presence of carbonate species in deionized water. It is further

supported by the findings of Javier Rivas et al. (2011) who reported an inhibitory effect of alkalinity on the ozonation of secondary effluent.

The combination of DON-N and alkalinity introduced a dual impact, combining the competition effect of DON-N in direct mechanism, and scavenging effect of carbonate species in indirect mechanism. This combination resulted in the highest inhibition observed for IBU removal, with a rate of 0.152 mg $L^{-1}h^{-1}$ (Figure 4.1.g).

Notably, in a multi-compound water matrix (Figure 4.1.h, and 4.1.i), the inhibitory effect of compounds on IBU removal was less than in a dual-compound matrix. Specifically, in the presence of both DON-N and alkalinity, the IBU net removal was only 45%. However, in a more complex composition involving DON-N, alkalinity, and ammonia with the same concentration as in dual-compound water matrix, the IBU net removal significantly increased to 82%. This substantial improvement can be attributed to the strong impact of ammonia in the ozonation of high-strength water matrix. As detailed in the previous chapter, the reaction of ammonia with ozone produces H^+, which engages in neutralization reactions with alkalinity (Equation (4.5) and Equation (4.6)). Consequently, the scavenger load, posed by alkalinity, in the water matrix is lower in the presence of ammonia, allowing the potential $OH^\bullet$ radicals to contribute more effectively to IBU removal. Further support of this findings comes from previous investigations that showed the concurrent decrease in alkalinity along with ammonia removal during ozonation (Tanaka and Matsumura, 2003).

During the model calibration in the previous chapter, it was demonstrated that ammonia exerts a significant influence on ozone consumption rate, highlighting the competitive nature of ammonia in ozone consumption. This competition effect, evident in a single-compound water matrix (Figure 4.1.c), led to a decrease in IBU removal rate to 77%, compared to complete removal in DW. In a dual-compound water matrix with ammonia and alkalinity, the net removal of IBU slightly increased to 80% (Figure 4.1.e), likely attributed to the aforementioned neutralization processes and more availability of generated $OH^\bullet$ radicals.

4.3.3 Transformation of water matrix during 1-h ozonation

Dissolved ozone level was negligible in all water matrices except for DW. This suggests that the transferred ozone into the liquid was rapidly consumed by water matrix components, even in single-compound water matrices.

Alkalinity dropped in the water matrix containing alkalinity and ammonia, due to the above-mentioned neutralization process in the presence of ammonia. This change was 12% in dual-compound water matrix (Figure 4.1.m) and 10% in multi-compound water matrix (Figure 4.1.p, and 4.2.q).

Regarding DON-N inhibition, competition played a significant role. In water matrix containing DON-N, more inhibition was observed on IBU removal. In a single-compound water matrix containing DON-N, an average of 12 mg NO_3-NL^{-1} was generated (Figure 4.1.I). In comparison, ammonia in a single-compound water matrix generated only 1 mg NO_3-NL^{-1} (Figure 4.1.l). In a dual-compound water matrix containing DON-N and ammonia, nitrate generation remained the same as in the absence of ammonia (Figure 4.1.n), despite having two nitrogen sources available for oxidation. However, in a multi-component water matrix (DON-N, NH_3-N, alkalinity) and digestate, nitrate generation increased to 16 and 22 mg NO_3-NL^{-1}, respectively (Figure 4.1.p and 4.1.q). This is attributed to the buffer effect of alkalinity on ammonia oxidation, as explained in the previous chapter. Nitrate generation occurs through two processes as per Equation (4.3) and Equation (4.4). The second process is highly dependent on the presence of alkalinity. In its absence, ammonia oxidation is limited, aligning with findings reported by (Yang and Liu, 2022), and consistent with this study.

4.4 CONCLUSION

This chapter presented a mathematical model designed for predicting the oxidation of persistent CECs during ozonation. The model predictions rely solely on fundamental water matrix characterizations as inputs, including the initial concentrations of organic and inorganic carbon and nitrogen. Unlike other prediction models that often necessitate preliminary experimental work, this model stands out by eliminating such prerequisites, particularly the determination of parameters like R_{CT}.

The primary focus of this study was on elucidating inhibitory factors that impact the removal of persistent CECs during the ozonation process. Remarkably, ibuprofen removal predictions demonstrated high accuracy across diverse water matrices, achieving an agreement of over 91% for all considered matrices.

Among the matrix components, DON-N exhibited the most inhibitory effect, with a K_i_DON (Inhibition Constant for DON-N) of 0.23 mg NL^{-1}. Following DON-N, ammonia, DOC, and alkalinity also exerted inhibitory influences. In scenarios involving dual-compound water matrices, the combined presence of DON and alkalinity resulted in the most substantial inhibition of IBU removal, resulting in a 65% less net removal.

4.5 ANNEXES

Annex 4.5.1. Removal of various CECs in single, dual and multi-components water matrix
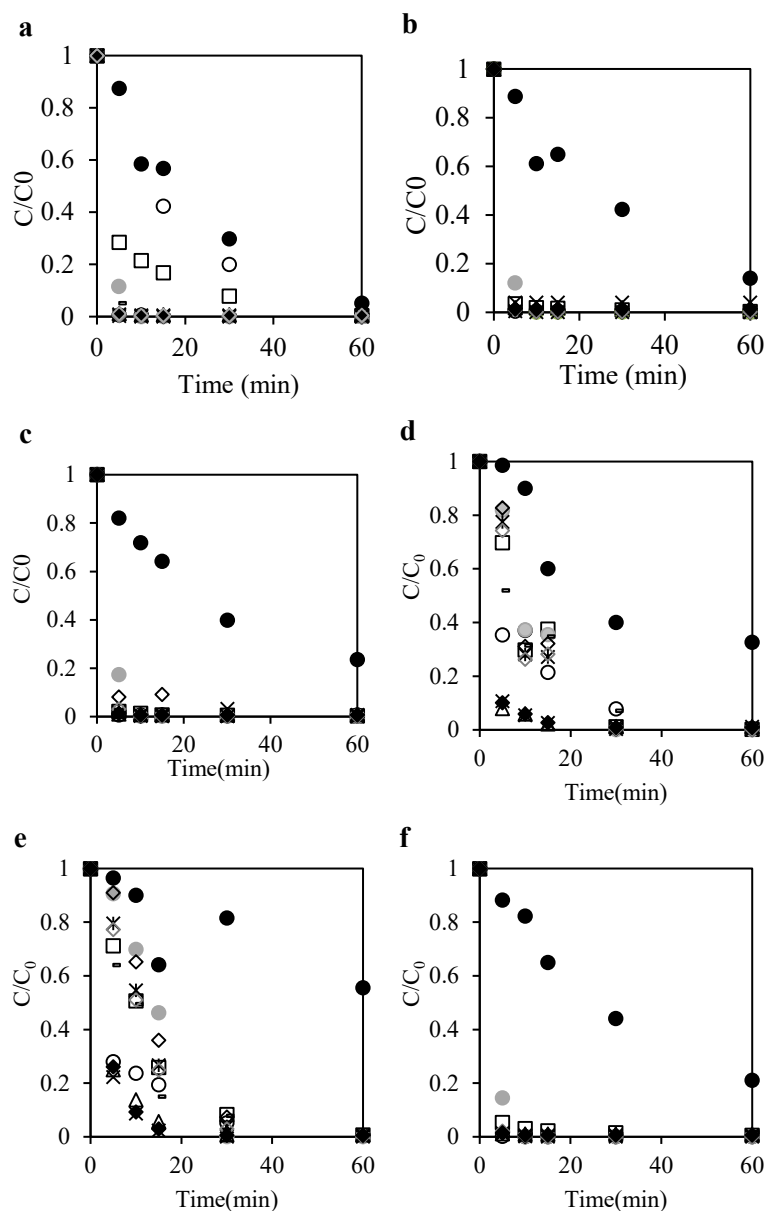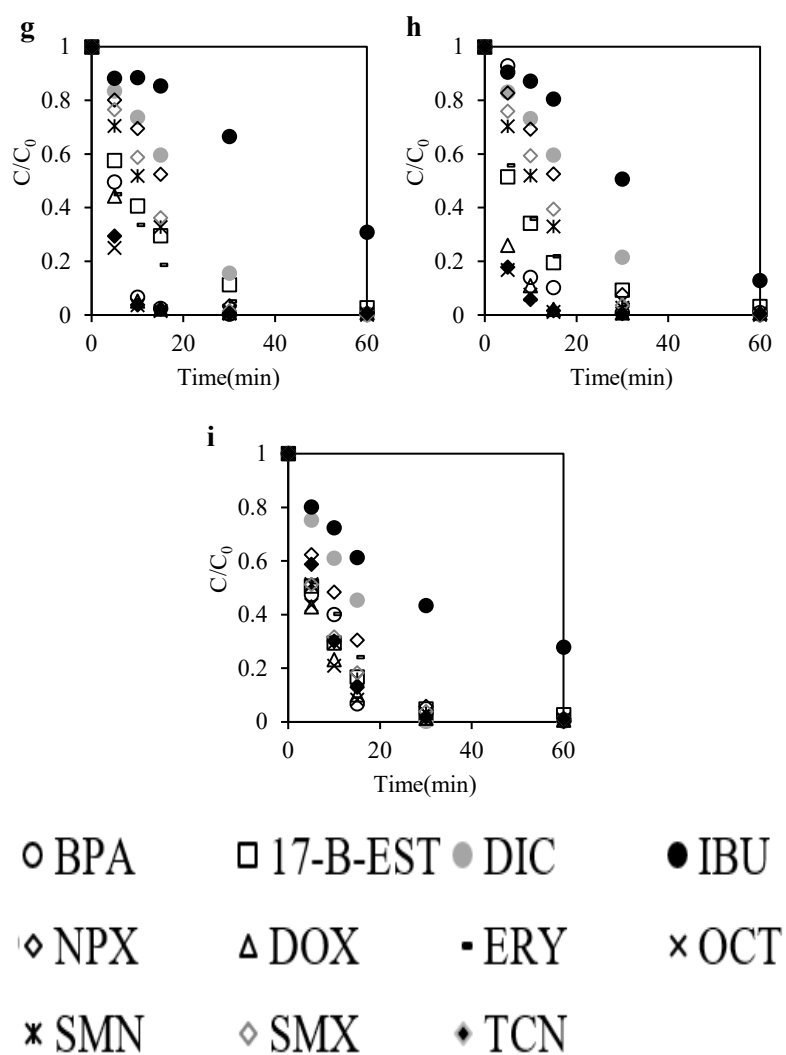
Figure A4.1. CECs removal during 1 h ozonation with (a) no competition, and in competition with single compound including (b) alkalinity, (c) ammonia, (d) DON-N, dual compounds including (e) DON-N and Alkalinity, (f) ammonia and alkalinity, (g) DON-N and ammonia, multi compound including (h) DON-N, alkalinity and ammonia, and (i) in the digestate supernatant. Alkalinity:200 mg/L, DON-N: 50 mg/L, am

5

PRACTICAL APPLICATION OF UVOX REDOX® FOR CECS REMOVAL FROM LIQUID DIGESTATE

This chapter explores the efficacy of a novel UV/ozone-based technology, UVOX Redox®, in removing prevalent pharmaceuticals, including antibiotics and non-steroidal anti-inflammatory drugs (NSAIDs), from the digestate of two biogas plants. In both cases, UVOX showed to be a feasible solution for pharmaceutical removal from digestate. Addition of hydrogen peroxide further increased the process efficiency, achieving $> 90\%$ removal of all compounds within an hour. The energy per order (E_{EO}) value for all the studied pharmaceuticals was less than the reported median E_{EO} for O_3 and UV treatment, showcasing notable energy efficiency in UVOX technology. Moreover, the research highlights that the presence of ions augments the removal efficiency when applying the UVOX technology. In addition, the research results revealed a significant correlation between the effectiveness of the UVOX technology and UV transmittance, with R^2 exceeding 90% for pharmaceuticals and 75% for Dissolved Organic Carbon (DOC). This finding suggests that UV transmittance can serve as a viable surrogate method for implementing this advanced oxidation process in practical applications.

5.1 INTRODUCTION

Organic waste constitutes a substantial proportion of global waste, averaging 46%, with varying rates across different countries (Worldbank.org). Anaerobic digestion (AD) plants present a sustainable solution by converting organic waste into renewable energy and valuable nutrients. The produced digestate is a nutrient-rich resource with potential applications in agriculture, serving as a fertilizer, irrigation fluid, and soil conditioner (Wang and Lee, 2021). However, the direct application of digestate to soil or its discharge can lead to undesirable consequences, including NH_3 and N_2O emissions (Crolla et al., 2013), acidification, eutrophication, and reducing worm populations through high ammonium-N loading rates (Moinard et al., 2021).

Furthermore, over the past few decades, the use of active pharmaceutical compounds such as antibiotics, non-steroidal anti-inflammatory drugs (NSAIDs), and hormones in farming for animal growth and disease control has been significantly increased (Kasumba et al., 2020; Nurk et al., 2019; Widyasari-Mehta et al., 2016). These compounds are typically non-biodegradable, with only 10-20% assimilated by animals. The concentration of these compounds in livestock manure varies between several to 15200 μg/kg (Yang et al., 2022b). During anaerobic digestion process of livestock manure, pharmaceutical can be removed from liquid phase by biodegradation or sorption onto biological sludge (Liu et al., 2018; Yang et al., 2022b). However, sorption is a phase transfer mechanism and cannot exclude the risk of pharmaceutical discharge into the environment. Furthermore, biodegradation fails to remove non-biodegradable pharmaceutical such as chlortetracycline (Qiang et al., 2019). Therefore, anaerobic digestion is reported to have a moderate effect on pharmaceutical with an average of 47 % to 72 % for different antibiotics for instance (Yang et al., 2022b). Different approaches including additives (Zhang et al., 2018; Zhou et al., 2021), pretreatment such as thermal method (Yin et al., 2020), advanced anaerobic system and co-digestion methods (Huang et al., 2018) have been investigated to improve removal of antibiotics during anaerobic digestion process. Although these methods were successful in increasing antibiotic removal during anaerobic digestion process, a significant portion of these compounds still is reported to end up in digestate derived from manure and slurries, with concentrations ranging from 120 μg/L for tetracycline to 66,400 μg/L for chlortetracycline, for instance (Kasumba et al., 2020; Nurk et al., 2019). Therefore, the discharge of digestate can pose potential environmental hazards and contribute to development of antibiotic-resistant bacteria (Gurmessa et al., 2020; Reygaert, 2018).

Furthermore, due to a lack of an available and cost-effective technology, turning digestate into an environmentally-friendly biofertilizer is not an option in different countries. Consequently, the only available alternative for disposing of digestate is to send it to landfills, which may not be an ideal solution from an environmental perspective.

To address these issues, a Novel Organic recovery using Mobil Advanced technology (NOMAD) was developed to serve decentralized rural plants, small treatment plants and small-scale AD markets. NOMAD streamlines the handling of digestate by installing all necessary technologies into two trucks, making it mobile across various AD plants. The NOMAD process encompasses several key steps, including pasteurization, solid-liquid separation, filtration, nutrient recovery, pharmaceutical removal through UVOX Redox® technology (a novel UV/O_3 system), and additional treatment such as reverse osmosis (RO), if necessary.

This hybrid technology has been already tested in several AD plants across Europe. This research specifically focuses on evaluating the effectiveness of UVOX Redox® in removing pharmaceuticals from digestate in two distinct AD plants. The first study site, located in Kozani, Greece, is a pig manure biogas plant that receives animal waste, urine, manure, and corn silage as feedstock. The resulting digestate is presently utilized as a land amendment by local farmers. The second site, situated in Malta, is associated with a sewage treatment plant where the biogas plant receives sludge from the treatment of urban wastewater, farmyard waste, and urban waste from the sewer collection network. The generated digestate is currently disposed of through landfilling.

The UVOX Redox® system is an UV-based Advanced oxidation process (AOPs) that employs a combination of ozone and UV light to enhance the degradation of pharmaceutical compounds, thereby increasing their removal efficiency. Among all existing methods, AOPs are known as the most effective techniques to remove persistent contaminants of emerging concern, which are not removed in biological treatment (De la Cruz et al., 2012; Dong et al., 2022; Kulišťáková, 2023). AOPs are characterized by generation of reactive oxidative species (ROS) such as OH$^\bullet$ radicals. Ozone, an AOP-like process, has demonstrated effectiveness in removing pharmaceuticals from both drinking water and wastewater (Bui et al., 2016; de Oliveira et al., 2020; Hansen et al., 2016). However, there are some limitations associated with ozonation, for instance low mineralization (Miklos et al., 2018). Furthermore, O_3 is less effective in degradation of organic compounds without electron-rich functional group (Lee et al., 2013). To overcome these limitations, the integration and combination of O_3 with an activated method has been suggested (Saeid et al., 2018). For instance, integration of O_3 with UV (254 nm) increases the degradation efficiency of organic matter (Gassie and Englehardt, 2019; Lin et al., 2014). In the presence of UV light, O_3 decomposes to form OH$^\bullet$ radicals that have 10^6 to 10^{12} times higher oxidation capacity than O_3 (Miklos et al., 2018; Von Sonntag, 2008). This integration combines two degradation pathways including the reaction of molecular ozone with organic matter, and the reaction of generated OH$^\bullet$ radicals with organic matter (Coha et al., 2021; Liu et al., 2021). The combination of UV/O_3 has been successfully applied for TOC removal (Keen et al., 2016; Wols and Hofman-Caris, 2012), and pharmaceutical removal from wastewater (Khan et al., 2020). The main drawback of this application is that both the ozone generator and the UV source

have a high electricity demand which results in higher cost (Miklos et al., 2018). The UVOX Redox®, however, is a novel UV/O_3 system that has been recently invented for further commercially application and development of AOPs. This innovative technology generates ozone from atmospheric oxygen through the use of a UV lamp, eliminating the need for oxygen supply tanks and ozone generators. Consequently, it significantly reduces both the electricity demand and the associated costs related to ozone generation (Ekowati et al., 2019). Promisingly, the UVOX Redox® system has undergone recent testing in swimming pool water, where it has been reported to effectively remove certain pharmaceutical compounds during treatment (Ekowati et al., 2019).

While promising, the UVOX Redox® technology has never been evaluated for the removal of pharmaceuticals from a high-strength water matrix. Digestate liquids are characterized by a substantial load of organic and inorganic materials, whereas the concentration of pharmaceuticals is significantly lower by several orders of magnitude. These organic and inorganic compounds can potentially impede the efficiency of UVOX Redox® through multiple mechanisms, including obstructing UV penetration and OH$^\bullet$ generation, influencing ozone solubility, as well as their competition effect to consume oxidative species. Therefore, the objective of this research was to (i) evaluate the effectiveness of UVOX Redox® for pharmaceutical removal from digestate in different AD plants and its role within the NOMAD technology, (ii) evaluate the contribution of OH$^\bullet$ radicals in the removal efficiency, (iii) optimize technology sequence in the NOMAD technology, and (iv) propose an easily-monitored surrogate method for removal efficiency.

In this study, the selection of pharmaceuticals included the most frequently utilized veterinary antibiotics in food processing animals, which encompassed doxycycline (DOX), tetracycline (TCN), oxytetracycline (OTC), sulfamethoxazole (SMX), sulfamethazine (SMN) (Yang et al., 2022a), as well as the widespread NSAIDs present in different types of sludge, including ibuprofen (IBU) and diclofenac (DIC) (Ajibola et al., 2021).

5.2 MATERIALS AND METHODS

5.2.1 Chemicals

All pharmaceuticals including doxycycline (DOX), tetracycline (TCN), oxytetracycline (OTC), sulfamethoxazole (SMX), sulfamethazine (SMN), ibuprofen (IBU), and diclofenac (DIC) were purchased from Sigma Aldrich, Chemie GmbH (Germany). Prior to the experiment, the digestate sample was spiked by these compounds to a final concentration of 100 μg/L each.

5.2.2 UVOX Redox® equipment within the NOMAD truck

The UVOX Redox® was purchased from WAPURE International GmbH (Germany) and installed on the truck as a part of the novel mobile technology for digestate treatment. This equipment consists of a UV chamber constructed from PE100 HDPE, four UV lamps with a total power consumption of 800 W housed within a quartz tube, an O_3-air Xyclon injector device, completed with a booster pump, a power module and relevant connecting cables. The setup also incorporates a UV-compact measurement device designed to record the percentage of UV light (254 nm) transmitted through a 10 mm liquid sample, hereafter referred to as UVT at T10.

The UVOX Redox® technology utilizes powerful UV lights to generate strong oxidative species. The process begins with the introduction of air into the inner compartment of the UVOX chamber, facilitated by a venturi (Xyclon injector) that creates a vacuum effect. Subsequently, atmospheric oxygen is converted into ozone as it is exposed to UV lamps emitting light at a wavelength of 185 nm. The resultant ozonated gas is then injected into the water via the Xyclon injector system. The water and gas mixture are subjected to further UV light exposure (254 nm) within the UVOX outer reaction chamber.

Through this process, ozone in the water generates $OH^{\bullet}$ radicals, leading to a notable increase in the relative redox potential from 2.07 (for O_3) to 2.8 (for $OH^{\bullet}$).

Before commencing the experiments, a baseline measurement was conducted using tap water, revealing a maximum UVT of 95% at T10 and a maximum dissolved ozone concentration of 2 mg L^{-1} over a 5-hour duration. A simplified process-flow diagram of the NOMAD truck and the different compartments of the UVOX Redox® is shown in Figure 5.1.
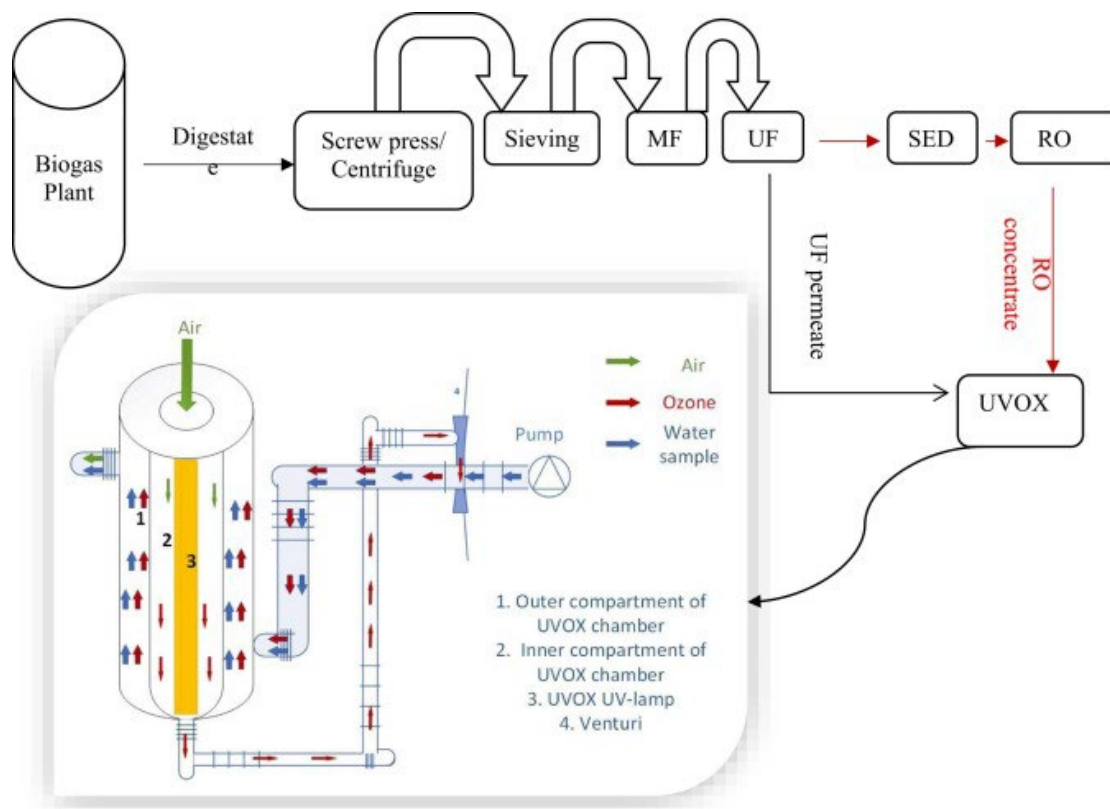
Figure 5.1. Simplified process-flow diagram of the different technologies in the NOMAD truck and the compartments and ozone generation mechanism of the UVOX Redox® technology. MF: Microfiltration, UF: Ultrafiltration, SED: Selective electrodialysis (nutrient recovery module), RO: Reverse osmosis. (Adapted from (UVOX.com)). The sequence of technologies before UVOX is shown by red- arrow in the first case study, and by black arrow in the second case study.

5.2.3 Design of experiments per study sites

The experiments were conducted at two distinct study sites, each with its unique design, aimed at assessing the effectiveness of the UVOX system in pharmaceutical removal. To determine its feasibility and establish the optimal treatment sequence within the mobile unit, the application of UVOX was executed on the digestate liquid after nutrient recovery and ion removal in the first case study (Greece), and before nutrient recovery in the second case study (Malta). In both study sites, the UVOX experiment was carried out in a recirculating mode, processing a minimum of 450 litters of the sample with flow rate of 13.5 m^3h^{-1} within a 22-hour timeframe. The experimental design for each study site is outlined as follows:

Case study 1: Pig manure biogas plant, Kozani, Greece

In the first biogas plant in Greece, the experiment was designed to assess the efficiency of UVOX system to remove pharmaceuticals, and the potential effect of hydrogen peroxide. This set of experiment was conducted after nutrient recovery module. Therefore, following the anaerobic digestion process, the digestate was pumped out of the fermenter and directed into a compressor separator device equipped with 0.5 mm slits situated on-site. The resulting liquid digestate was then collected and transferred to truck containers for further separation. This separation process involved a series of sieves, followed by microfiltration (MF) down to 1 micron and ultrafiltration (UF). Subsequently, the liquid fraction underwent treatment in a selective electrodialysis (SED) module. This specialized module was constructed by combining standard ion exchange membranes and monovalent selective ion exchange membranes to fractionate and concentrate nutrient ions from the digestate, particularly for struvite recovery.

The effluent from the SED process then underwent reverse osmosis (RO), and the resulting RO concentrate was utilized in the UVOX experiment. Notably, the RO concentrate was characterized by a substantial load of organic material and exhibited coloration, resulting in an initial UV transmittance reading of zero in the UVOX system. Consequently, the RO concentrate was diluted until the UV intensity reached a minimum threshold, as detected by the UV-compact sensor. The working solution, comprising the diluted RO concentrate, featured a DOC concentration of 200 mg L^{-1}, with no detectable ammonia and a pH level of 8. Before initiating the experiments, this solution was spiked with a pharmaceutical cocktail, each compound present at a concentration of 100 μg/L. Along with the baseline measurement (mentioned in section 2.2.), two more experiments were conducted in Greece, with and without hydrogen peroxide (Table 5.1).

Case study 2: Sewage Treatment Plant, Malta

In the second biogas plant in Malta, the experiments were primarily aimed at assessing the potential impact of matrix components, particularly ions, on the removal of pharmaceutical compounds. Therefore, the selective electrodialysis (SED) module was omitted prior to the use of the UVOX system. Following the anaerobic digestion process, the resulting digestate was directed to centrifuges situated at the treatment plant. The liquid digestate supernatant, subsequently, was collected and transferred to the truck containers integrated into the ultrafiltration system. Thereafter, the liquid fraction was subjected to the UVOX experiment, following appropriate dilution until a minimum UV transmittance reading was recorded by the UV-compact sensor. The diluted digestate supernatant was characterized by a DOC of 365 mg L^{-1}, ammonia of 354 mg NH$_4$-N/L, and a pH level of 8. This working solution was spiked with the pharmaceuticals (100 μg/L each) prior to the experiments, and the experiments were conducted as shown in Table 5.1.

Table 5.1. Experimental design for pharmaceutical removal in both case studies

Case study	Exp.	Treatment	Sampling time	H_2O_2 /DOC ratio:	Objective
Greece	G1	UVOX	2 min, 20 min, 1 h, 2 h, 5 h, 22 h in both the experiments	0	Pharmaceutical removal
	G2	UVOX+H_2O_2		6.6	Effect of H_2O_2 in removal
Malta	M1	UVOX		0	Pharmaceutical removal
	M2	UVOX+H_2O_2		1.6	Effect of H_2O_2 dosage in removal
	M3	UVOX+H_2O_2	2 min, 20 min, 1 h, 2 h, 5 h, 22 h in all the experiments	6.6	
	M4	UVOX+TBA		0	To assess the potential contribution of OH˙ radicals

Experiment M4 was designed based on the quenching method (Guo et al., 2022) to assess the potential generation of OH˙ radicals in the UVOX system. Tert-butanol (TBA) was added in a molar ratio of TBA/O_3 of 7 (based on the maximum dissolved ozone measured in exp M1).

5.2.4 On-site measurement

pH was measured using a portable pH-meter (WTW-3310), temperature was recorded with an in-line temperature sensor, UV transmittance (%) at T10 was recorded using an in-line UV-compact sensor, and dissolved ozone was measured manually by using Hach Ozone AccuVac® (MR) ampules and a portable spectrometer DR-1900.

5.2.5 Analytical determinations

Dissolved organic carbon (DOC) were determined using a TOC analyser from Shimadzu (the Netherlands). The collected samples for pharmaceutical analysis were spiked with sodium thiosulfate to a final concentration of 80 mg L^{-1} to remove the residue of the oxidant, and kept in the freezer (-18 °C) in glass stoppered bottle wrapped in aluminium foil prior to the analysis. The analyses were performed by Laboratorios Tecnológicos de Levante (Valencia, Spain) (Certificate no. 121/LE1782) where the following methods were applied: For antibiotics, the sample was stirred and filtered by filter of 13 mm PTFE Hydrophilic, 0.45 um Teknokroma (Ref TR-F1-0021). The filtrate was collected in vial and analysed by direct injection into high-performance liquid chromatography (Agilent HPLC Agilent 1260), equipped with triple quadrupole-mass spectrometer (Agilent QQQ Agilent 6460). The applied column was Eclipse plus C18 (2.1 × 100 mm, 1.8 um) with mobile Phase A: Water 0.1% formic acid, and mobile Phase B: acetonitrile 0.1% formic acid with the flow of 0.3 mL/min. The linear range was between 0.5 to 500 ppb with detection limit of 0.5 μg/L.

For NSAIDs, the sample was stirred and filtered by filter of 13 mm PTFE Hydrophilic, 0.45 um Teknokroma (Ref TR-F1-0021), and the filtrate was collected in vial and analysed by direct injection into the same HPLC-QQQ but equipped with Poroshell 120 Phenyl-Hexyl column (3.0 × 100 mm, 2.7 mm) with mobile phase A: Water 0.1 mM ammonium fluoride, mobile phase B: methanol 0.1 mM ammonium fluoride with the flow of 0.4 mL/min. The linear range was between 0.1 to 100 ppb with detection limit of 0.1 μg/L.

5.2.6 Energy consumption in UVOX Redox® technology

With AOPs being energy-intensive processes (Miklos et al., 2018), assessment of operational energy consumption is crucial for economic purposes. The energy consumption in UVOX system was calculated by using electrical energy per order (E_{EO}) proposed by International Union of Pure and Applied Chemistry (IUPAC) and described by Bolton et al. (2001). Since in UVOX system ozone is generated by the means of UV irradiation, it is considered as an UV-based AOP system. Therefore, for each pharmaceutical, the energy consumption of UV lamp ($E_{EO, UV}$), was determined by Equation (5.1)

$$E_{EO,UV} = \frac{1000 \times W \times t}{V \times log\left(\frac{C_0}{C_t}\right)} \qquad (5.1)$$

Where, $E_{EO,UV}$ is electrical energy per order (kW h m^{-3}) for UV irradiation, W is the total power of the UV lamp (kW), V is the total volume of recirculated water (L) within the

treatment time t (h), C_0 and C_t are the concentration (mg L^{-1}) of the target contaminant at time 0 and time t, respectively.

The equivalent energy per order in case of using H_2O_2 ($E_{EO,H2O2}$) can be calculated as per Equation (5.2) (Katsoyiannis et al., 2011; Rosenfeldt et al., 2006)

$$E_{EO,H2O2} = E_{EQ,H2O2} \times C_{H2O2}$$ (5.2)

Where, $E_{EQ,H2O2}$ is the equivalent electrical energy consumption per mole of utilized H_2O_2, and it is equal to 0.241 kWh M^{-1} based on what was reported by Guo et al. (2018) and Sgroi et al. (2021). C_{H2O2} is the concentration (M) of H_2O_2. The energy per order was then determined as per Equation (5.3)

$$E_{EO} = E_{EO,UV} + E_{EO,H2O2}$$ (5.3)

5.3 RESULTS AND DISCUSSION

5.3.1 Pharmaceutical removal in both case studies (Exp. G1 and G2) and (Exp. M1-M3)

During the experiment with UVOX treatment (Exp. G1), no target compound was found after 22 hours treatment in the water collected from the UVOX process. By adding extra H_2O_2 to the system (Exp. G2), the removal efficiency for all the studied compounds increased and a faster removal was observed during the treatment. A complete removal of all compounds was achieved in 1 h, except for ibuprofen which required 5 h for complete removal (Figure 5.2). Figure 5.2 shows the removal profile in both treatment in the first 5 h.
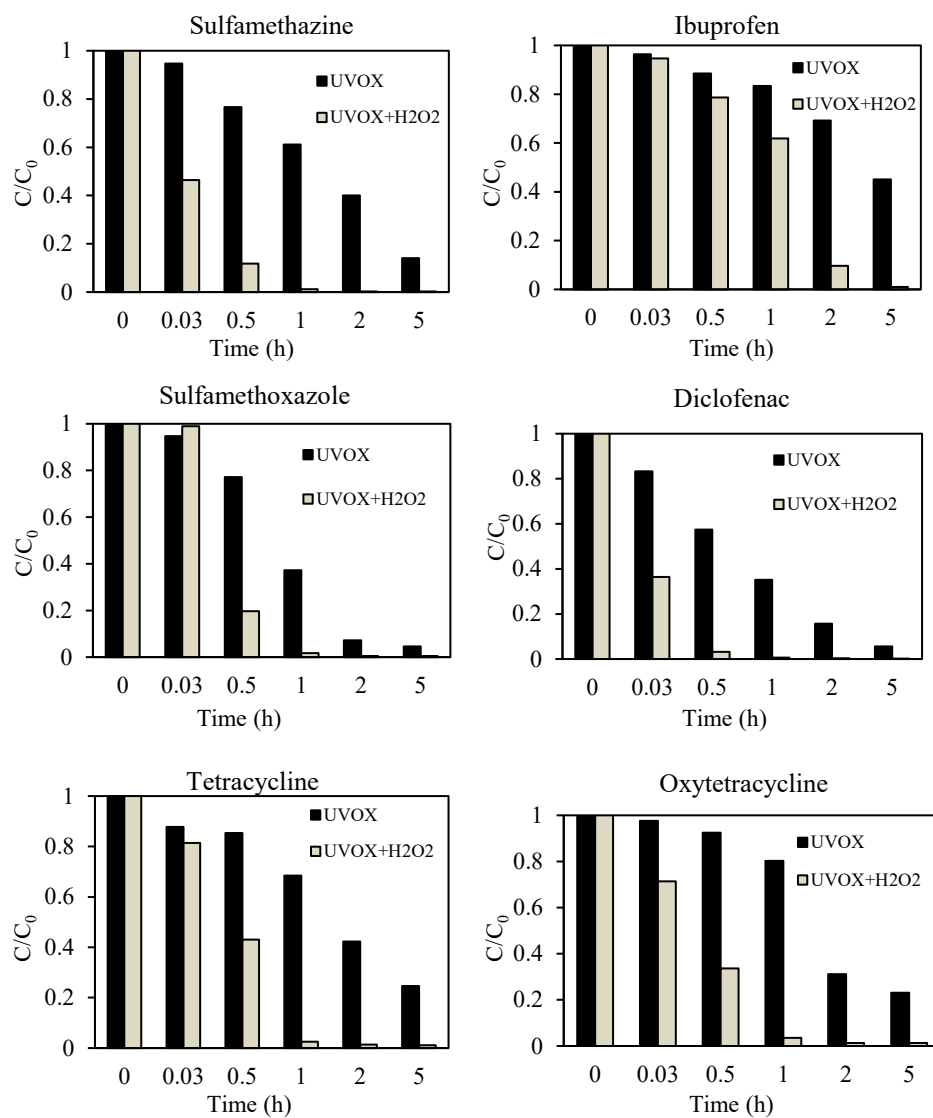
Figure 5.2. Removal as function of time for six pharmaceuticals from liquid digestate after ion removal in nutrient recovery module by using UVOX and UVOX+H₂O₂ in first case study: biogas plant, Greece (Exp. G1 and G2)

In the second study site (Malta), pharmaceutical removal was notably faster compared to the first study site. Regardless of the H_2O_2 dosage, all the target compounds were effectively removed within 2 hours. As depicted in Figure 5.3, increasing the H_2O_2/DOC ratio from 0 to 1.6 and 6.6 resulted in only a slight improvement in the removal efficiency of the target compounds. For instance, the removal of sulfamethazine increased from 79% to 88% and 90%, and the removal of sulfamethoxazole increased from 90% to 94% and 98%.
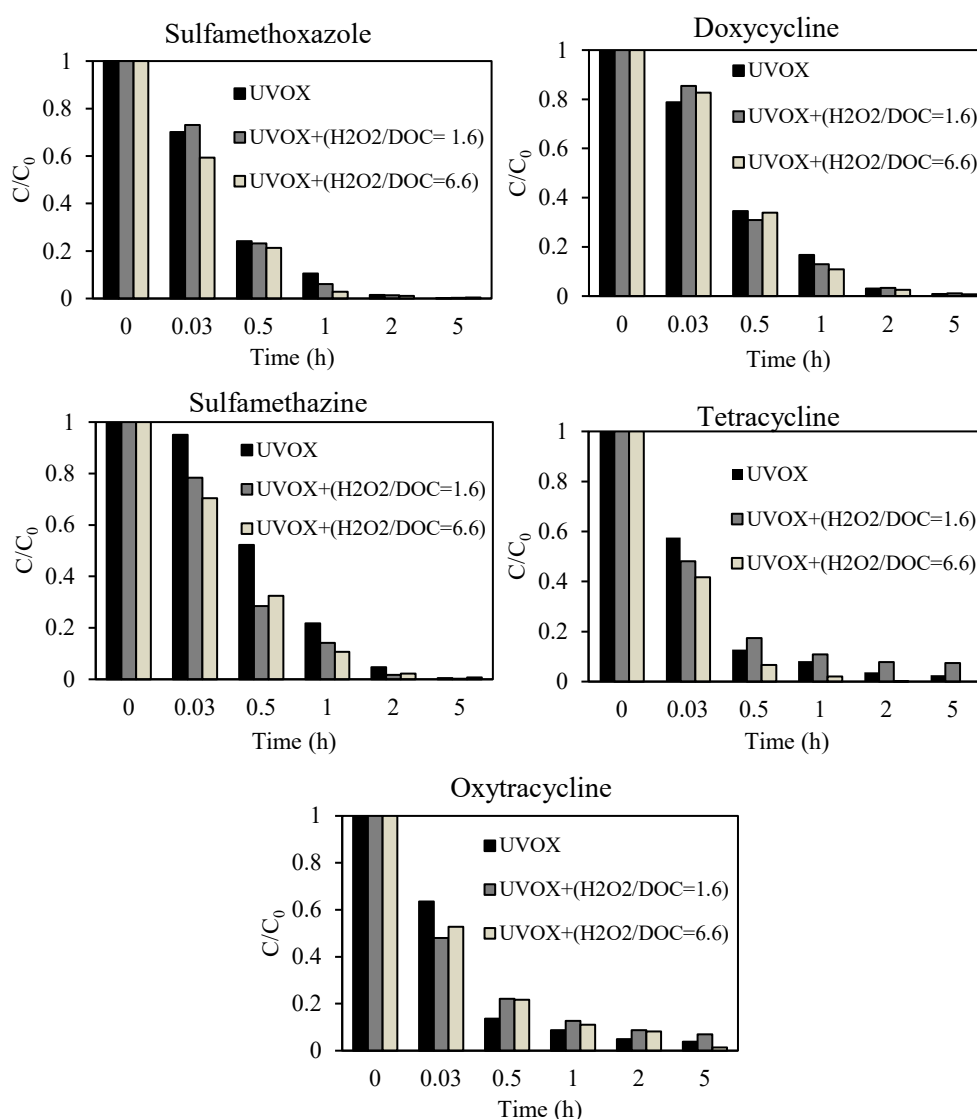
Figure 5.3. Removal as function of time for five pharmaceuticals from liquid digestate using UVOX and UVOX+H_2O_2 in second case study: treatment plant, Malta

Both figures illustrate distinct removal profiles for various compounds. The enhancement in the removal efficiency in the presence of H_2O_2 in first case study aligns with the finding of Liu et al. (2016) who reported an increase in antibiotic removal by adding H_2O_2 to UV-based AOPs, and with the findings of Martini et al. (2018), who reported an enhancement in antibiotic removal in the presence of H_2O_2 in O_3-based AOPs. Furthermore, the second case study exhibited a faster removal rate compared to the first. As elaborated and discussed further below, the removal of pharmaceuticals can be influenced by factors such as the removal mechanism within the UVOX chamber, the molecular structure of pharmaceuticals, as well as the effect of the psychochemical characteristics of the digestate matrix influenced by the previous technologies prior to the UVOX treatment.

Effect of O_3/ $OH^•$ generation mechanism, and added H_2O_2 on removal process

Oxidation of pharmaceutical compounds and organic matter involves two mechanisms: (i) a direct mechanism, in which molecular ozone selectively targets and degrades specific compounds that contain electron-rich functional groups (Asghar et al., 2022; Feng et al., 2016); and (ii) an indirect mechanism in which ozone decomposes and via a chain of reactions produces $OH^•$ radicals which oxidizes the organic matter non-selectively (Khan et al., 2020). Within the UVOX chamber, $OH^•$ radicals are generated through the irradiation of O_3 in water with UV light at 254 nm. Therefore, the effectiveness of the indirect mechanism via $OH^•$ radicals is significantly dependent on the penetration of UV light into the water sample.

During the UVOX treatment, the low UVT at the initial stage of digestate treatment, gradually increased over time in both case studies. As Figure 5.4 shows, the UVT in the first case study (Exp. G1), rose from 0.3% to 38%, and in the second case study (Exp. M1), it increased from 0.33% to 41% after 22 hours.
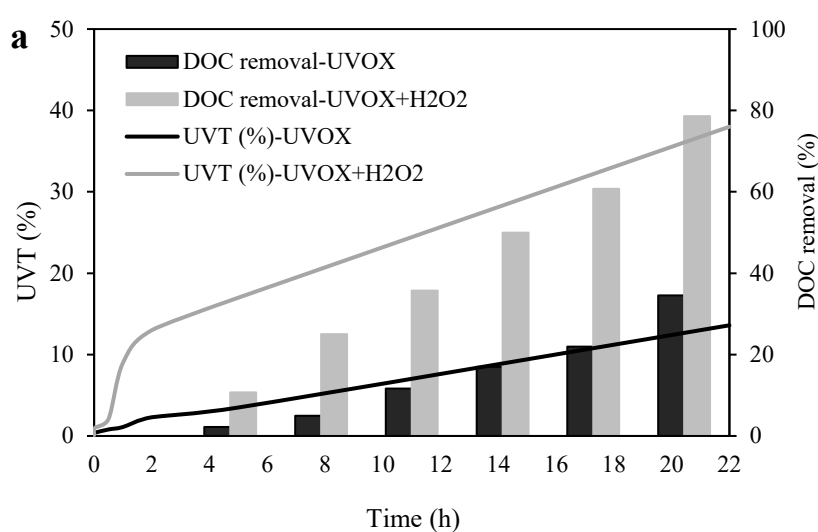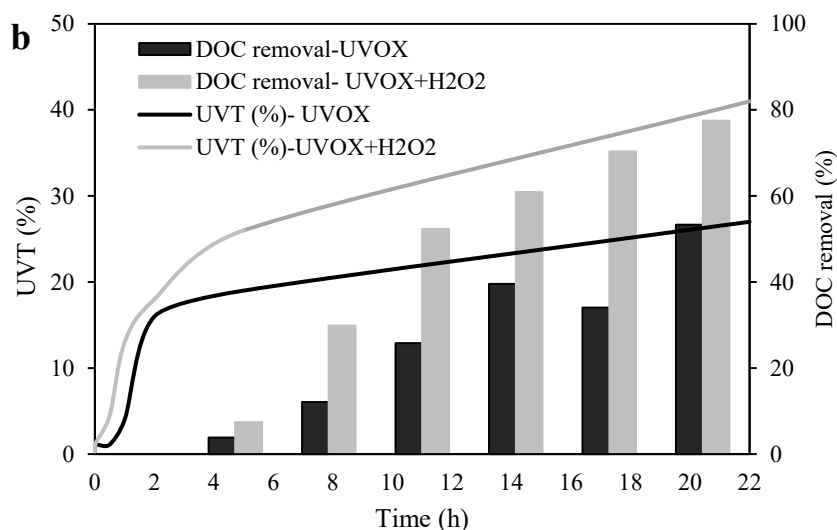
Figure 5.4. UV transmittance (UVT) pattern during UVOX treatment with and without H_2O_2 in (a) first case study (Greece), and (b) second case study (Malta)

The initial low UVT can be attributed to the presence of organic matter, including aromatic compounds responsible for the brownish-grey colour in digestate (Marcilhac et al., 2014). These aromatic compounds absorb UV light, hindering its penetration into the water sample, and adversely impact $OH^•$ radical formation and the indirect removal mechanism. This phenomenon is consistent with the findings of Yang et al. (2021c) who reported changes in specific UV absorbance along with the degradation of aromatic compounds. Therefore, at the early stage of UVOX treatment, due to low UV penetration, pharmaceutical oxidation primarily depends on the direct mechanism of molecular ozone.

The indirect removal mechanism, however, can accelerate in the UVOX treatment by adding H_2O_2, which increases a chain of reaction leading to $OH^•$ radical formation (Merényi et al., 2010; Rekhate and Srivastava, 2020). The substantial increase in DOC removal with H_2O_2 compared to without H_2O_2 (Figure 5.4), indicates the efficiency of the indirect mechanism. Furthermore, the removal of pharmaceuticals was increased with H_2O_2; for instants, the removal of the most persistent pharmaceutical, ibuprofen, increased from 65% to >98% with H_2O_2 (Figure 5.2). This aligns with previous reports on the enhanced performance of ozone-based and UV-based advanced oxidation processes with the addition of H_2O_2 (Adil et al., 2020; Martini et al., 2018).

The rapid increase in UVT in the first 2 hours with H_2O_2, coinciding with the removal of all target pharmaceuticals and the disappearance of digestate coloration, was followed by a slower rate of increase (Figure 5.4), potentially indicating a gradual oxidation of organic matter. This might be attributed to the initial addition of H_2O_2 as a single shot at the beginning of the experiment. Considering the decomposition of H_2O_2 over time, gradual addition might optimize the process further. This aligns with previous research by St.

Laurent et al. (2007) and Woodard and Curran (2006) who noted that while H_2O_2 in contact with UV light or O_3 produces $OH^•$ radicals, the compound tends to decompose over time into O_2 and H_2O.

The final experiment (Exp. M4) aimed to assess the respective contributions of O_3 and $OH^•$ to the removal process by introducing tert-butanol (TBA) as a quencher. The results (Figure 5.5) demonstrated a positive effect of combination of O_3 and $OH^•$ radicals on DOC removal, emphasizing the substantial contribution of $OH^•$ to the UVOX treatment's efficiency. A statistical comparison of the results revealed that DOC removal in the presence of the quencher was significantly lower than its absence (p-value= 0.009 <0.05). Specifically, DOC removal in the 22-hour treatment with the quencher was 27% lower than that observed in the UVOX treatment without the quencher. This aligns with the findings of Guo et al. (2022) who reported that in a quencher/O_3 molar ratio between 5 to 10, TBA effectively quenches all $OH^•$ radicals due to its high concentration and fast reaction with $OH^•$.

In contrast, the observed pattern during the initial 1-hour treatment indicated that quenching $OH^•$ radicals did not significantly affect DOC removal. It confirms that the primary removal mechanism in this phase involved the reaction between molecular ozone and organic compounds.
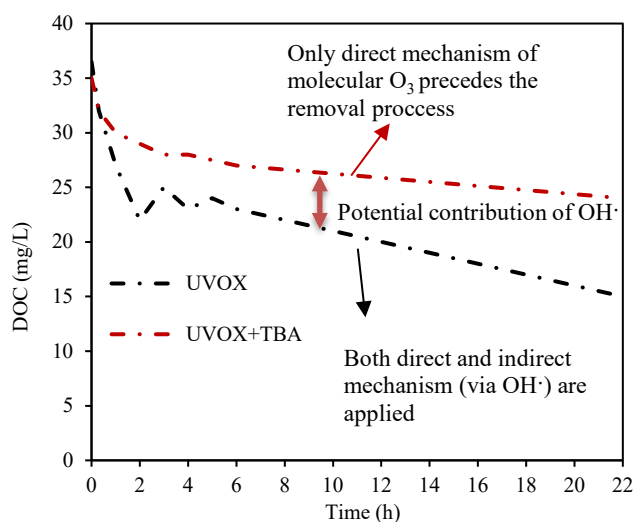
Figure 5.5. Effect of the TBA quencher on DOC removal (TBA/max dissolved O₃: 7)
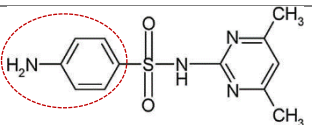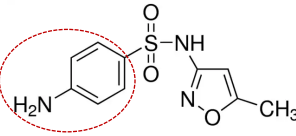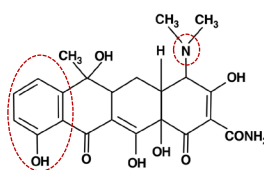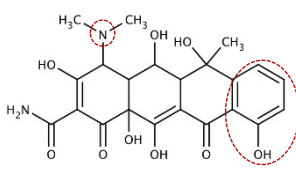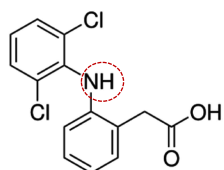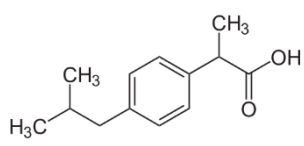
Effect of molecular structure on removal of pharmaceuticals

Within the UVOX experiments, various compounds exhibited distinct removal patterns, indicating the influence of their molecular structures. For instance, in Exp. G1, sulfamethoxazole was effectively removed within 2 hours, while ibuprofen's removal did not exceed 65%, even after 5 hours. As illustrated in Table 5.2, compounds containing electron-rich functional group, such as the aniline group in sulfamethazine and sulfamethoxazole, the amine and phenyl groups in tetracycline and oxytetracycline, and the aromatic amine in diclofenac, readily undergo electrophilic ozone reactions (Antoniou et al., 2013; Huber et al., 2005). Nevertheless, compounds lacking electron-rich functional groups, like ibuprofen, exhibit slower removal with ozone. As indicated in Table 5.2, ibuprofen has a carboxyl group on its aromatic ring, which acts as a withdrawal functional group, reducing the negative charge density of the aromatic ring (Antoniou et al., 2013; Moradi et al., 2023). Therefore, the electrophilic reaction of ozone is less effective in removing ibuprofen, and its removal primarily depends on OH· radicals, a stronger oxidant that non-selectively targets all organic compounds (Khan et al., 2020). Consequently, the addition of H_2O_2 substantially enhanced ibuprofen removal, reaching 90% within 2 hours (Figure 5.2).

Diclofenac, on the other hand, contains withdrawal groups in both aromatic rings, namely the carboxyl group in one ring and the chloride group in another (Table 5.2). Nevertheless, the electron-rich aromatic amine situated between the two rings readily undergoes the electrophilic reaction with ozone (Antoniou et al., 2013). Therefore, diclofenac was effectively removed even in the absence of H_2O_2, with an 85% removal within 2 hours, underscoring the selectivity of ozone reactions.

The comparatively slow removal of ibuprofen during UVOX treatment has also been reported by Ekowati et al. (2019) during application of UVOX to remove micropollutant from swimming pool, where there was minimal inhibition by organic matter, unlike in this study. In their study, no significant ibuprofen removal was reported during UVOX treatment, but the combination of UVOX and chlorination resulted in complete ibuprofen removal within 25 hours (Ekowati et al., 2019). This discrepancy could be attributed to the involvement of other highly reactive oxidative species with a higher redox potential than O_3, such as Cl· with a redox potential of 2.4 V (Guo et al., 2020).

Table 5.2. Molecular structure of investigated pharmaceuticals and their electron-rich functional groups highlighted by red circles for potential electrophilic ozone reactions
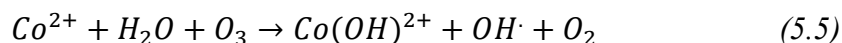
Compound	Molecular structure
Sulfamethazine	
Sulfamethoxazole	
Tetracycline	
Oxytetracycline	
Diclofenac	
Ibuprofen	

Sequence order of technologies in NOMAD truck and its effect on removal

The second case study in Malta demonstrated faster and more effective removal compared to the first case study in Greece. For instance, sulfamethazine achieved complete removal within 2 hours in Malta, even without the use of H_2O_2, whereas in Greece, the removal efficiency for the same compound reached only 58% within 2 hours and 78% within 5 hours (Figure 5.2 and Figure 5.3). Furthermore, the removal of DOC in the first case study over 22 hours reached up to 34%, while in the second case study, without the use of H_2O_2, a removal of 58% was observed (Figure 5.4).

Despite maintaining similar operational conditions in both case studies, the accelerated removal observed in Malta prompts an exploration into the potential influence of specific compounds on the underlying mechanisms governing pharmaceutical removal. In the first case study (Exp. G1 and G2 in Greece), the procedural sequence involved nutrient recovery through Selective electrodialysis (SED) preceding the UVOX treatment. Conversely, in the second case study (Exp. M1 to M4 in Malta), the digestate supernatant underwent direct UVOX treatment. As a result, the liquid in Malta (Exp. M1 to M4) inherently exhibited a higher concentration of ions compared to the liquid in Greece (Exp. G1 and G2).

The presence of specific ions can enhance the solubility and decomposition of ozone due to their catalytic effect, thus promoting the generation of reactive oxidative species (ROS), such as $OH^\bullet$ radicals. For instance, Psaltou et al. (2019) reported an increase in ozone decomposition, $OH^\bullet$ formation, and pCBA degradation in the presence of Fe^{2+} and Co^{2+}. This is attributed to the catalytic impact of these metals on the ozonation process, with direct reactions of Fe^{2+} with ozone (Equation (5.4)), and Co^{2+} with O_3 (Equation (5.5)), resulting in $OH^\bullet$ production (Aihara et al., 2021; Kasprzyk-Hordern et al., 2003).

$$Fe^{2+} + H_2O + O_3 \rightarrow Fe^{3+} + OH^\cdot + OH^- + O_2 \qquad (5.4)$$

$$Co^{2+} + H_2O + O_3 \rightarrow Co(OH)^{2+} + OH^\cdot + O_2 \qquad (5.5)$$

In our study, the water sample treated in Greece underwent the nutrient recovery step, during which monovalent and divalent ions were removed before UVOX treatment. For instance, the concentration of Fe^{2+} in the digestate supernatant was 12.5 mg L^{-1}, whereas after the SED process, it was below the detection limit. Lyngsie et al. (2018) also observed a positive effect of Fe^{2+} in removing dimethoxyhydroquinone in the O_3/H_2O_2 process, which supports the result of this study.

Based on these findings, it is recommended that further studies explore the feasibility of incorporating cobalt or iron, rather than H_2O_2, to enhance pharmaceutical removal performance in the UVOX unit. This suggestion is particularly relevant as these ions can maintain stability for more extended periods, and both serve as micronutrients essential for plant growth (Gomes et al., 2021).

5.3.2 Energy consumption in UVOX redox® technology

To evaluate the efficiency of AOPs, electric cost is considered as the main operational cost (Cardoso et al., 2016; Mehrjouei et al., 2014). Bolton et al. (2001) introduced the concept of energy per order (E_{EO}) as a metric for comparing the effectiveness of various treatments within AOPs. In current research, the second case study demonstrated

enhanced results in pharmaceutical removal, attributed to the sequence of applied technologies. Therefore, an energy efficiency analysis was conducted for the experiments in this case study, and the resulting E_{EO} values are presented in Table 5.3. In UVOX treatment, the determined E_{EO} for all the studied compounds was <0.087 kW h m^{-3}, showcasing notable energy efficiency of UVOX technology in compare with other O_3-based and UV-based AOPs. Within AOPs, a comprehensive review by Miklos et al. (2018) ranks ozonation as the most energy-efficient AOP-like treatment, with a median E_{EO} of 0.15 kW h m^{-3} followed by UV/O_3 treatment with a median E_{EO} of 0.7 kW h m^{-3} and UV/H_2O_2 with a median E_{EO} of 0.75 kW h m^{-3}.

It worth noting that O_3 used in UVOX treatment is generated by a UV irradiation without employing an ozone generator, resulting in lower energy consumption than conventional O_3 and UV/O_3 treatments. For instance, in a pilot-scale treatment to remove different micropollutant from municipal wastewater, the reported E_{EO} for sulfamethoxazole in UV/O_3 treatment was 0.068 kW h m^{-3} and in O_3 treatment was 0.245 kW h m^{-3} (Sgroi et al., 2021). While in our study the E_{EO} value for the same compound was 0.059 kW h m^{-3}.

The addition of H_2O_2 increased the E_{EO} for all the studied compounds, reflecting its equivalent energy per order (as per Equation (5.2)), consistent with the result reported by Sgroi et al. (2021). However, in all cases, the E_{EO} remained below the median E_{EO} reported for conventional UV/O_3 and UV/H_2O_2 treatments (Miklos et al., 2018), underscoring the efficiency of UVOX treatment.

Table 5.3. Electrical energy per order (E_{EO} (kW h m^{-3})) for the removal of the studied pharmaceutical

	E_{EO} (kW h m^{-3})	
	UVOX	UVOX/H_2O_2
Sulfamethoxazole	0.059	0.086
Sulfamethazine	0.087	0.107
Tetracycline	0.054	0.083
Oxytetracycline	0.056	0.11
Doxycycline	0.058	0.149

The E_{EO} values in Table 5.3 were determined based on the total volume of diluted digestate (450 L) recirculating during the treatment time. It is important to note that in full-scale practice the required water for dilution, will be recirculated from the effluent of the UVOX unit. This recirculation process ensures that the extra water for dilution does not contribute to additional water usage but rather is part of a closed-loop system. In this context, to maintain the same dilution factor applied in this study (60 litters of digestate in a final volume of 450 L), the input digestate should get a flow rate of 1.8 m³ h⁻¹, and the recirculated treated water a flow rate of 11.7 m³ h⁻¹, resulting in a total working sample flow of 13.5 m³ h⁻¹. This recirculation approach reflects a practical strategy for managing water usage in full-scale applications. To provide insights into the potential energy consumption in this scenario, the E_{EO} calculation was repeated for the volume of digestate recirculating within the treatment time without dilution (60 litters of digestate with a flow of 1.8 m³ h⁻¹). In this context, the recalculated E_{EO} values for the same compounds ranged between 0.44 kW h m⁻³ to 0.65 kW h m⁻³ in UVOX treatment and between 0.31 kW h m⁻³ to 0.8 kW h m⁻³ for UVOX/H_2O_2 treatment. Importantly, these values still fall within the range of energy-efficient treatments, aligning with previous comprehensive review by Miklos et al. (2018) that shows AOPs with an E_{EO} value <1 kWh m⁻³ represent a practical and feasible range for full-scale applications.

5.3.3 Surrogate-based monitoring

In this study, a significant correlation was observed between the rising trend of UV transmittance (UVT) and the removal of DOC (Figure 5.4). Given that the UVOX Redox® is equipped with a compact UV monitor, developing an UV-based surrogate method for UVOX efficiency was explored. The correlation between UVT and DOC, as well as between UVT and sulfamethoxazole (SMX), a representative pharmaceutical compound found in digestate, was evaluated in Exp. G1 and G2. As depicted in Figure 5.6, the logarithmic decrease of DOC and SMX correlates with the logarithmic increase in UVT. The data showed the best fit with an exponential formula, as shown in Equation (5.6) for DOC in the absence of H_2O_2 (Exp. G1), Equation (5.7) for DOC in the presence of H_2O_2 (Exp. G2), Equation (5.8) for SMX in the absence of H_2O_2 (Exp. G1), and Equation (5.9) for SMX in the presence of H_2O_2 (Exp. G2). These results are in line with the findings of Yang et al. (2021c) who proposed an exponential correlation between UV absorbance and the degradation of organic matter.

$$\ln \frac{DOC_0}{DOC} = 1.03 e^{0.112 \ln(UVT/UVT_0)} \qquad (5.6)$$

$$\ln \frac{DOC_0}{DOC} = 1.28 e^{0.23 \ln(UVT/UVT_0)} \qquad (5.7)$$

$$\ln \frac{SMX_0}{SMX} = 1.9 e^{1.62 \ln(UVT/UVT_0)} \qquad (5.8)$$

$$\ln \frac{SMX_0}{SMX} = 2.44e^{1.27\ln(UVT/UVT_0)} \tag{5.9}$$
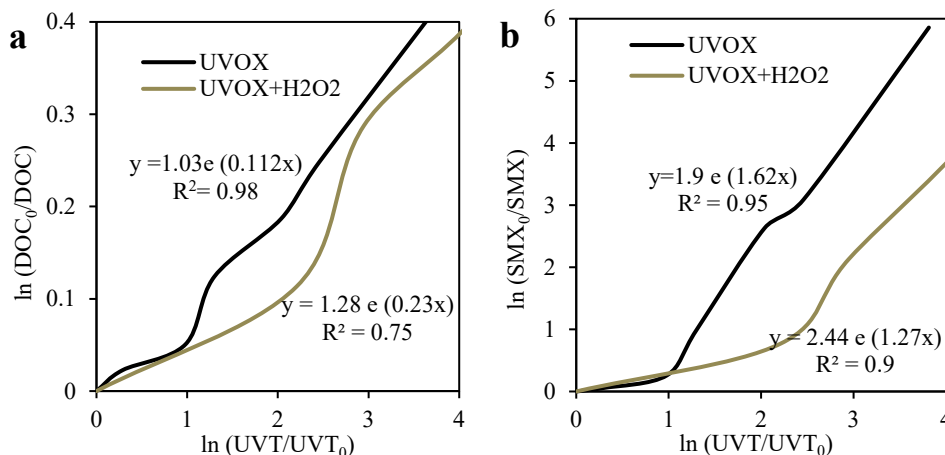
Figure 5.6. Oxidation of (a) DOC and (b) SMX as a function of the UVT when treating the digestate in the UVOX (black line) and in the UVOX with the addition of H_2O_2 (grey line).

The correlation observed in this study stems from the influence of organic matter reactivity and affinity towards oxidants. The reactivity of organic matter is predominantly determined by active aromatic sites and their strong affinity for oxidants (Chon et al., 2015). Initially, when UVT is low, the generation of OH˙ radical is limited, and the dominant removal mechanism involves direct oxidation through molecular ozone. As discussed earlier, the aromatic ring provides an electron-rich site for the reaction with molecular ozone, resulting in the oxidation of aromatic rings. Therefore, the UV absorbance associated with the aromatic compounds decreases. The decrease in UV absorbance corresponds to an increase in UVT. Chon et al. (2015) noted that the oxidation of aromatic compounds leads to a decrease in UV absorbance in the water matrix, supporting the finding of this study. The elevated UVT facilitates an increased generation of OH˙ radicals, thereby contributing to the removal process.

Various studies support the outcomes of this investigation. Chys et al. (2017) established a correlation between UV absorbance at 254 nm and the removal of trace organic matter during the ozonation of municipal wastewater. Similarly, Park et al. (2017) identified a correlation between the oxidation of trace organic compounds and UV absorbance at 254 nm, and total fluorescence (TF). Furthermore, recent work by Yang et al. (2021c) demonstrated a correlation between the removal of micropollutants and UV absorbance at 254 nm. All these findings support the results of the present study, underscoring the

efficacy of UV-based surrogate methods in monitoring the removal of target compounds and organic matter during treatment processes.

The surrogate method was applied in the second case study for Exp. M1 and M3 to predict DOC and SMX removal using the obtained equations. The level of agreement between the actual measured data and the predicted values was assessed using the normalized root mean squared deviation (NRMSD) as expressed in Equation (5.10) (Oehmen et al., 2010).

$$NRMSD = \frac{\sqrt{\frac{\sum_{i=1}^{n}(x_{meas,i}-x_{pred,i})^2}{n}}}{x_{meas,max}-x_{meas,min}} \qquad (5.10)$$

Where, x_{meas} and x_{pred} are measured and predicated data, $x_{meas,max}$ and $x_{meas,min}$ are the maximum and minimum measured concentration, and n is the number of data points. Validation of the surrogate method in the second case study (Exp. M1 and M3) showed high predictive accuracy for DOC removal, with NRMSD values of 0.12 in UVOX treatment and 0.14 in UVOX/H_2O_2 treatment, corresponding to approximately 87% and 86% predictive capability. However, for SMX removal, the agreement was lower at 77%. It is worth noting that these surrogate-based equations can potentially be improved by considering shorter sampling time intervals.

5.4 CONCLUSIONS

This study delivers crucial insights into the application and effectiveness of the UVOX Redox® technology within the NOMAD mobile unit, which is specifically designed for nutrient recovery and pharmaceutical removal. The sequencing of technologies within this innovative mobile system has a profound impact on removal efficiency. Notably, the direct treatment of liquid digestate following solid/liquid separation and preceding the nutrient recovery module resulted in a faster removal of over 90% of pharmaceuticals within a maximum of 2 hours, even without the addition of H_2O_2. However, when the UVOX treatment was applied after the nutrient recovery modules, the efficiency of UVOX decreased, and achieving 90% removal of pharmaceuticals required a longer period (e.g., 90% removal of sulfamethazine took 5 hours). Furthermore, this research introduced an easily-monitored surrogate method, UVT, which exhibits a strong correlation with DOC and pharmaceutical removal. The outcomes of this study hold the potential to enhance the practical implementation of this innovative technology, aligning with the broader objectives of establishing sustainable solutions for digestate recycling and promoting the advancement of circular economy strategies and goals.

5.5 ANNEXES

Annex 5.5.1 Greece biogas plant

Location: Serbia, Kozani

Feedstock: Animal faeces, urine and manure (including spoiled straw), corn silage

Feedstock Composition: Animal faeces, urine and manure (including spoiled straw), corn silage (Generally, the feedstock consists of 50 m_3 (tonnes) of pig waste and 2 tonnes of corn silage)

Capacity: 21900 tpa

Process: Mesophilic. The liquid feedstock is transported into the digester where a mesophilic (~ 37 - 42 ° C) anaerobic digestion process occurs. The biogas produced is transferred through a compressor to a CHP system, where the excess moisture is removed and cooled, and then channelled into an internal combustion engine for the co-generation of electricity and heat.

Energy Generation: annual generation of 854 MWh

Digestate Disposal: Land application; provided for free to local farmers who provide corn silage feedstock

Site location: The biogas plant is situated in an area of 9379 m^2. It is located near the town of Serbia in Kozani. The location of the plant and the nearby road network is presented in Figure A5.1.
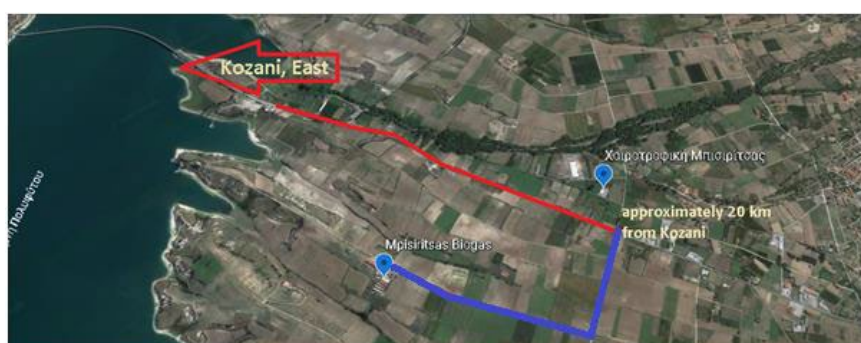
Figure A5.1. Biogas plant location, Serbia, Kozani

Annex 5.5.2 Malta Biogas plant

Location: Ta' Barkat, limits of Xgħajra, Malta

Feedstock: Urban Wastewater

Feedstock Composition: Sludges from treatment of urban wastewater and farmyard waste mixed with urban waste in the sewer collection network

Capacity: 243000 tpa

Energy Generation: Annual power generation of the plant is approximately 4000 MWh

Digestate Disposal: Landfill

Process: Mesophilic. The Malta South Sewage Treatment Plant is a mesophilic anaerobic digestion plant, which biologically converts sewage sludge and grease into biogas and digestate. The biogas is used for heat and power generation through a CHP process, whilst the digestate is dewatered and then disposed directly to landfill.

Site location: The plant is located on the outskirts of the towns of Xgħajra. The location of the Ta' Barkat Sewage Treatment Plant is shown in Figure A5.2.

Figure A5.2. Ta'Barkat Sewage Treatment Plant Biogas Location, Malta

Annex 5.5.3. NOMAD Bioresource recovery model
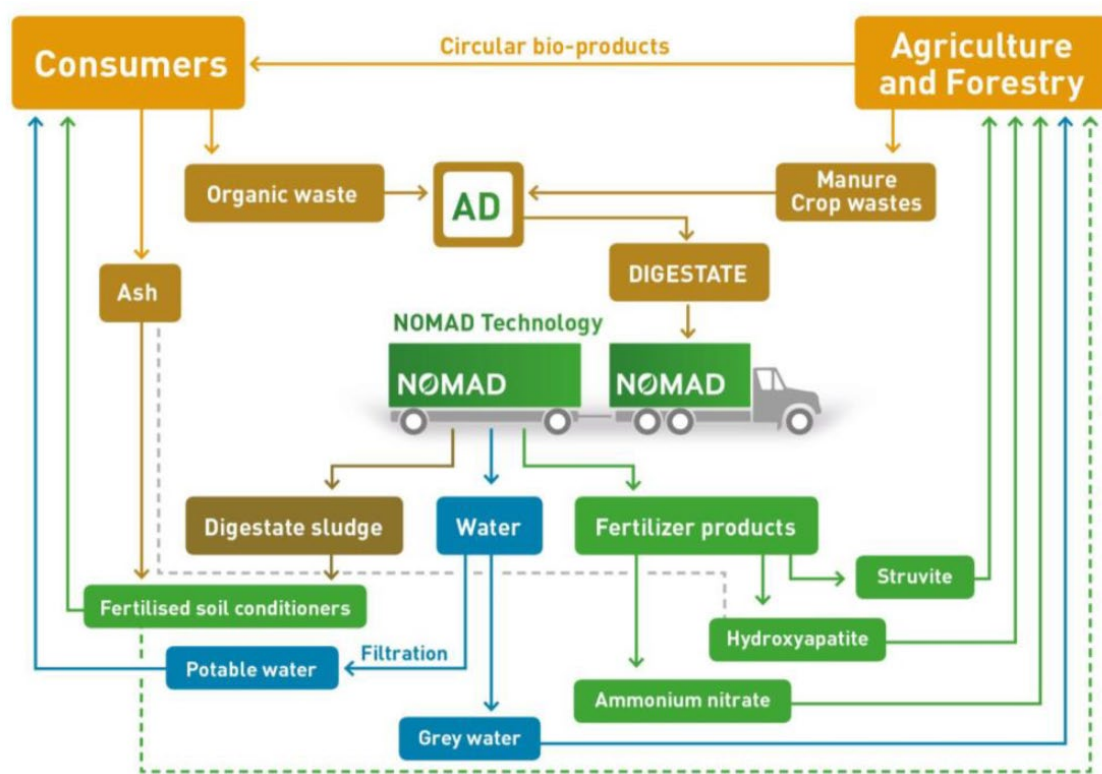
Figure A5.3. NOMAD's circular bioresource recovery model

6

CONCLUSIONS AND FURTHER PERSPECTIVES

6.1 CONCLUSIONS

This research aimed to evaluate the feasibility of ozone-based Advanced Oxidation Processes (AOPs) for eliminating contaminants of emerging concern (CECs) from liquid digestate, with the primary objective of enhancing the management and potential reuse of digestate supernatant. The main focus of this study was to determine ozone dosage for the removal of CECs, considering the influence of the digestate matrix. Additionally, the research aimed to introduce a mathematical model describing the ozonation process within digestate, develop this model further to predict CECs removal, and compare the efficiency of ozonation when applied independently versus when integrated with an activation method. The following key conclusions were drawn from this thesis:

6.1.1 Removal of contaminants of emerging concern from liquid digestate

To the date of conducting this research, there was no post-anaerobic digestion (AD) treatment employed to eliminate contaminants of emerging concern (CECs) from digestate. Currently, digestate supernatant is utilized in agricultural fields without undergoing additional treatment for CECs removal, or it is disposed of in landfills, an environmentally unsustainable practice.

In the second chapter of this thesis, the viability of ozonation as a potential post-AD treatment to remove CECs from digestate supernatant was assessed. Ozonation was conducted using a lab-scale bubble column reactor with a continuous supply of ozone. While the lab-scale ozonation resulted in an ozone dose of 1.49 mg O_3/mg DOC in a 5-hour treatment, nearly all the investigated CECs were successfully removed at a lower maximum ozone dose of 0.48 mg O_3/mg DOC. The presence of the digestate matrix led to a considerable reduction in the kinetic ozonation rate, approximately 1% compared to the removal rate observed in demineralized water.

Incorporating a combined treatment approach involving ozone and hydrogen peroxide (O_3/H_2O_2) demonstrated an additional benefit. The introduction of H_2O_2 significantly decreased the ozone demand by a minimum of 59% for all the studied compounds. The acute toxicity of the digestate, measured through the inhibition of *Vibrio fisheries* luminescence, exhibited an 18.1% reduction during 5 hours of ozonation and a 34% reduction during 5 hours of O_3/H_2O_2 treatment.

Despite the substantial consumption of ozone, the required ozone dose (mg O_3/mg DOC) for the complete removal of all CECs from digestate supernatant fell within the range or was lower than that reported range for other (waste-)water matrices. This suggests that ozonation can be considered as a potential post-AD treatment strategy to generate a cleaner stream before discharge or land application.

6.1.2 Mathematical modelling of ozonation process of high strength liquid digestate

The second chapter of this thesis showed the impact of digestate, characterized by a high-strength matrix of organic matter, on ozone consumption during treatment. Due to the energy-intensive nature of ozone technology, anticipating ozone consumption before treatment is crucial for assessing its cost-effectiveness as a potential post-AD treatment. The general trend observed was an increase in ozone consumption influenced by the digestate matrix, yet limited knowledge existed regarding the key parameters governing the ozonation process. To address this, in the third chapter, a long-term ozonation was conducted until steady state trend for each component was obtained.

Third chapter addresses a research gap in ozone modeling by integrating ammonia into the ozone decomposition matrix (the Petersen matrix) and considering the impact of alkalinity on the oxidation of other components. It contributes fundamental insights into the ozonation process within complex water matrices like digestate. The key conclusions of this chapter are outlined below:

- The proposed model effectively predicts ozone consumption in digestate based solely on initial values of organic/inorganic carbon and nitrogen.

- The model elucidates the oxidation of primary components in the digestate matrix by ozone, their interactions with other components, and the influence of buffer capacity on the ozonation process.

- The model demonstrates strong internal validity, surpassing 91%, and external validity, exceeding 88%, in describing the ozonation process in high-strength water matrices. Additionally, it proves highly effective in describing ozonation in lower-strength water matrices, down to concentrations as low as 14 mg DOC L^{-1}.

- The model highlights that relying solely on kinetic rates is insufficient for explaining component oxidation in a complex water matrix. It underscores the necessity of considering interactions between water matrix components to accurately describe the process and predict ozone consumption before experimental work.

6.1.3 Development of the mathematical ozone process model for CECs prediction in diverse water matrices

Chapter 4 builds upon the calibrated model developed in the previous chapter, extending its application to predict the removal of contaminants of emerging concern (CECs) in diverse water matrices. The primary focus of this chapter was to elucidate inhibitory factors impacting the removal of persistent CECs during the ozonation process.

Specifically tailored to describe the ozonation process in the digestate matrix, the calibrated model served as the foundation for creating a simplified mathematical model to predict CECs removal under the influence of digestate matrix components. To develop the model, a comprehensive assessment of the individual and combined effects of matrix components on CECs removal was conducted. Ibuprofen (IBU) was chosen as a representative persistent CECs to be assessed within the model.

The experimental work showed that in single-component water matrices, Dissolved Organic Nitrogen (DON-N) demonstrated the most inhibitory effect, resulting in a 32% lower IBU removal compared to demineralized water (DW). In dual-component water matrices, the combination of DON-N and alkalinity showed the highest inhibition, with only 45% of IBU being removed. Notably, multi-component water matrices exhibited a positive interaction of matrix components, resulting in a remarkable 90% IBU removal within a 1-hour treatment.

The previously calibrated model was further enhanced by integrating IBU removal rates into the mathematical framework, incorporating inhibition factors for each matrix component on IBU removal rates. IBU removal predictions demonstrated high accuracy across diverse water matrices, achieving an agreement of over 83% for all considered matrices. The resulting inhibition constants, estimated using the parameter estimation tool in Aquasim software, aligned well with experimental data. DON-N exhibited the most inhibitory effect, with an estimated Inhibition Constant for DON-N (K_i_DON) of 2.325 mg NL^{-1}. Following DON-N, ammonia, DOC, and alkalinity also exerted inhibitory influences.

This chapter presents a tailored mathematical model for predicting the abatement of persistent CECs during ozonation, relying solely on fundamental water matrix characterizations. In contrast to other prediction models that often require preliminary experimental work, this model eliminates such prerequisites, including the determination of parameters like R_{CT}.

6.1.4 Practical application of integrated ozonation system (UVOX Redox®) for pharmaceutical removal from liquid digestate in biogas plants

The preceding chapters have demonstrated the feasibility of ozonation as a post- AD treatment for removing contaminants of emerging concern (CECs) from digestate in lab-scale experiments. However, the limitations of ozone effectiveness in removing compounds lacking an electron-rich functional group were evident. Additionally, ozonation did not lead to complete mineralization, and the experimental work highlighted a high energy per order (E_{EO}) for the removal of all the studied CECs.

In response to these challenges, the chapter 5 explored a pilot-scale hybrid system that integrates the application of UV, as an activation method, to the ozone treatment. The focus was on a novel UV/O_3 system (UVOX Redox®) within a mobile technology (NOMAD), designed for digestate treatment in small-scale treatment plant and decentralized AD plants. NOMAD, a mobile technology equipped with filtration, nutrient recovery, and pharmaceutical removal units installed on a truck, offers mobility within AD plants. The findings of this chapter underscored the efficiency of UVOX treatment for CECs removal from digestate.

The sequencing of technologies within this innovative mobile system significantly influenced CECs removal efficiency. Direct treatment of liquid digestate, following solid/liquid separation and preceding the nutrient recovery module, resulted in a rapid removal of over 90% of pharmaceuticals within a maximum of 2 hours, even without the addition of H_2O_2. However, when the UVOX treatment was applied after the nutrient recovery module, the efficiency decreased, and achieving 90% removal of pharmaceuticals required a longer period (e.g., 90% removal of sulfamethazine took 5 hours). This decrease in efficiency could potentially be attributed to the elimination of metals during the nutrient recovery process. The presence of metals, such as irons, in digestate has the potential to promote catalytic ozonation, thereby improving removal efficiency when applying the ozonation system prior to the nutrient recovery module.

Beyond its high removal efficiency, UVOX stands out for reducing costs and energy due to its unique ozone generation system, omitting the need for an ozone generator and oxygen supply tank. The E_{EO} value below the median reported for ozone-based and UV-based AOPs, specifically less than 1 kWh m^{-3}, represents a practical and feasible range for full-scale applications.

Furthermore, this chapter introduced an easily-monitored surrogate method, UVT, displaying a strong correlation with Dissolved Organic Carbon (DOC) and pharmaceutical removal.

The outcomes of this study hold the potential to enhance the practical implementation of this innovative technology, aligning with broader objectives of establishing sustainable solutions for digestate recycling and promoting the advancement of circular economy strategies and goals.

6.2 FUTURE PERSPECTIVE

- This research has demonstrated that ozonation can reduce the toxicity of digestate towards the organism *Vibrio fisheries*. However, assessing the toxicity of endocrine-disrupting compounds, such as hormones, necessitates further testing to evaluate the acute toxicity, estrogenic, and (anti) androgenic effects (Heffron et al., 2016; Sohoni and Sumpter, 1998). For future studies, the application of in

vitro Yeast Estrogen Screening (YES) and Yeast Androgen Screening (YAS) assays is recommended, especially when ozonation is applied in anaerobic digestion plants fed by animal wastes.

- Although this research showcased the abatement of the studied contaminants of emerging concern (CECs), the disappearance of parent compounds doesn't always indicate successful treatment due to potentially active and even more toxic oxiadation by-products. Determining the by-products and metabolites of the parent compounds can enhance the understanding of toxicity and contribute to a better comprehension of the removal mechanisms.

- This research aimed to create a simplified model for understanding the ozonation process in a high-strength water matrix. Given that the main focus was on core ozonation mechanisms where ozone is the primary oxidant, the role of active radicals in the model was not explicitly addressed. Future research is required to develop the model by measuring key radical concentrations and incorporating their reactions into the model, especially in scenarios where hydroxyl radicals (OH•) are the primary oxidants, such as ozonation at high alkaline pH levels. This approach could provide valuable insights into the ozonation process by explicitly differentiating radical reactions from ozone reactions.

- It was demonstrated that the application of H_2O_2 increases removal efficiency in the hybrid system (UV/O$_3$) in the absence of ions. However, in the presence of ions, removal with and without H_2O_2 was not significantly different. Another recommendation is the exploration of catalytic ozonation rather than the addition of H_2O_2, by utilizing the already present metals in the digestate. Future studies could investigate the feasibility of incorporating cobalt or iron, instead of H_2O_2, to enhance pharmaceutical removal performance in the UVOX unit. This suggestion is particularly relevant as these ions can maintain stability for more extended periods and serve as micronutrients essential for plant growth.

REFERENCES

Abril, C., Santos, J.L., Martín, J., Aparicio, I. and Alonso, E. 2020. Occurrence, fate and environmental risk of anionic surfactants, bisphenol A, perfluorinated compounds and personal care products in sludge stabilization treatments. Science of The Total Environment 711, 135048.

Adil, S., Maryam, B., Kim, E.-J. and Dulova, N. 2020. Individual and simultaneous degradation of sulfamethoxazole and trimethoprim by ozone, ozone/hydrogen peroxide and ozone/persulfate processes: A comparative study. Environmental Research 189, 109889.

Ahmed, M.B., Zhou, J.L., Ngo, H.H., Guo, W., Thomaidis, N.S. and Xu, J. 2017. Progress in the biological and chemical treatment technologies for emerging contaminant removal from wastewater: A critical review. Journal of Hazardous Materials 323, 274-298.

Aihara, H., Watanabe, S., Shibata, A., Mahardiani, L., Otomo, R. and Kamiya, Y. 2021. Oxidative decomposition of ammonium ion with ozone in the presence of cobalt and chloride ions for the treatment of radioactive liquid waste. Progress in Nuclear Energy 139, 103872.

Ajibola, A.S., Fawole, S.T., Ajibola, F.O. and Adewuyi, G.O. 2021. Diclofenac and Ibuprofen Determination in Sewage Sludge Using a QuEChERS Approach: Occurrence and Ecological Risk Assessment in Three Nigerian Wastewater Treatment Plants. Bulletin of Environmental Contamination and Toxicology 106(4), 690-699.

Akhiar, A., Battimelli, A., Torrijos, M. and Carrere, H. 2017. Comprehensive characterization of the liquid fraction of digestates from full-scale anaerobic co-digestion. Waste Management 59, 118-128.

Antoniou, M.G. and Andersen, H.R. 2012. Evaluation of pretreatments for inhibiting bromate formation during ozonation. Environmental Technology 33(15), 1747-1753.

Antoniou, M.G., Hey, G., Rodríguez Vega, S., Spiliotopoulou, A., Fick, J., Tysklind, M., la Cour Jansen, J. and Andersen, H.R. 2013. Required ozone doses for removing pharmaceuticals from wastewater effluents. Science of The Total Environment 456-457, 42-49.

APHA 1992. Standard Methods for the examiniation of water and wastewater. American Public Health Organisation, p. 5-6/5-11.

Arikan, O.A., Sikora, L.J., Mulbry, W., Khan, S.U. and Foster, G.D. 2007. Composting rapidly reduces levels of extractable oxytetracycline in manure from therapeutically treated beef calves. Bioresource Technology 98(1), 169-176.

Asghar, A., Lutze, H.V., Tuerk, J. and Schmidt, T.C. 2022. Influence of water matrix on the degradation of organic micropollutants by ozone based processes: A review on oxidant scavenging mechanism. Journal of Hazardous Materials 429, 128189.

Ashfaq, M., Nawaz Khan, K., Saif Ur Rehman, M., Mustafa, G., Faizan Nazar, M., Sun, Q., Iqbal, J., Mulla, S.I. and Yu, C.-P. 2017. Ecological risk assessment of pharmaceuticals in the receiving environment of pharmaceutical wastewater in Pakistan. Ecotoxicology and Environmental Safety 136, 31-39.

Audenaert, W.T.M., Callewaert, M., Nopens, I., Cromphout, J., Vanhoucke, R., Dumoulin, A., Dejans, P. and Van Hulle, S.W.H. 2010. Full-scale modelling of an ozone reactor for drinking water treatment. Chemical Engineering Journal 157(2), 551-557.

Audenaert, W.T.M., Vandevelde, M., Van Hulle, S.W.H. and Nopens, I. 2013. Impact of Dissolved Organic Matter (DOM) on Parameter Sensitivity of a Kinetic Ozone Decomposition Model. Ozone: Science & Engineering 35(5), 338-349.

Bader, H. and Hoigné, J. 1981. Determination of ozone in water by the indigo method. Water Research 15(4), 449-456.

Bahr, C., Schumacher, J., Ernst, M., Luck, F., Heinzmann, B. and Jekel, M. 2007. SUVA as control parameter for the effective ozonation of organic pollutants in secondary effluent. Water Science and Technology 55(12), 267-274.

Balachandran, R., Zhao, M., Dong, B., Brown, I., Raghavan, S. and Keswani, M. 2014. Role of ammonia and carbonates in scavenging hydroxyl radicals generated during megasonic irradiation of wafer cleaning solutions. Microelectronic Engineering 130, 82-86.

Bolton, J.R., Bircher, K.G., Tumas, W. and Tolman, C.A. 2001. Figures-of-merit for the technical development and application of advanced oxidation technologies for both electric- and solar-driven systems (IUPAC Technical Report). 73(4), 627-637.

Buffle, M.-O., Schumacher, J., Meylan, S., Jekel, M. and von Gunten, U. 2006. Ozonation and Advanced Oxidation of Wastewater: Effect of O3 Dose, pH, DOM and HO•-Scavengers on Ozone Decomposition and HO• Generation. Ozone: Science & Engineering 28(4), 247-259.

Bühler, R.E., Staehelin, J. and Hoigné, J. 1984. Ozone decomposition in water studied by pulse radiolysis. 1. HO2/O2- and HO3/O3- as intermediates. Journal of Physical Chemistry 88(12), 2560-2564.

126

Bui, X.T., Vo, T.P.T., Ngo, H.H., Guo, W.S. and Nguyen, T.T. 2016. Multicriteria assessment of advanced treatment technologies for micropollutants removal at large-scale applications. Science of The Total Environment 563-564, 1050-1067.

Cabeza, Y., Candela, L., Ronen, D. and Teijon, G. 2012. Monitoring the occurrence of emerging contaminants in treated wastewater and groundwater between 2008 and 2010. The Baix Llobregat (Barcelona, Spain). Journal of Hazardous Materials 239-240, 32-39.

Carbajo, J.B., Petre, A.L., Rosal, R., Herrera, S., Letón, P., García-Calvo, E., Fernández-Alba, A.R. and Perdigón-Melón, J.A. 2015. Continuous ozonation treatment of ofloxacin: Transformation products, water matrix effect and aquatic toxicity. Journal of Hazardous Materials 292, 34-43.

Cardoso, J.C., Bessegato, G.G. and Boldrin Zanoni, M.V. 2016. Efficiency comparison of ozonation, photolysis, photocatalysis and photoelectrocatalysis methods in real textile wastewater decolorization. Water Research 98, 39-46.

Česen, M., Lenarčič, K., Mislej, V., Levstek, M., Kovačič, A., Cimrmančič, B., Uranjek, N., Kosjek, T., Heath, D., Dolenc, M.S. and Heath, E. 2018. The occurrence and source identification of bisphenol compounds in wastewaters. Sci Total Environ 616-617, 744-752.

Chen, H. and Wang, J. 2021. Degradation and mineralization of ofloxacin by ozonation and peroxone (O3/H2O2) process. Chemosphere 269, 128775.

Chiriac, F.L., Paun, I., Pirvu, F., Pascu, L.F. and Galaon, T. 2021. Occurrence and Fate of Bisphenol A and its Congeners in Two Wastewater Treatment Plants and Receiving Surface Waters in Romania. Environ Toxicol Chem 40(2), 435-446.

Chon, K., Salhi, E. and von Gunten, U. 2015. Combination of UV absorbance and electron donating capacity to assess degradation of micropollutants and formation of bromate during ozonation of wastewater effluents. Water Research 81, 388-397.

Chys, M., Audenaert, W.T.M., Deniere, E., Mortier, S.T.F.C., Van Langenhove, H., Nopens, I., Demeestere, K. and Van Hulle, S.W.H. 2017. Surrogate-Based Correlation Models in View of Real-Time Control of Ozonation of Secondary Treated Municipal Wastewater—Model Development and Dynamic Validation. Environmental Science & Technology 51(24), 14233-14243.

Coha, M., Farinelli, G., Tiraferri, A., Minella, M. and Vione, D. 2021. Advanced oxidation processes in the removal of organic substances from produced water: Potential, configurations, and research needs. Chemical Engineering Journal 414.

Crolla, A., Kinsley, C. and Pattey, E. (2013) The Biogas Handbook. Wellinger, A., Murphy, J. and Baxter, D. (eds), pp. 302-325, Woodhead Publishing.

Cruz-Alcalde, A., Esplugas, S. and Sans, C. 2020. Characterization and fate of EfOM during ozonation applied for effective abatement of recalcitrant micropollutants. Separation and Purification Technology 237, 116468.

De la Cruz, N., Giménez, J., Esplugas, S., Grandjean, D., De Alencastro, L.F. and Pulgarín, C. 2012. Degradation of 32 emergent contaminants by UV and neutral photo-fenton in domestic wastewater effluent previously treated by activated sludge. Water Research 46(6), 1947-1957.

de Oliveira, M., Frihling, B.E.F., Velasques, J., Filho, F.J.C.M., Cavalheri, P.S. and Migliolo, L. 2020. Pharmaceuticals residues and xenobiotics contaminants: Occurrence, analytical techniques and sustainable alternatives for wastewater treatment. Science of The Total Environment 705, 135568.

de Vera, G.A., Gernjak, W., Weinberg, H., Farré, M.J., Keller, J. and von Gunten, U. 2017. Kinetics and mechanisms of nitrate and ammonium formation during ozonation of dissolved organic nitrogen. Water Research 108, 451-461.

Dietrich, C.C., Rahaman, M.A., Robles-Aguilar, A.A., Latif, S., Intani, K., Müller, J. and Jablonowski, N.D. 2020. Nutrient Loaded Biochar Doubled Biomass Production in Juvenile Maize Plants (Zea mays L.). Agronomy 10(4).

Dong, G., Chen, B., Liu, B., Cao, Y., de Jourdan, B., Stoyanov, S.R., Ling, J., Ye, X., Lee, K. and Zhang, B. 2022. Comparison of O3, UV/O3, and UV/O3/PS processes for marine oily wastewater treatment: Degradation performance, toxicity evaluation, and flocs analysis. Water Research 226, 119234.

Ekowati, Y., Ferrero, G., Farré, M.J., Kennedy, M.D. and Buttiglieri, G. 2019. Application of UVOX Redox® for swimming pool water treatment: Microbial inactivation, disinfection byproduct formation and micropollutant removal. Chemosphere 220, 176-184.

Eslami, A., Amini, M.M., Yazdanbakhsh, A.R., Rastkari, N., Mohseni-Bandpei, A., Nasseri, S., Piroti, E. and Asadi, A. 2015. Occurrence of non-steroidal anti-inflammatory drugs in Tehran source water, municipal and hospital wastewaters, and their ecotoxicological risk assessment. Environ Monit Assess 187(12), 734.

Ezzariai, A., Hafidi, M., Khadra, A., Aemig, Q., El Fels, L., Barret, M., Merlina, G., Patureau, D. and Pinelli, E. 2018. Human and veterinary antibiotics during composting of sludge or manure: Global perspectives on persistence, degradation, and resistance genes. Journal of Hazardous Materials 359, 465-481.

Farkas, L., Monzini, I., Takács, E., Wojnárovits, L., Vörös, M., Vágvölgyi, C., Janáky, C. and Alapi, T. 2024. Comparison of the effectiveness of UV, UV/VUV photolysis, ozonation, and ozone/UV processes for the removal of sulfonamide antibiotics. Journal of Environmental Chemical Engineering 12(1), 111845.

Feng, M., Yan, L., Zhang, X., Sun, P., Yang, S., Wang, L. and Wang, Z. 2016. Fast removal of the antibiotic flumequine from aqueous solution by ozonation: Influencing factors, reaction pathways, and toxicity evaluation. Science of The Total Environment 541, 167-175.

Fernández, P., Alder, A.C., Suter, M.J.F. and Giger, W. 1996. Determination off the quaternary ammonium surfactant ditallowdimethylammonium in digested sludges and marine sediments by supercritical fluid extraction and liquid chromatography with postcolumn ion-pair formation. Analytical Chemistry 68(5), 921-929.

Gassie, L.W. and Englehardt, J.D. 2019. Mineralization of greywater organics by the ozone-UV advanced oxidation process: Kinetic modeling and efficiency. Environmental Science: Water Research and Technology 5(11), 1956-1970.

Gomes, D.G., Pieretti, J.C., Rolim, W.R., Seabra, A.B. and Oliveira, H.C. (2021) Advances in Nano-Fertilizers and Nano-Pesticides in Agriculture. Jogaiah, S., Singh, H.B., Fraceto, L.F. and Lima, R.d. (eds), pp. 111-143, Woodhead Publishing.

Gomes, J., Costa, R., Quinta-Ferreira, R.M. and Martins, R.C. 2017. Application of ozonation for pharmaceuticals and personal care products removal from water. Science of The Total Environment 586, 265-283.

Guerra, P., Kim, M., Shah, A., Alaee, M. and Smyth, S.A. 2014. Occurrence and fate of antibiotic, analgesic/anti-inflammatory, and antifungal compounds in five wastewater treatment processes. Science of the Total Environment 473-474, 235-243.

Guo, K., Wu, Z. and Fang, J. (2020) Contaminants of Emerging Concern in Water and Wastewater. Hernández-Maldonado, A.J. and Blaney, L. (eds), pp. 367-408, Butterworth-Heinemann.

Guo, K., Wu, Z., Yan, S., Yao, B., Song, W., Hua, Z., Zhang, X., Kong, X., Li, X. and Fang, J. 2018. Comparison of the UV/chlorine and UV/H2O2 processes in the degradation of PPCPs in simulated drinking water and wastewater: Kinetics, radical mechanism and energy requirements. Water Research 147, 184-194.

Guo, Y., Long, J., Huang, J., Yu, G. and Wang, Y. 2022. Can the commonly used quenching method really evaluate the role of reactive oxygen species in pollutant abatement during catalytic ozonation? Water Research 215, 118275.

Gurmessa, B., Pedretti, E.F., Cocco, S., Cardelli, V. and Corti, G. 2020. Manure anaerobic digestion effects and the role of pre- and post-treatments on veterinary antibiotics and antibiotic resistance genes removal efficiency. Science of The Total Environment 721, 137532.

Hansen, K.M.S., Andersen, H.R. and Ledin, A. 2010. Ozonation of estrogenic chemicals in biologically treated sewage. Water Science and Technology 62(3), 649-657.

Hansen, K.M.S., Spiliotopoulou, A., Chhetri, R.K., Escolà Casas, M., Bester, K. and Andersen, H.R. 2016. Ozonation for source treatment of pharmaceuticals in hospital wastewater – Ozone lifetime and required ozone dose. Chemical Engineering Journal 290, 507-514.

Hassani, G., Babaei, A.A., Takdastan, A., Shirmardi, M., Yousefian, F. and Mohammadi, M.J. 2016. Occurrence and fate of 17β-estradiol in water resources and wastewater in Ahvaz, Iran. Global Nest Journal 18(4), 855-866.

He, Y., Cai, Y., Fan, S., Meng, T., Zhang, Y., Li, X. and Zhang, Y. 2022. Hydroxyl radicals can significantly influence the toxicity of ofloxacin transformation products during ozonation. Journal of Hazardous Materials 438, 129503.

Heffron, K.T., Gaines, K.F., Novak, J.M., Canam, T. and Collard, D.A. 2016. 17β-Estradiol influent and effluent concentrations in wastewater: demographic influences and the risk to environmental health. Environ Monit Assess 188(5), 288.

Henze, M., Gujer, W., Mino, T. and Loosdrecht, M. (2000) Activated Sludge Models ASM1, ASM2, ASM2D, ASM3.

Hirsch, R., Ternes, T., Haberer, K. and Kratz, K.L. 1999. Occurrence of antibiotics in the aquatic environment. Science of the Total Environment 225(1-2), 109-118.

Hollender, J., Zimmermann, S.G., Koepke, S., Krauss, M., McArdell, C.S., Ort, C., Singer, H., von Gunten, U. and Siegrist, H. 2009. Elimination of Organic Micropollutants in a Municipal Wastewater Treatment Plant Upgraded with a Full-Scale Post-Ozonation Followed by Sand Filtration. Environmental Science & Technology 43(20), 7862-7869.

Hu, Z., Liu, Y., Chen, G., Gui, X., Chen, T. and Zhan, X. 2011. Characterization of organic matter degradation during composting of manure–straw mixtures spiked with tetracyclines. Bioresource Technology 102(15), 7329-7334.

Huang, B., Wang, H.-C., Cui, D., Zhang, B., Chen, Z.-B. and Wang, A.-J. 2018. Treatment of pharmaceutical wastewater containing β-lactams antibiotics by a pilot-scale anaerobic membrane bioreactor (AnMBR). Chemical Engineering Journal 341, 238-247.

Huber, M.M., GÖbel, A., Joss, A., Hermann, N., LÖffler, D., McArdell, C.S., Ried, A., Siegrist, H., Ternes, T.A. and von Gunten, U. 2005. Oxidation of Pharmaceuticals during Ozonation of Municipal Wastewater Effluents: A Pilot Study. Environmental Science & Technology 39(11), 4290-4299.

Javier Rivas, F., Sagasti, J., Encinas, A. and Gimeno, O. 2011. Contaminants abatement by ozone in secondary effluents. Evaluation of second-order rate constants. Journal of Chemical Technology & Biotechnology 86(8), 1058-1066.

Kafaei, R., Papari, F., Seyedabadi, M., Sahebi, S., Tahmasebi, R., Ahmadi, M., Sorial, G.A., Asgari, G. and Ramavandi, B. 2018. Occurrence, distribution, and potential sources of antibiotics pollution in the water-sediment of the northern coastline of the Persian Gulf, Iran. Science of The Total Environment 627, 703-712.

Kasprzyk-Hordern, B., Ziółek, M. and Nawrocki, J. 2003. Catalytic ozonation and methods of enhancing molecular ozone reactions in water treatment. Applied Catalysis B: Environmental 46(4), 639-669.

Kasumba, J., Appala, K., Agga, G.E., Loughrin, J.H. and Conte, E.D. 2020. Anaerobic digestion of livestock and poultry manures spiked with tetracycline antibiotics. Journal of Environmental Science and Health - Part B Pesticides, Food Contaminants, and Agricultural Wastes 55(2), 135-147.

Katsoyiannis, I.A., Canonica, S. and von Gunten, U. 2011. Efficiency and energy requirements for the transformation of organic micropollutants by ozone, O3/H2O2 and UV/H2O2. Water Research 45(13), 3811-3822.

Keen, O.S., Love, N.G., Aga, D.S. and Linden, K.G. 2016. Biodegradability of iopromide products after UV/H2O2 advanced oxidation. Chemosphere 144, 989-994.

Kermia, A.E.B., Fouial-Djebbar, D. and Trari, M. 2016. Occurrence, fate and removal efficiencies of pharmaceuticals in wastewater treatment plants (WWTPs) discharging in the coastal environment of Algiers. Comptes Rendus Chimie 19(8), 963-970.

Khadra, A., Ezzariai, A., Merlina, G., Capdeville, M.-J., Budzinski, H., Hamdi, H., Pinelli, E. and Hafidi, M. 2019. Fate of antibiotics present in a primary sludge of WWTP during their co-composting with palm wastes. Waste Management 84, 13-19.

Khan, A.H., Khan, N.A., Ahmed, S., Dhingra, A., Singh, C.P., Khan, S.U., Mohammadi, A.A., Changani, F., Yousefi, M., Alam, S., Vambol, S., Vambol, V., Khursheed, A. and Ali, I. 2020. Application of advanced oxidation processes followed by different treatment technologies for hospital wastewater treatment. Journal of Cleaner Production 269, 122411.

Kim, M.S., Cha, D., Lee, K.-M., Lee, H.-J., Kim, T. and Lee, C. 2020. Modeling of ozone decomposition, oxidant exposures, and the abatement of micropollutants during ozonation processes. Water Research 169, 115230.

Konieczny, K., Kwiecińska, A. and Gworek, B. 2011. The recovery of water from slurry produced in high density livestock farming with the use of membrane processes. Separation and Purification Technology 80(3), 490-498.

Kosma, C.I., Lambropoulou, D.A. and Albanis, T.A. 2014. Investigation of PPCPs in wastewater treatment plants in Greece: Occurrence, removal and environmental risk assessment. Science of the Total Environment 466-467, 421-438.

Kulišťáková, A. 2023. Removal of pharmaceutical micropollutants from real wastewater matrices by means of photochemical advanced oxidation processes – A review. Journal of Water Process Engineering 53, 103727.

Kumar, V., Lakkaboyana, S.K., Sharma, N., Chakraborty, P., Umesh, M., Pasrija, R., Thomas, J., Kalebar, V.U., Jayaraj, I., Awasthi, M.K., Das, T., Oladipo, A.A., Barcelo, D. and Dumee, L.F. 2023. A critical assessment of technical advances in pharmaceutical removal from wastewater – A critical review. Case Studies in Chemical and Environmental Engineering 8, 100363.

Kuo, C.-H., Yuan, F. and Hill, D.O. 1997. Kinetics of Oxidation of Ammonia in Solutions Containing Ozone with or without Hydrogen Peroxide. Industrial & Engineering Chemistry Research 36(10), 4108-4113.

Kwon, J.W. and Rodriguez, J.M. 2014. Occurrence and removal of selected pharmaceuticals and personal care products in three wastewater-treatment plants. Archives of Environmental Contamination and Toxicology 66(4), 538-548.

Lado Ribeiro, A.R., Moreira, N.F.F., Li Puma, G. and Silva, A.M.T. 2019. Impact of water matrix on the removal of micropollutants by advanced oxidation technologies. Chemical Engineering Journal 363, 155-173.

Lee, W., Choi, S., Kim, H., Lee, W., Lee, M., Son, H., Lee, C., Cho, M. and Lee, Y. 2023. Efficiency of ozonation and O3/H2O2 as enhanced wastewater treatment processes for micropollutant abatement and disinfection with minimized byproduct formation. Journal of Hazardous Materials 454, 131436.

Lee, Y., Gerrity, D., Lee, M., Bogeat, A.E., Salhi, E., Gamage, S., Trenholm, R.A., Wert, E.C., Snyder, S.A. and Von Gunten, U. 2013. Prediction of micropollutant elimination during ozonation of municipal wastewater effluents: Use of kinetic and water specific information. Environmental Science and Technology 47(11), 5872-5881.

Lei, H. and Snyder, S.A. 2007. 3D QSPR models for the removal of trace organic contaminants by ozone and free chlorine. Water Research 41(18), 4051-4060.

Libralato, G., Ghirardini Annamaria, V. and Francesco, A. 2010. How toxic is toxic? A proposal for wastewater toxicity hazard assessment. Ecotoxicology and Environmental Safety 73(7), 1602-1611.

Lim, S., Shi, J.L., von Gunten, U. and McCurry, D.L. 2022. Ozonation of organic compounds in water and wastewater: A critical review. Water Research 213, 118053.

Lin, A.Y.-C., Lin, C.-F., Chiou, J.-M. and Hong, P.K.A. 2009. O3 and O3/H2O2 treatment of sulfonamide and macrolide antibiotics in wastewater. Journal of Hazardous Materials 171(1), 452-458.

Lin, C., Zhang, W., Yuan, M., Feng, C., Ren, Y. and Wei, C. 2014. Degradation of polycyclic aromatic hydrocarbons in a coking wastewater treatment plant residual by an O3/ultraviolet fluidized bed reactor. Environmental Science and Pollution Research 21(17), 10329-10338.

Liu, B., Chen, B., Zhang, B., Song, X., Zeng, G. and Lee, K. 2021. Photocatalytic ozonation of offshore produced water by TiO2 nanotube arrays coupled with UV-LED irradiation. Journal of Hazardous Materials 402.

Liu, H., Pu, C., Yu, X., Sun, Y. and Chen, J. 2018. Removal of tetracyclines, sulfonamides, and quinolones by industrial-scale composting and anaerobic digestion processes. Environmental Science and Pollution Research 25(36), 35835-35844.

Liu, Y., He, X., Fu, Y. and Dionysiou, D.D. 2016. Degradation kinetics and mechanism of oxytetracycline by hydroxyl radical-based advanced oxidation processes. Chemical Engineering Journal 284, 1317-1327.

Liu, Z., Yang, Y., Shao, C., Ji, Z., Wang, Q., Wang, S., Guo, Y., Demeestere, K. and Hulle, S.V. 2020. Ozonation of trace organic compounds in different municipal and industrial wastewaters: Kinetic-based prediction of removal efficiency and ozone dose requirements. Chemical Engineering Journal 387, 123405.

Lovato, M.E., Martín, C.A. and Cassano, A.E. 2009. A reaction kinetic model for ozone decomposition in aqueous media valid for neutral and acidic pH. Chemical Engineering Journal 146(3), 486-497.

Lyngsie, G., Krumina, L., Tunlid, A. and Persson, P. 2018. Generation of hydroxyl radicals from reactions between a dimethoxyhydroquinone and iron oxide nanoparticles. Scientific Reports 8(1), 10834.

Marcilhac, C., Sialve, B., Pourcher, A.-M., Ziebal, C., Bernet, N. and Béline, F. 2014. Digestate color and light intensity affect nutrient removal and competition phenomena in a microalgal-bacterial ecosystem. Water Research 64, 278-287.

Martín, J., Camacho-Muñoz, D., Santos, J.L., Aparicio, I. and Alonso, E. 2012. Occurrence of pharmaceutical compounds in wastewater and sludge from wastewater treatment plants: Removal and ecotoxicological impact of wastewater discharges and sludge disposal. Journal of Hazardous Materials 239-240, 40-47.

Martini, J., Orge, C.A., Faria, J.L., Pereira, M.F.R. and Soares, O.S.G.P. 2018. Sulfamethoxazole degradation by combination of advanced oxidation processes. Journal of Environmental Chemical Engineering 6(4), 4054-4060.

Mehrjouei, M., Müller, S. and Möller, D. 2014. Catalytic and photocatalytic ozonation of tert-butyl alcohol in water by means of falling film reactor: Kinetic and cost-effectiveness study. Chemical Engineering Journal 248, 184-190.

Merényi, G., Lind, J., Naumov, S. and Sonntag, C.v. 2010. Reaction of Ozone with Hydrogen Peroxide (Peroxone Process): A Revision of Current Mechanistic Concepts Based on Thermokinetic and Quantum-Chemical Considerations. Environmental Science & Technology 44(9), 3505-3507.

Merkus, V.I., Leupold, M.S., Rockel, S.P., Lutze, H.V. and Schmidt, T.C. 2023. Effects of organic matter and alkalinity on the ozonation of antiviral purine derivatives as exemplary micropollutant motif. Water Research 243, 120387.

Miao, H.F., Cao, M., Xu, D.Y., Ren, H.Y., Zhao, M.X., Huang, Z.X. and Ruan, W.Q. 2015. Degradation of phenazone in aqueous solution with ozone: Influencing factors and degradation pathways. Chemosphere 119, 326-333.

Miklos, D.B., Remy, C., Jekel, M., Linden, K.G., Drewes, J.E. and Hübner, U. 2018. Evaluation of advanced oxidation processes for water and wastewater treatment – A critical review. Water Research 139, 118-131.

Mohapatra, D., Brar, K., Tyagi, R. and Surampalli, R. 2011. Occurrence of bisphenol A in wastewater and wastewater sludge of CUQ treatment plant. Journal of Xenobiotics 1.

Moinard, V., Redondi, C., Etiévant, V., Savoie, A., Duchene, D., Pelosi, C., Houot, S. and Capowiez, Y. 2021. Short- and long-term impacts of anaerobic digestate spreading on earthworms in cropped soils. Applied Soil Ecology 168, 104149.

Monlau, F., Sambusiti, C., Ficara, E., Aboulkas, A., Barakat, A. and Carrère, H. 2015. New opportunities for agricultural digestate valorization: Current situation and perspectives. Energy and Environmental Science 8(9), 2600-2621.

Moradi, N., Vazquez, C.L., Hernandez, H.G., Brdjanovic, D., van Loosdrecht, M.C.M. and Rincón, F.R. 2023. Removal of contaminants of emerging concern from the supernatant of anaerobically digested sludge by O3 and O3/H2O2: Ozone requirements, effects of the matrix, and toxicity. Environmental Research 235, 116597.

Muller, M., Combalbert, S., Delgenès, N., Bergheaud, V., Rocher, V., Benoît, P., Delgenès, J.-P., Patureau, D. and Hernandez-Raquet, G. 2010. Occurrence of estrogens in sewage sludge and their fate during plant-scale anaerobic digestion. Chemosphere 81(1), 65-71.

Nawrocki, J. and Kasprzyk-Hordern, B. 2010. The efficiency and mechanisms of catalytic ozonation. Applied Catalysis B: Environmental 99(1), 27-42.

Nurk, L., Knörzer, S., Jacobi, H.F. and Spielmeyer, A. 2019. Elimination of sulfonamides and tetracyclines during anaerobic fermentation - A "Cheshire Cat" phenomenon. Sustainable Chemistry and Pharmacy 13.

Oehmen, A., Lopez-Vazquez, C.M., Carvalho, G., Reis, M.A.M. and van Loosdrecht, M.C.M. 2010. Modelling the population dynamics and metabolic diversity of organisms relevant in anaerobic/anoxic/aerobic enhanced biological phosphorus removal processes. Water Research 44(15), 4473-4486.

Park, M., Anumol, T., Daniels, K.D., Wu, S., Ziska, A.D. and Snyder, S.A. 2017. Predicting trace organic compound attenuation by ozone oxidation: Development of indicator and surrogate models. Water Research 119, 21-32.

Paucar, N.E., Kim, I., Tanaka, H. and Sato, C. 2019. Effect of O3 Dose on the O3/UV Treatment Process for the Removal of Pharmaceuticals and Personal Care Products in Secondary Effluent. ChemEngineering 3(2).

Petrie, B., Lopardo, L., Proctor, K., Youdan, J., Barden, R. and Kasprzyk-Hordern, B. 2019. Assessment of bisphenol-A in the urban water cycle. Science of The Total Environment 650, 900-907.

Pisarenko, A.N., Stanford, B.D., Yan, D., Gerrity, D. and Snyder, S.A. 2012. Effects of ozone and ozone/peroxide on trace organic contaminants and NDMA in drinking water and water reuse applications. Water Research 46(2), 316-326.

Presumido, P.H., Montes, R., Quintana, J.B., Rodil, R., Feliciano, M., Puma, G.L., Gomes, A.I. and Vilar, V.J.P. 2022. Ozone membrane contactor to intensify gas/liquid mass transfer and contaminants of emerging concern oxidation. Journal of Environmental Chemical Engineering 10(6), 108671.

Psaltou, S., Karapatis, A., Mitrakas, M. and Zouboulis, A. 2019. The role of metal ions on p-CBA degradation by catalytic ozonation. Journal of Environmental Chemical Engineering 7(5), 103324.

Qiang, H., Yang, Y., Li, N., Song, Y. and Li, Y. 2019. Effect of chlortetracycline concentration on mesophilic anaerobic digestion characteristics and antibiotic degradation of chicken manure. Trans. CSAE 35, 181-190.

Reichert, P. 1994. AQUASIM – A TOOL FOR SIMULATION AND DATA ANALYSIS OF AQUATIC SYSTEMS. Water Science and Technology 30(2), 21-30.

Rekhate, C.V. and Srivastava, J.K. 2020. Recent advances in ozone-based advanced oxidation processes for treatment of wastewater- A review. Chemical Engineering Journal Advances, 100031.

Reygaert, W.C. 2018. An overview of the antimicrobial resistance mechanisms of bacteria. AIMS Microbiol 4(3), 482-501.

Rosenfeldt, E.J., Linden, K.G., Canonica, S. and von Gunten, U. 2006. Comparison of the efficiency of {radical dot}OH radical formation during ozonation and the advanced oxidation processes O3/H2O2 and UV/H2O2. Water Research 40(20), 3695-3704.

Saeid, S., Tolvanen, P., Kumar, N., Eränen, K., Peltonen, J., Peurla, M., Mikkola, J.-P., Franz, A. and Salmi, T. 2018. Advanced oxidation process for the removal of ibuprofen from aqueous solution: A non-catalytic and catalytic ozonation study in a semi-batch reactor. Applied Catalysis B: Environmental 230, 77-90.

Sagristà, E., Larsson, E., Ezoddin, M., Hidalgo, M., Salvadó, V. and Jönsson, J.Å. 2010. Determination of non-steroidal anti-inflammatory drugs in sewage sludge by direct hollow fiber supported liquid membrane extraction and liquid chromatography–mass spectrometry. Journal of Chromatography A 1217(40), 6153-6158.

Sgroi, M., Snyder, S.A. and Roccaro, P. 2021. Comparison of AOPs at pilot scale: Energy costs for micro-pollutants oxidation, disinfection by-products formation and pathogens inactivation. Chemosphere 273, 128527.

Sharma, V.K. and Graham, N.J.D. 2010. Oxidation of Amino Acids, Peptides and Proteins by Ozone: A Review. Ozone: Science and Engineering 32(2), 81-90.

Shi, J., Chen, Q., Liu, X., Zhan, X., Li, J. and Li, Z. 2013. Sludge/water partition and biochemical transformation of estrone and 17β-estradiol in a pilot-scale step-feed anoxic/oxic wastewater treatment system. Biochemical Engineering Journal 74, 107-114.

Sim, W.-J., Lee, J.-W., Lee, E.-S., Shin, S.-K., Hwang, S.-R. and Oh, J.-E. 2011. Occurrence and distribution of pharmaceuticals in wastewater from households, livestock farms, hospitals and pharmaceutical manufactures. Chemosphere 82(2), 179-186.

Singer, P.C. and Zilli, W.B. 1975. Ozonation of ammonia in wastewater. Water Research 9(2), 127-134.

Sohoni, P. and Sumpter, J.P. 1998. Several environmental oestrogens are also anti-androgens. Journal of Endocrinology 158(3), 327-339.

Song, Y., Breider, F., Ma, J. and von Gunten, U. 2017. Nitrate formation during ozonation as a surrogate parameter for abatement of micropollutants and the N-nitrosodimethylamine (NDMA) formation potential. Water Research 122, 246-257.

St. Laurent, J.B., de Buzzaccarini, F., De Clerck, K., Demeyere, H., Labeque, R., Lodewick, R. and van Langenhove, L. (2007) Handbook for Cleaning/Decontamination of Surfaces. Johansson, I. and Somasundaran, P. (eds), pp. 57-102, Elsevier Science B.V., Amsterdam.

Stadlmair, L.F., Letzel, T., Drewes, J.E. and Grassmann, J. 2018. Enzymes in removal of pharmaceuticals from wastewater: A critical review of challenges, applications and screening methods for their selection. Chemosphere 205, 649-661.

Tanaka, J. and Matsumura, M. 2003. Application of ozone treatment for ammonia removal in spent brine. Advances in Environmental Research 7(4), 835-845.

Tang, K., Ooi, G.T.H., Spiliotopoulou, A., Kaarsholm, K.M.S., Sundmark, K., Florian, B., Kragelund, C., Bester, K. and Andersen, H.R. 2020. Removal of Pharmaceuticals, Toxicity and Natural Fluorescence by Ozonation in Biologically Pre-Treated Municipal Wastewater, in Comparison to Subsequent Polishing Biofilm Reactors. Water 12(4).

Tang, K., Spiliotopoulou, A., Chhetri, R.K., Ooi, G.T.H., Kaarsholm, K.M.S., Sundmark, K., Florian, B., Kragelund, C., Bester, K. and Andersen, H.R. 2019. Removal of pharmaceuticals, toxicity and natural fluorescence through the ozonation of biologically-treated hospital wastewater, with further polishing via a suspended biofilm. Chemical Engineering Journal 359, 321-330.

Ternes, T.A., Kreckel, P. and Mueller, J. 1999. Behaviour and occurrence of estrogens in municipal sewage treatment plants - II. Aerobic batch experiments with activated sludge. Science of the Total Environment 225(1-2), 91-99.

Thalla, A.K. and Vannarath, A.S. 2020. Occurrence and environmental risks of nonsteroidal anti-inflammatory drugs in urban wastewater in the southwest monsoon region of India. Environ Monit Assess 192(3), 193.

Tomiyasu, H., Fukutomi, H. and Gordon, G. 1985. Kinetics and mechanism of ozone decomposition in basic aqueous solution. Inorganic Chemistry 24(19), 2962-2966.

UVOX.com THE UVOX REDOX® PROCESS.

Vinayagam, V., Murugan, S., Kumaresan, R., Narayanan, M., Sillanpää, M., Viet N Vo, D., Kushwaha, O.S., Jenis, P., Potdar, P. and Gadiya, S. 2022. Sustainable adsorbents for the removal of pharmaceuticals from wastewater: A review. Chemosphere 300, 134597.

Von Sonntag, C. 2008 Advanced oxidation processes: Mechanistic aspects, pp. 1015-1021.

Wang, H., Zhang, S., He, X., Yang, Y., Yang, X. and Van Hulle, S.W.H. 2023a. Comparison of macro and micro-pollutants abatement from biotreated landfill

leachate by single ozonation, O3/H2O2, and catalytic ozonation processes. Chemical Engineering Journal 452, 139503.

Wang, J. and Chen, H. 2020. Catalytic ozonation for water and wastewater treatment: Recent advances and perspective. Science of The Total Environment 704, 135249.

Wang, J. and Wang, S. 2020. Reactive species in advanced oxidation processes: Formation, identification and reaction mechanism. Chemical Engineering Journal 401, 126158.

Wang, J. and Wang, S. 2021. Toxicity changes of wastewater during various advanced oxidation processes treatment: An overview. Journal of Cleaner Production 315, 128202.

Wang, W., Chang, J.-S. and Lee, D.-J. 2023b. Anaerobic digestate valorization beyond agricultural application: Current status and prospects. Bioresource Technology 373, 128742.

Wang, W. and Lee, D.-J. 2021. Valorization of anaerobic digestion digestate: A prospect review. Bioresource Technology 323, 124626.

Widyasari-Mehta, A., Hartung, S. and Kreuzig, R. 2016. From the application of antibiotics to antibiotic residues in liquid manures and digestates: A screening study in one European center of conventional pig husbandry. Journal of Environmental Management 177, 129-137.

Wols, B.A. and Hofman-Caris, C.H.M. 2012. Review of photochemical reaction constants of organic micropollutants required for UV advanced oxidation processes in water. Water Research 46(9), 2815-2827.

Woodard and Curran, I. (2006) Industrial Waste Treatment Handbook (Second Edition). Woodard and Curran, I. (eds), pp. 149-334, Butterworth-Heinemann, Burlington.

Worldbank.org Trends in Solid Waste Management.

Yan, S., Liu, Y., Lian, L., Li, R., Ma, J., Zhou, H. and Song, W. 2019. Photochemical formation of carbonate radical and its reaction with dissolved organic matters. Water Research 161, 288-296.

Yang, C.-W., Hsiao, W.-C. and Chang, B.-V. 2016. Biodegradation of sulfonamide antibiotics in sludge. Chemosphere 150, 559-565.

Yang, G., Xie, S., Yang, M., Tang, S., Zhou, L., Jiang, W., Zhou, B., Li, Y. and Si, B. 2022a. A critical review on retaining antibiotics in liquid digestate: Potential risk and removal technologies. Science of The Total Environment 853, 158550.

Yang, L., Si, B., Tan, X., Xu, J., Xu, W., Zhou, L., Chen, J., Zhang, Y. and Zhou, X. 2022b. Valorization of livestock manure for bioenergy production: A perspective

on the fates and conversion of antibiotics. Resources, Conservation and Recycling 183, 106352.

Yang, X., Liu, Z., Manhaeghe, D., Yang, Y., Hogie, J., Demeestere, K. and Van Hulle, S.W.H. 2021a. Intensified ozonation in packed bubble columns for water treatment: Focus on mass transfer and humic acids removal. Chemosphere 283, 131217.

Yang, X., Tao, Y. and Murphy, J.G. 2021b. Kinetics of the oxidation of ammonia and amines with hydroxyl radicals in the aqueous phase. Environmental Science: Processes & Impacts 23(12), 1906-1913.

Yang, Y. and Liu, H. 2022. The mechanisms of ozonation for ammonia nitrogen removal: An indirect process. Journal of Environmental Chemical Engineering 10(5), 108525.

Yang, Y., Liu, Z., Demeestere, K. and Van Hulle, S. 2021c. Ozonation in view of micropollutant removal from biologically treated landfill leachate: Removal efficiency, OH exposure, and surrogate-based monitoring. Chemical Engineering Journal 410, 128413.

Yin, F., Dong, H., Zhang, W., Zhu, Z. and Shang, B. 2020. Additional function of pasteurisation pretreatment in combination with anaerobic digestion on antibiotic removal. Bioresource Technology 297, 122414.

Yu, Y., Chen, L., fang, Y., Jia, X. and Chen, J. 2019. High temperatures can effectively degrade residual tetracyclines in chicken manure through composting. Journal of Hazardous Materials 380, 120862.

Yue, C., Dong, H., Zhang, W., Zhu, Z., Yin, F. and Wang, S. 2020. Effects of Membrane Concentration Processes on Flux, Nutrient Recovery, and Antibiotic Isolation for Anaerobically Digested Slurry from Swine Manure. Transactions of the ASABE 63(6), 1639-1647.

Zhang, X. and Li, R. 2018. Variation of antibiotics in sludge pretreatment and anaerobic digestion processes: Degradation and solid-liquid distribution. Bioresource Technology 255, 266-272.

Zhang, Z., Gao, P., Cheng, J., Liu, G., Zhang, X. and Feng, Y. 2018. Enhancing anaerobic digestion and methane production of tetracycline wastewater in EGSB reactor with GAC/NZVI mediator. Water Research 136, 54-63.

Zhou, H., Cao, Z., Zhang, M., Ying, Z. and Ma, L. 2021. Zero-valent iron enhanced in-situ advanced anaerobic digestion for the removal of antibiotics and antibiotic resistance genes in sewage sludge. Science of the Total Environment 754.

LIST OF ACRONYMS

17-β-EST	17-β-Estradiol
AD	Anaerobic digestion
AOD	Applied Ozone Dose
AOPs	Advanced Oxidation Processes
ARBs	Antibiotic-Resistant Bacteria
BPA	Bisphenol A
CECs	Contaminants of Emerging Concern
CTC	Chlortetracycline
DIC	Diclofenac
DOC	Dissolved Organic Carbon
DOM	Dissolved Organic Material
DON	Dissolved Organic Nitrogen
DOX	Doxycycline
DW	Demineralized Water
IBU	Ibuprofen
NOM	Natural Organic Matter
NOMAD	Novel Organic recovery using Mobil Advanced technology
NPX	Naproxen
NRMSD	Normalised Root Mean Squared Deviation

NSAIDs	Nonsteroidal Anti-Inflammatory Drugs
OTC	Oxytetracycline
ROS	Reactive Oxidative Species
RSM	Response Surface Methodology
SED	Selective Electrodialysis
SHB	Staehelin, Hoigné, and Bühler
SMN	Sulfamethazine
SMX	Sulfamethoxazole
TCN	Tetracycline
TFG	Tomiyasu, Fukutomi and Gordon
TOC	Total Organic Carbon
TOD	Transferred Ozone dose
UOD	Utilized Ozone dose
UVA	UV Absorbance
UVT	UV Transmittance
WWTPs	Wastewater Treatment Plants

LIST OF TABLES

LIST OF FIGURES

ABOUT THE AUTHOR

Nazanin Moradi was born on September 20th, 1984, in Mahshahr, Iran. She obtained her bachelor's degree in Applied Chemistry from Arak University, Iran, in 2008. Short after, Nazanin started her career at Water and Wastewater Consulting Engineers Co. (WWCERD) in Iran, accumulating 12 years of experience.

Continuing her educational journey, she earned a master's degree in Environmental Engineering from Isfahan University, Iran, in 2018. During her master's program, Nazanin conducted research on catalytic treatment for removing Contaminants of Emerging Concern (CECs) from pool water and wastewater.

In 2020, Nazanin initiated her PhD at IHE-Delft, concentrating on the removal of Contaminants of Emerging Concern (CECs) from digestate supernatant through ozone-based advanced oxidation. This research has been conducted in collaboration with the international NOMAD project, funded by the European Union's Horizon 2020 research and innovation program.

Journals publications

Moradi, N., Rubio-Rincón, F.J., Hernandez, H.G., Brdjanovic, D., van Loosdrecht, M.C.M., Lopez-Vazquez, C. 2024. Mathematical modelling of ozonation process of high-strength liquid digestate. Chemical Engineering. (Submitted)

Moradi, N., Lopez-Vazquez, C., Garcia Hernandez, H., Proskynitopoulou, V., Vouros, A., Garagounis, I., Lorentzou, S., Panopoulos, K.D., Brdanovic, D., van Loosdrecht, M.C.M, and Rubio- Rincón, F.J. 2024. Practical application of UVOX Redox® for pharmaceutical removal from liquid digestate in two biogas plants. Environmental Technology and Innovation, 33, 103473. https://doi.org/10.1016/j.eti.2023.103473

Moradi, N., Vazquez, C.L., Hernandez, H.G., Brdjanovic, D., van Loosdrecht, M.C.M. and Rincón, F.R., 2023. Removal of contaminants of emerging concern from the supernatant of anaerobically digested sludge by O_3 and O_3/H_2O_2: Ozone requirements, effects of the matrix, and toxicity. Environmental Research 235, 116597. https://doi.org/10.1016/j.envres.2023.116597.

Moradi, N., Amin, M. M., Fatehizadeh, A. ; Ghasemi, Z., 2018. Degradation of UV-filter Benzophenon-3 in aqueous solution using TiO_2 coated on quartz tubes. Journal of Environmental Health Science and Engineering, 16 (2): 213-228.

Fatehizadeh, A., Taheri, E., Amin, M.M., Mahdavi, M., Moradi, N., 2018. Sodium and potassium removal from brackish water by nanofiltration membrane: single and binary salt mixtures. Desalination and water treatment. 103: 65-71.

Netherlands Research School for the
Socio-Economic and Natural Sciences of the Environment

D I P L O M A

for specialised PhD training

The Netherlands research school for the
Socio-Economic and Natural Sciences of the Environment
(SENSE) declares that

Nazanin Moradi

born on the 20th of September 1984 in Mahshahr, Iran

has successfully fulfilled all requirements of the
educational PhD programme of SENSE.

Delft, 28 October 2024

Chair of the SENSE board

Prof. dr. Martin Wassen

The SENSE Director

Prof. Philipp Pattberg

The SENSE Research School has been accredited by the Royal Netherlands Academy of Arts and Sciences (KNAW)

K O N I N K L I J K E   N E D E R L A N D S E
A K A D E M I E   V A N   W E T E N S C H A P P E N

The SENSE Research School declares that **Nazanin Moradi** has successfully fulfilled all requirements of the educational PhD programme of SENSE with a work load of 38.7 EC, including the following activities:

SENSE PhD Courses

o Environmental research in context (2020)
o Research in context activity: Video Guideline for sludge preparation (2022)
o Micropollutant in water cycle (2022)

Selection of Other PhD and Advanced MSc Courses

o Introduction to R and R studio, Wageningen University (2021)
o Effective Negotiation: Win-Win Communication, TU Delft (2021)
o Cross cultural communication, TU Delft (2020)
o Teamwork, Leadership and Group Dynamics, TU Delft (2021)
o Using Creativity to Maximize Productivity and Innovation in your PhD, TU Delft (2021)
o Brain management, TU Delft (2021)
o Anaerobic wastewater treatment, IHE-Delft (2022)
o Aquasim Model, IHE Delft (2022)
o Advanced Chemistry, University of Kentucky, USA (2022)
o Introduction to chemistry: reactions and ratios, Duke University, USA (2023)

External training at a foreign research institute

o MOOC Open Science: Sharing your Research with the World (2020)

Management and Didactic Skills Training

o Supervising 1 MSc student with thesis entitled 'Removal of Antibiotics from Digestate' (2021)
o Teaching assistance activities in MSc program on the Module entitled "Experimental methods for wastewater treatment" (2022)

Oral Presentations

o *Pharmaceutical Removal from Digestate Supernatant, Comparing Known Technologies.* 6th IWA International Conference on eco-Technologies for Wastewater Treatment, 26-29 June 2023, Girona, Spain

SENSE coordinator PhD education

Dr. ir. Peter Vermeulen

Organic waste constitutes a significant portion of global waste, prompting the need for sustainable solutions. Anaerobic Digestion (AD) emerges as a vital process, converting organic waste into renewable energy and digestate. The latter, while rich in nutrients, faces restrictions in direct application due to environmental and health concerns. This thesis addresses this challenge through the exploration of ozone-based Advanced Oxidation Processes (AOPs) as a post-AD treatment for liquid digestate. The research highlights the efficacy of ozonation in removing contaminants of emerging concern (CECs) from digestate, overcoming complexities within the digestate matrix. A mathematical model is established to predict ozone consumption, offering fundamental insights into the ozonation process in complex water matrices. Building upon this model, the thesis extends its focus to diverse water matrices, demonstrating the predictive accuracy of CECs removal. Furthermore, the exploration extends to a pilot-scale UVOX Redox® system, a hybrid of UV light and ozone, proving its efficiency, cost-effectiveness, and energy reduction in removing CECs from digestate. The findings of this thesis contribute to sustainable digestate management and offer practical and innovative strategies for digestate treatment, aligned with broader goals of circular bioeconomy practices.

9 789073 445673